ANALYSIS OF MULTI-STAGE CENTRIFUGAL

PUMPS USING TRANSFER MATRICES

A Thesis

by

J. HOWARD KELLY

Submitted to the Office of Graduate Studies of
Texas A&M University
in partial fulfillment of the requirements for the degree of

MASTER OF SCIENCE

December 1989

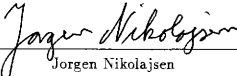Major Subject: Mechanical Engineering

ANALYSIS OF MULTI–STAGE CENTRIFUGAL
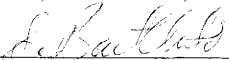
PUMPS USING TRANSFER MATRICES

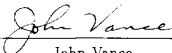A Thesis
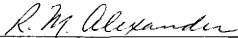
by

J. HOWARD KELLY

Approved as to style and content by:

Jorgen Nikolajsen	John Vance
(Chair of Committee)	(Member)
S. Bart Childs	for Michael Rabins
(Member)	(Head of Department)

December 1989

ABSTRACT

Analysis of Multi–Stage Centrifugal Pumps

Using Transfer Matrices. (December 1989)

J. Howard Kelly, B.S., Texas A&M University

Chair of Advisory Committee: Dr. Jorgen Nikolajsen

This report describes the background, theory, and verification of the FORTRAN program PATH. This program is used to analyze multi–stage centrifugal pumps using the transfer matrix method. It is capable of being used to conduct a static analysis in order to find the linearized stiffness and damping coefficients of the end bearings. It is also able to account for seal and impeller forces, seal misalignments, and a nonrotating flexible housing along with its supports.

The program is written to perform a dynamic analysis of the pump. Complex eigenvalues are computed for use in conducting a critical speed and stability investigation. Dynamic analysis capability is made complete with the program's ability to calculate mode shapes and model the pump response to mass imbalance.

DEDICATION

I wish to dedicate this work to my parents James and Katie.

ACKNOWLEDGEMENTS

NOMENCLATURE

$$a_i \quad = \text{semi-major axis of ellipse } [m]$$

$$A \quad = \text{cross sectional area } [m^2]$$

$$b_i \quad = \text{semi-minor axis of ellipse } [m]$$

$C_{xx}, C_{xy}, C_{x\theta}, C_{x\phi}$

$C_{yx}, C_{yy}, C_{y\theta}, C_{y\phi}$

$C_{\theta x}, C_{\theta y}, C_{\theta\theta}, C_{\theta\phi}$

$C_{\phi x}, C_{\phi y}, C_{\phi\theta}, C_{\phi\phi} \quad = \text{linear damping force coefficients } [N \ s/m]$

$$e_n \quad = \text{eccentricity of unbalance } [m]$$

$$e_x, e_y \quad = \text{components of bearing eccentricity } [m]$$

$$E \quad = \text{modulus of elasticity } [N/m^2]$$

$$f \quad = \text{scaling factor}$$

$$F_x, F_y \quad = \text{force components } [N]$$

$$g \quad = \text{function minimized in static iteration process}$$

$$G \quad = \text{modulus of rigidity } [N/m^2]$$

$$h \quad = \text{incremental vector in static iteration process}$$

$$i \quad = \text{used to denote an imaginary number}$$

$$I \quad = \text{geometric moment of inertia } [m^4]$$

$$J \quad = \text{Jacobian matrix in static iteration process}$$

$$J_T \quad = \text{transverse mass moment of inertia } [kg \ m^2]$$

$$J_P \quad = \text{polar mass moment of inertia } [kg \ m^2]$$

$$k, K \quad = \text{stiffness force coefficient } [N/m]$$

$$K_{xx}, K_{xy}, K_{x\theta}, K_{x\phi}$$

$$K_{yx}, K_{yy}, K_{y\theta}, K_{y\phi}$$

$$K_{\theta x}, K_{\theta y}, K_{\theta\theta}, K_{\theta\phi}$$

$$K_{\phi x}, K_{\phi y}, K_{\phi\theta}, K_{\phi\phi} \quad = \text{linear stiffness force coefficients } [N/m]$$

$$l_n \quad = \text{length of station n } [m]$$

$$m_n \quad = \text{mass of station n } [kg]$$

$$M_{xx}, M_{xy}, M_{x\theta}, M_{x\phi}$$

$$M_{yx}, M_{yy}, M_{y\theta}, M_{y\phi}$$

$$M_{\theta x}, M_{\theta y}, M_{\theta\theta}, M_{\theta\phi}$$

$$M_{\phi x}, M_{\phi y}, M_{\phi\theta}, M_{\phi\phi} \quad = \text{linear inertia force coefficients } [N\ s^2/m]$$

$$M_\phi, M_\theta \quad = \text{moment about x and y axis's } [N\ m]$$

$$P \quad = \text{polynomial function}$$

$$s \quad = \text{complex root } (\lambda + i\omega) \ [rad/s]$$

$$t \quad = \text{time } [s]$$

$$V_x, V_y \quad = \text{shear force in x and y directions } [N]$$

$$x, y \quad = \text{displacements in x and y directions } [m]$$

$$\bar{x}, \bar{y} \quad = \text{complex displacement in x and y directions } [m]$$

$$x_{r_i}, y_{r_i} \quad = \text{real components of complex displacements } [m]$$

$$x_{c_i}, y_{c_i} \quad = \text{imaginary components of complex displacements } [m]$$

$$\dot{x}, \dot{y} \quad = \text{velocity in x and y directions } [m/s]$$

$$\ddot{x}, \ddot{y} \quad = \text{acceleration in x and y directions } [m/s^2]$$

x^*, y^* = modified eccentricity components $[m]$

$\delta x, \delta y$ = absolute change in displacement of the shaft $[m]$

α = X-sectional shape factor for shear deformation of shaft

α_n = C.G. angle of imbalance $[deg]$

γ = direction angle of impeller force $[deg]$

γ_i = elliptical phase angle of whirl orbit $[deg]$

δ = logarithmic decrement of damped vibrations

$\delta_x, \delta_y, \delta_\theta, \delta_\phi$ = seal misalignments in corresponding directions $[m]$

θ_n = angle about y–axis $[rad]$

$\dot{\theta}_n$ = angular velocity about y–axis $[rad/s]$

λ = damping exponent of free vibration $[rad/s]$

π = 180 degrees converted to radians

ϕ = phase angle associated with imbalance $[deg]$

ϕ_n = angle about x–axis $[rad]$

$\ddot{\phi}_n$ = angular acceleration about x–axis $[rad/s^2]$

ψ = elliptical orientation angle of whirl orbit $[deg]$

ω = natural frequency of vibration $[rad/s]$

ω_d = damped natural frequency of vibration $[rad/s]$

Ω = running speed of shaft $[rpm]$

subscripts

B = bearing

$B1$ = left bearing

B_2 = right bearing

BS = bearing support

H = housing

I = impeller

LHS = left hand side of pump

n = station number

N = number of stations

RHS = right hand side of pump

S = shaft

SL = seal

x, y, θ, ϕ = direction components

superscripts

T = transpose of matrix

$\prime$ = substation between lumped mass and massless beam

TABLE OF CONTENTS

LIST OF TABLES

LIST OF FIGURES

CHAPTER I

INTRODUCTION

The objective of this project is to produce a computer code capable of analyzing high performance multi-stage centrifugal pumps using the transfer matrix technique with eigenvalues derived from the characteristic polynomial (Murphy and Vance (1983)). This program is able to take into account the following features of the pump:

1) Nonlinear bearings with linearized 2×2 stiffness and damping matrices.

2) Up to 25 linear seals with 4×4 stiffness, damping, and inertia matrices.

3) Flexible pump housing on flexible, damped supports.

4) Seal misalignments.

5) Steady-state impeller forces.

The program enables the user to perform the following analyses:

1) Determine instability threshold speed.

2) Determine damped natural frequencies and mode shapes.

3) Find steady unbalance response of the system, including displacements at each station and reactions at each support.

4) Calculate steady state eccentricity of the bearings and the seals and use this eccentricity to obtain the bearing stiffness and damping coefficients.

These analyses can be performed interactively.

Format and style based on ASME Journal of Vibration, Acoustics, Stress, and Reliability in Design.

Prohl (1945) and Myklestad (1944) were the first to introduce the transfer matrix method as a technique for calculating the natural frequencies and mode shapes of flexible beams. Koenig (1961) described a technique by which this method could be applied to finding the response to imbalances, as well as the natural frequencies. Twelve years later, Lund (1973) set forth a procedure by which the stability and damped critical speeds of a flexible rotor in fluid-film bearings could be found by calculating the complex eigenvalues of the system.

Pilkey and Chang (1971) proposed a new idea for finding critical speeds with the transfer matrix method. They set forth a method that avoids iterative searches and instead takes advantage of the characteristic determinant being a polynomial. The natural frequencies could now be found as roots of this polynomial. Though submitted as a faster technique that would avoid missing critical speeds, it was not brought to fruition for ten years. It was at this time that Murphy and Vance (1983) wrote a paper describing a program using this method with damping included. In their paper, they proved that this method converges faster than a Lund–type program and no critical speeds are missed.

All of these papers mentioned thus far regard only single spool systems. Bohm (1966) described a transfer matrix method for calculating critical speeds of multiple spool systems. Hibner (1975) improved upon this scheme by considering bearings with nonlinear viscous damping and shear flexibility. Li and Gunter (1978) developed a program for "computing the stability of a linear dual-rotor system using the parallel transfer matrix technique". Nelson and Meacham (1982) produced a program to

analyze dual rotor systems using finite elements with either the direct or component mode synthesis method.

Gajan (1987) described in his thesis a computer code developed to specifically analyze multi-stage centrifugal pumps. His program was a modification of a more general rotor dynamics program developed by Nelson, et.al. (1981) based on using the finite element method. Centrifugal pumps have seals as well as nonlinear bearings to support the weight of the rotor. This condition means that the pump is statically indeterminate, which implies that the bearing eccentricities are unknown. Therefore, the bearing stiffness and damping coefficients are unknown. Gajan modified Nelson's program by developing an iterative scheme to home in on the static bearing eccentricities. He also made available a means of considering seal misalignments and full 4×4 seal stiffness, damping, and inertia coefficient matrices.

The flexible housing option in program PATH is made available for use in analyzing vertical pumps as well as horizontal centrifugal pumps with housing. A vertical water pump has been chosen to be analyzed in order to demonstrate the effects of including the housing in the model. A typical vertical, multistage, deepwell pump is shown in Figure 1 from Dicmas (1987). A number of models have been suggested in the literature for use in analyzing vertical pumps. Some models differentiate on whether or not to include the stiffness of the base plate connection to the foundation, and if so, whether to use moment stiffnesses, direct stiffnesses, cross-coupled stiffnesses, or all the above. Lee, et al. (1985) demonstrated the importance of modeling the base-plate-to-foundation stiffness in a paper on the analysis of an idealized

vertical pump. Previous analyses had assumed infinite stiffness for this connection. The pump model used by Lee, et al. is shown in Figure 2. They use a torsional stiffness model, K_t for the baseplate-to-foundation connection and also include the stiffness K of the discharge pipe. It was demonstrated that both the base-plate-to-foundation stiffness and the stiffness of the discharge "significantly affected the natural frequencies and modes" of the vertical pump model.

Smith and Woodward (1988) presented a paper describing the field vibration analysis of "several large motor-driven vertical cooling water pumps which experienced excessive wear of the impellers, wear rings and seals after a short period of operation". They discovered that the problem was due to the operating speed being too close to a natural frequency of the system. It was shown that the "natural frequency was a direct function of the stiffness of the bolted connections between the concrete [foundation], the pump, and the motor". Though a detailed computer analysis was never conducted, they suggested the lumped mass model shown in Figure 3. The basis of this suggestion is that the stiffness of the baseplate-to-foundation can greatly affect the natural frequency of the pump and should thus be included in any numerical analysis.

None of the previous mentioned papers included the effects of the vertical pump casing in their analyses. Chang and Braun (1987) included the casing in the analysis of a vertical multistage cryogenic pump. They showed that "a subsynchronous mode associated with the cantilever bending of the pump casing bundle was correctly predicted" by including the housing in the model. Finite element representations of

2	Impeller
6	Shaft, Pump
8	Ring, Impeller
10	Shaft, Head
12	Shaft, Drive
13	Packing
17	Gland
29	Ring, Lantern
39	Bushing, Bearing
55	Bell, Suction
63	Bushing, Stuffing Box
64	Collar, Protecting
66	Nut, Shaft Adjusting
70	Coupling, Shaft
77	Lubricator
79	Bracket, Lubricator
83	Stuffing Box
84	Collet, Impeller Lock
85	Tube, Shaft Enclosing
101	Pipe, Column
103	Bearing, Line Shaft, Enclosed
183	Nut, Tubing
185	Plate, Tension, Tubing
187	Head, Surface Discharge
189	Flange, Top Column
191	Coupling, Column Pipe
193	Retainer Bearing, Open Lineshaft
195	Adapter, Tubing
197	Case, Discharge
199	Bowl, Intermediate
203	Case, Suction
209	Strainer
211	Pipe, Suction

OPEN LINESHAFT TYPE
SEMI-OPEN IMPELLER

ENCLOSED LINESHAFT TYPE
ENCLOSED IMPELLER

Figure 1. Turbine type, vertical, multistage, deepwell pump.
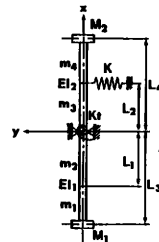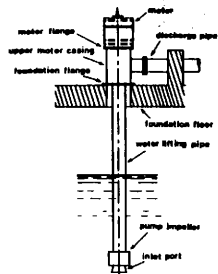
Figure 2. Idealized vertical model.
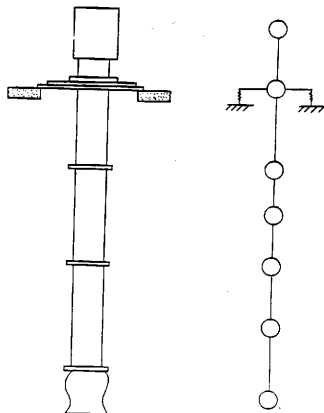
Figure 3.   Lumped mass vertical pump model with baseplate.

vertical pumps have also been presented in the literature by Hinata, et al. (1985) and Cornman (1986).

Gajan's program, as well as Murphy's was developed for a single spool system. The project proposed here will improve upon each program by having the capability of taking the flexible pump housing into account. This is particularly important when analyzing vertical pumps which have long flexible housings. It also takes advantage of the simplicity and speed of transfer matrices in the static analysis. By combining the advantages of Gajan's program with Murphy's program along with the use of transfer matrices and the inclusion of a flexible housing, this should be the fastest, most encompassing pump program available.

CHAPTER II

THEORETICAL DEVELOPMENT (STATIC)

One of the primary objectives of this project is to compute the static equilibrium position of the shaft using transfer matrices. This is done in order to calculate the linearized bearing coefficients for use in the dynamic analysis. The transfer matrix method has been extensively described in the literature. For a simple introduction, refer to Steidel (1979). For a more extensive overview, see Leckie and Pestel (1960). In using the transfer matrix method, the shaft is broken up into a series of lumped masses and massless beams. For the static case, referring to Figure 4, the transfer equations are derived for the y-z plane. The transfer across lumped mass number n is obtained by summing the forces in the y_n direction and summing the moments in the ϕ_n direction.

$$\sum F_{y_n} = 0 \Rightarrow V'_{y_n} - V_{y_n} + \Gamma_{y_n} - W_{y_n} = 0$$

$$\sum M_{\phi_n} = 0 \Rightarrow M'_{\phi_n} - M_{\phi_n} + \Gamma_{\phi_n} = 0$$

(1)
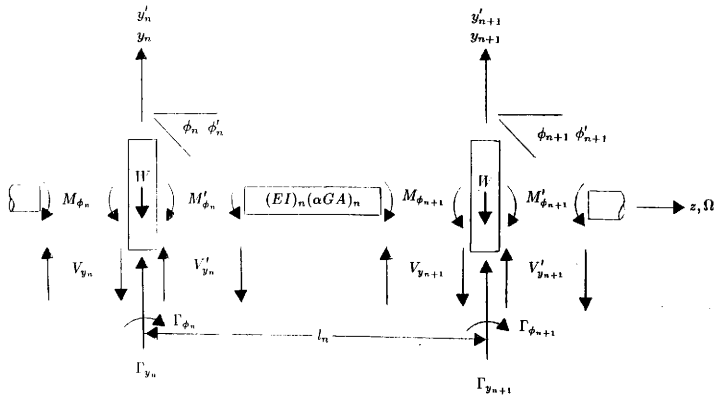
Figure 4. Discrete shaft model for static analysis in y–z plane.

where Γ_y represents the bearing and seal forces in the y direction, W_y depicts the weight and impeller forces in the y direction, and Γ_ϕ symbolizes the seal moments around the x-axis. The transfer across the massless beam number n is obtained in the same manner.

$$\sum F'_{y_n} = 0 \Rightarrow V_{y_{n+1}} - V'_{y_n} = 0$$

$$\sum M'_{\phi_n} = 0 \Rightarrow M_{\phi_{n+1}} - M'_{\phi_n} - V'_{y_n} l_n = 0 \tag{2}$$

Rearranging the terms of equations 1 and 2 results in equations 3.

$$V'_{y_n} = V_{y_n} - \Gamma_{y_n} + W_{y_n}$$

$$M'_{\phi_n} = M_{\phi_n} - \Gamma_{\phi_n}$$

$$V_{y_{n+1}} = V'_{y_n} \tag{3}$$

$$M_{\phi_{n+1}} = M'_{\phi_n} + V'_{y_n} l_n$$

Using beam theory, the deflections are derived.

$$y'_n = y_n$$

$$\phi'_n = \phi_n$$

$$y_{n+1} = y_n - \phi_n l_n + (\frac{l_n^3}{3EI} + \frac{l_n}{\alpha GA}) V_{y_{n+1}} - \frac{M_{\phi_{n+1}} l_n^2}{2EI} \tag{4}$$

$$\phi_{n+1} = \phi_n - \frac{V_{y_{n+1}} l_n^2}{2EI} + \frac{M_{\phi_{n+1}} l_n}{EI}$$

Substituting the solutions for $V_{y_{n+1}}$ and $M_{\phi_{n+1}}$ of equation 3 into the second half of equations 4 gives

$$y_{n+1} = y_n - \phi_n l_n - (\frac{l_n^3}{6} - \frac{l_n EI}{\alpha GA}) \frac{V'_{y_n}}{EI} - \frac{M'_{\phi_n} l_n^2}{2EI}$$

$$\phi_{n+1} = \phi_n + \frac{V'_{y_n} l_n^2}{2EI} + \frac{M'_{\phi_n} l_n}{EI} \tag{5}$$

Similarly, referring to Figure 5, the transfer equations are derived for the x-z plane.

$$V'_{z_n} = V_{z_n} - \Gamma_{z_n} + W_{z_n}$$

$$M'_{\theta_n} = M_{\theta_n} - \Gamma_{\theta_n}$$

$$V_{z_{n+1}} = V'_{z_n}$$

$$M_{\theta_{n+1}} = M'_{\theta_n} - V'_{z_n} l_n$$

$$x'_n = x_n \qquad (6)$$

$$\theta'_n = \theta_n$$

$$x_{n+1} = x_n + l_n\theta_n - \left(\frac{l_n^3}{6} - \frac{l_n EI}{\alpha GA}\right)\frac{V'_{z_n}}{EI} + \frac{M'_{\theta_n} l_n^2}{2EI}$$

$$\theta_{n+1} = \theta_n - \frac{V'_{z_n} l_n^2}{2EI} + \frac{M'_{\theta_n} l_n}{EI}$$

II.1 Nonlinear Bearing Forces

This program considers pumps with two nonlinear journal bearings with multiple seals between the bearings. The bearing force, attitude angle, stiffness coefficients, and damping coefficients are all functions of the eccentricity ratio, the ratio of the bearing eccentricity to the radial clearance between the shaft and the bearing. The bearing eccentricity is the displacement of the journal relative to the bearing centerline (see Figure 6). These parameters are shown in Figures 7 and 8 from Lund (1965), and Figures 9 and 10 from Woodcock (1971).

The bearing force is represented in Figure 7 as the inverse Sommerfield number

$$S^{-1} = \frac{F_B}{LD\mu N}\left(\frac{C}{R}\right)^2 \qquad (7)$$
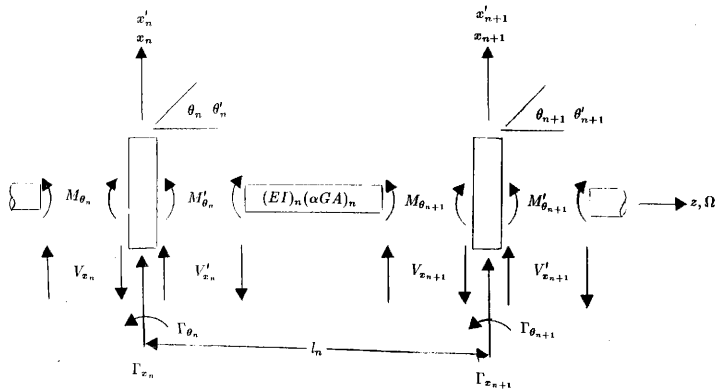
Figure 5. Discrete shaft model for static analysis in x-z plane.
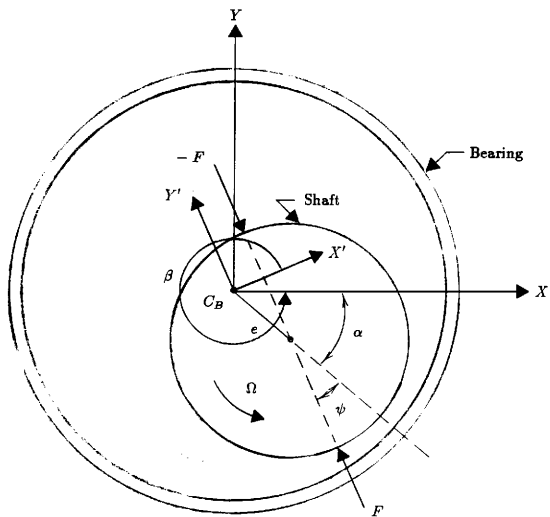
Figure 6.   Schematic of bearing forces acting on shaft with eccentricity and attitude angle.
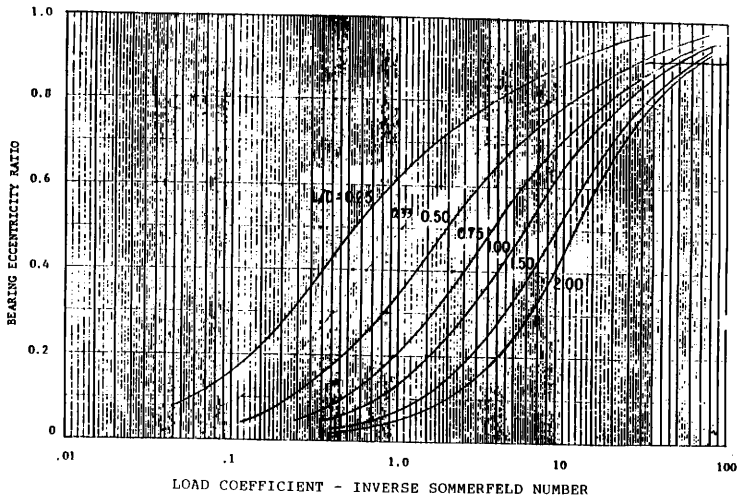
Figure 7. Load - eccentricity relationship.
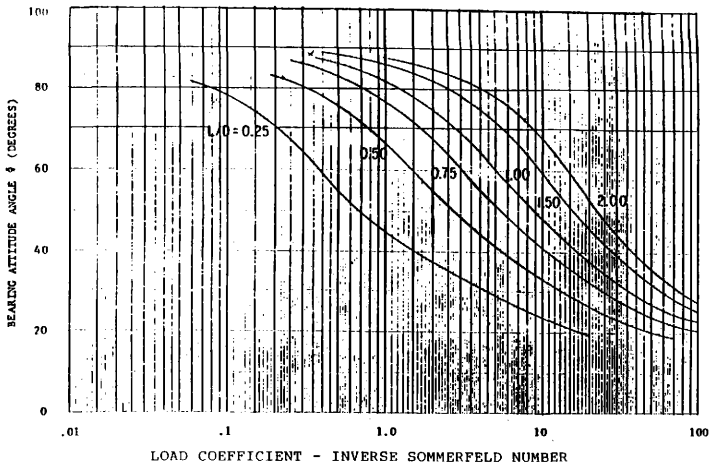
Figure 8. Load - attitude angle relationship.
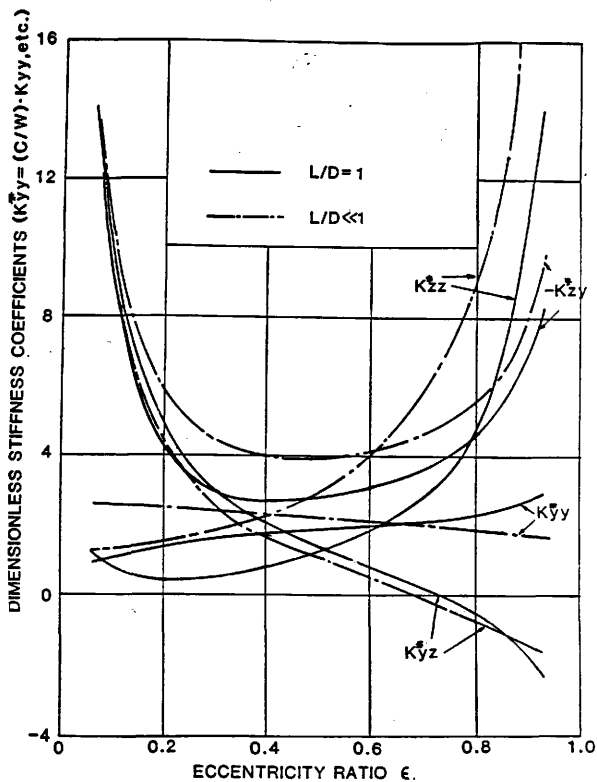
Figure 9. Dimensionless stiffness coefficients versus eccentricity.
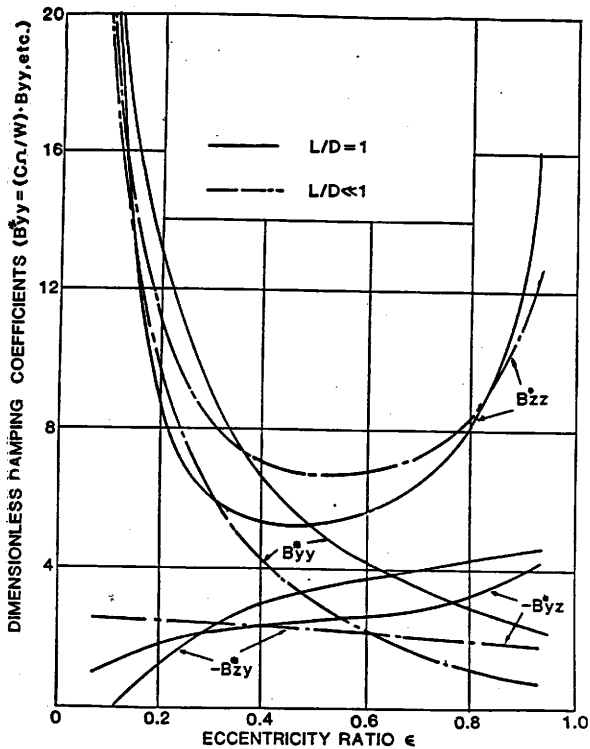
Figure 10. Dimensionless damping coefficients versus eccentricity.

where F_B is the absolute bearing force, L is the axial length of the bearing, $D = 2R$ is the diameter of the journal, μ is the viscosity of the fluid film, N is the the shaft speed in rps, and C is the radial clearance between the shaft and the bearing, Vance (1988). The attitude angle of Figure 8 is the angle ψ of Figure 6 between the lines of action of the force and eccentricity.

The dimensionless coefficients of Figures 9 and 10 are given in the direction of the load. The conversion to coefficients with physical dimensions along with the transformation to the defined coordinate system is given as

$$
\begin{aligned}
K_{zz} &= \frac{F}{C} * [K_{xx}\cos^2(\beta) - (K_{xy} + K_{yx})\cos(\beta)\sin(\beta) + K_{yy}\sin^2(\beta)] \\
K_{zy} &= \frac{F}{C} * [K_{xy}\cos^2(\beta) - (K_{yy} - K_{xx})\cos(\beta)\sin(\beta) - K_{yx}\sin^2(\beta)] \\
K_{yz} &= \frac{F}{C} * [K_{yx}\cos^2(\beta) - (K_{yy} - K_{xx})\cos(\beta)\sin(\beta) - K_{xy}\sin^2(\beta)] \\
K_{yy} &= \frac{F}{C} * [K_{yy}\cos^2(\beta) + (K_{xy} + K_{yx})\cos(\beta)\sin(\beta) + K_{xx}\sin^2(\beta)] \\
C_{zz} &= \frac{F}{C} * [C_{xx}\cos^2(\beta) - (C_{xy} + C_{yx})\cos(\beta)\sin(\beta) + C_{yy}\sin^2(\beta)] \\
C_{zy} &= \frac{F}{C} * [C_{xy}\cos^2(\beta) - (C_{yy} - C_{xx})\cos(\beta)\sin(\beta) - C_{yx}\sin^2(\beta)] \\
C_{yz} &= \frac{F}{C} * [C_{yx}\cos^2(\beta) - (C_{yy} - C_{xx})\cos(\beta)\sin(\beta) - C_{xy}\sin^2(\beta)] \\
C_{yy} &= \frac{F}{C} * [C_{yy}\cos^2(\beta) + (C_{zy} + C_{yz})\cos(\beta)\sin(\beta) + C_{xx}\sin^2(\beta)]
\end{aligned}
\tag{8}
$$

where, referring to Figure 6

$$
\beta = 1.5\pi - \alpha + \psi \tag{9}
$$

The damping coefficients C_{xx}–C_{yy} are not included in the static analysis, but are interpolated for at the end of the analysis for use in dynamic calculations.

Figure 11 is a simple schematic of a flexible shaft with linear seals, linearized bearings, and linear bearing supports connecting the bearing housing to the ground. In equation form,

$$e_y = y_S - y_B$$

$$e_x = x_S - x_B$$

(10)

where e_y and e_x are the y and x components of the bearing eccentricity, y_S and x_S are the absolute displacements of the shaft, and y_B and x_B are the absolute displacements of the bearing as seen in Figure 12.

Given an initial eccentricity, the nonlinear static bearing forces can be calculated in either of two ways. They can be found in linearized form using the stiffness coefficients where

$$F_x = -K_{xx}x - K_{xy}y$$

$$F_y = -K_{yx}x - K_{yy}y$$

(11)

They can also be found in basic nonlinear form by interpolating from tables for the absolute bearing forces (see Figures 7 and 8). These two options are further discussed in section II.6. The forces F_x and F_y are included in the variables Γ_{x_n} and Γ_{y_n} of equations (6) and (3), respectively, across the bearings at station n.

In order to account for the bearing support flexibility for the one spool case, it is first seen, referring to Figure 11, that

$$y_B = -\frac{F_{B_y}}{K_{BS_y}}$$

(12)

where F_{B_y} is the bearing force in the y–direction and K_{BS_y} is the bearing support stiffness coefficient in the y–direction. Substituting this into equation (10) and rearranging terms gives

$$y_S = e_y - \frac{F_{B_y}}{K_{BS_y}}$$

(13)
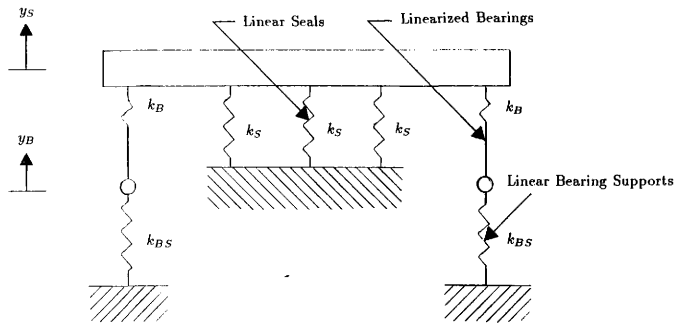
Figure 11. Flexible shaft with linear seals, linearized bearings, and linear bearing supports.
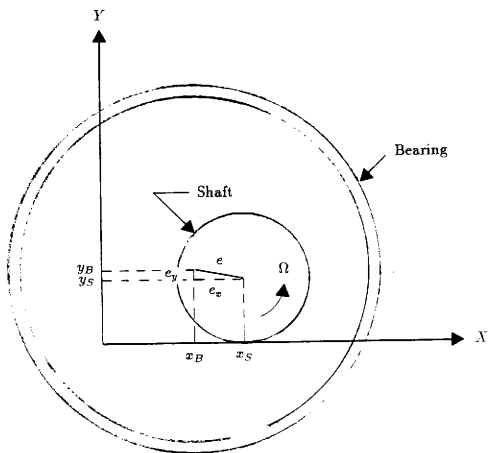
Figure 12.   Bearing eccentricity.

It has already been shown that e_y is the y-component of the bearing eccentricity, from which we obtain F_{B_y}. In the same fashion,

$$x_S = e_x - \frac{F_{B_x}}{K_{BS_x}} \tag{14}$$

where x is the absolute x-displacement of the shaft, e_x is the x-component of the bearing eccentricity, F_{B_x} is the bearing force in the x-direction, and K_{BS_x} is the bearing support stiffness in the x-direction. The equations across a lumped mass are represented here in matrix form.

$$\left\{ \begin{array}{c} x \\ y \\ \theta \\ \phi \\ V_x \\ V_y \\ M_\theta \\ M_\phi \\ 1 \end{array} \right\}'_n = \left[\begin{array}{ccccc} 1 & 0 & \ldots & a_{19} \\ 0 & 1 & \ldots & a_{29} \\ \vdots & \vdots & \ddots & \vdots \\ a_{81} & a_{82} & \ldots & a_{89} \\ 0 & 0 & \ldots & 1 \end{array} \right]'_n \left\{ \begin{array}{c} x \\ y \\ \theta \\ \phi \\ V_x \\ V_y \\ M_\theta \\ M_\phi \\ 1 \end{array} \right\}_n \tag{15}$$

Using equations (13) and (14), the bearing supports are accounted for by using the following equation.

$$\begin{aligned} a'_{19} &= a_{19} - \frac{F_{B_x}}{K_{BS_x}} \\ a'_{29} &= a_{29} - \frac{F_{B_y}}{K_{BS_y}} \\ a'_{59} &= a_{59} - a_{51}\frac{F_{B_x}}{K_{BS_x}} - a_{52}\frac{F_{B_y}}{K_{BS_y}} \\ a'_{69} &= a_{69} - a_{61}\frac{F_{B_x}}{K_{BS_x}} - a_{62}\frac{F_{B_y}}{K_{BS_y}} \end{aligned} \tag{16}$$

Substituting the results of equations (16) into equation (15) accounts for the bearing supports for the one spool case. The derivation accounting for the support flexibility with the housing is found in section 2.5.

II.2 Seal Forces

For this program, the seal forces are linear functions of the displacements (Childs (1981)). In matrix form, the transfer across a mass station with a seal is

$$
\left\{ \begin{array}{c} x \\ y \\ \theta \\ \phi \\ V_x \\ V_y \\ M_\theta \\ M_\phi \\ 1 \end{array} \right\}_n^{'} \cdot = \begin{bmatrix} 1 & 0 & 0 & 0 & \cdots & 0 \\ \vdots & \vdots & \vdots & \vdots & \ddots & \vdots \\ K_{xx} & K_{xy} & K_{x\theta} & K_{x\phi} & \cdots & a_{59} \\ K_{yx} & K_{yy} & K_{y\theta} & K_{y\phi} & \cdots & a_{69} \\ K_{\theta x} & K_{\theta y} & K_{\theta\theta} & K_{\theta\phi} & \cdots & a_{79} \\ K_{\phi x} & K_{\phi y} & K_{\phi\theta} & K_{\phi\phi} & \cdots & a_{89} \\ 0 & 0 & 0 & 0 & \cdots & 1 \end{bmatrix}_n^{'} \left\{ \begin{array}{c} x \\ y \\ \theta \\ \phi \\ V_x \\ V_y \\ M_\theta \\ M_\phi \\ 1 \end{array} \right\}_n \tag{17}
$$

The variables a_{59}–a_{89} represent all constant forces and moments acting on the seal station, such as weight and seal forces due to misalignments.

II.3 Seal Misalignments

Nikolajsen and Kelly (1989) demonstrated that "the stability of a rotor with three or more fluid–film bearings or seals is strongly affected by the radial misalignment of the bearings and seals." Referring to Figure 13, δ_y represents the misalignment of the seal with respect to the bearing centerline in the y direction. For this simple example, the seal forces caused by the misalignment are

$$
F_y = -k_y(e_y - \delta_y) \tag{18}
$$

or

$$
F_y = -k_y e_y + k_y \delta_y \tag{19}
$$

where e_y is the displacement of the shaft relative to the bearing centerline.

This simple example can be extended to include the four degrees of freedom x, y, θ, and ϕ for each seal. The seal force, representing $k_y \delta_y$, can be included into equation (17) by substituting in the following formulas.

$$a_{59} = W_x - K_{xx}\delta x - K_{xy}\delta y - K_{x\theta}\delta\theta - K_{x\phi}\delta\phi$$

$$a_{69} = W_y - K_{yx}\delta x - K_{yy}\delta y - K_{y\theta}\delta\theta - K_{y\phi}\delta\phi$$

$$a_{79} = -K_{\theta x}\delta x - K_{\theta y}\delta y - K_{\theta\theta}\delta\theta - K_{\theta\phi}\delta\phi$$

$$a_{89} = -K_{\phi x}\delta x - K_{\phi y}\delta y - K_{\phi\theta}\delta\theta - K_{\phi\phi}\delta\phi$$

$$(20)$$

II.4   Impeller Forces

The impeller forces are hydrodynamic forces exerted on the impellers and transmitted to the shaft. These forces have been recognized to cause rotor dynamic problems in high speed pumps (Jery, et al. (1984)). For any position of the impeller (see Figure 14), the forces on the impeller can be represented by

$$\left\{ \begin{array}{c} F_x \\ F_y \end{array} \right\} = \left\{ \begin{array}{c} F_{0x} \\ F_{0y} \end{array} \right\} + [A] \left\{ \begin{array}{c} x \\ y \end{array} \right\} \tag{21}$$

The forces F_{0x} and F_{0y} are the lateral forces "generated when the impeller center coincides with the volute center" Jery, et al. (1984). Data for these forces has been compiled by Domm and Hergt (1970), Agostinelli, et al. (1960), and Iversen, et al. (1960), among others. For this analysis, the volute center is considered coincidental with the bearing centerline. Small offsets x, y in the impeller center generate the remainder of the forces represented with the stiffness matrix $[A]$ (reference Chamieh, (1983), Chamieh, et al. (1982), and Jery and Franz (1982)).
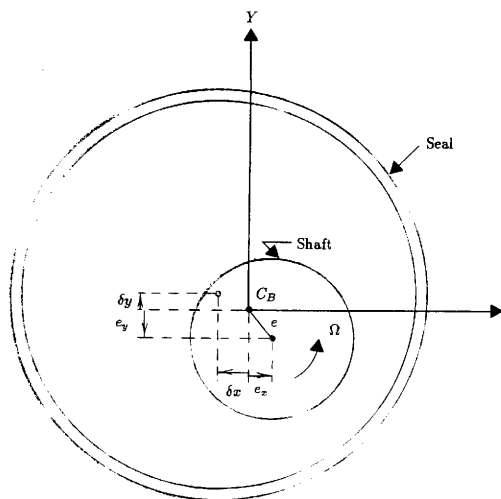
Figure 13. Seal misalignment with respect to bearing centerline.
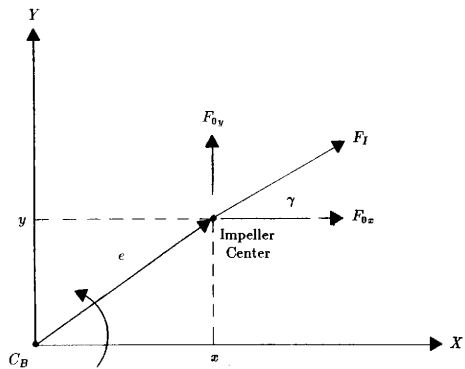
Figure 14. Impeller coordinate system and force notation.

For this project, the forces F_{0x} and F_{0y} are read in for each shaft speed Ω to be analyzed as a force magnitude F_I and direction γ as depicted in Figure 14. The force is broken up into its x and y components in equation (22) which can then be accounted for in the static force terms W_x and W_y of equations (6) and (3), respectively.

$$F_{I_x} = F_I \cos \gamma$$
$$F_{I_y} = F_I \sin \gamma$$
(22)

The stiffness matrix $[A]$ is also read in for each shaft speed Ω and contains cross-coupled as well as direct coefficients.

$$[A] = \begin{bmatrix} K_{xx} & K_{xy} \\ K_{yx} & K_{yy} \end{bmatrix}_I$$
(23)

The stiffness matrix is accounted for in the same way as that for the bearings and seals.

II.5   Flexible Housing

A major distinction between this project and that of Gajan and Murphy is the inclusion of a flexible housing in the analysis. This will result in a more accurate modeling of vertical pumps in particular. The transfer across lumped masses and massless beams is the same as in the one spool case. The main obstacle in multi-spool analysis is crossing over bearings and seals which connect the shaft to the housing (see Figure 15). In order to keep the size of the equations small in the following explanation, it is necessary to define two matrix variables.

$$\{ X \} = \begin{Bmatrix} x \\ y \\ \theta \\ \phi \end{Bmatrix} , and \; \{ V \} = \begin{Bmatrix} V_x \\ V_y \\ M_\theta \\ M_\phi \end{Bmatrix}$$
(24)
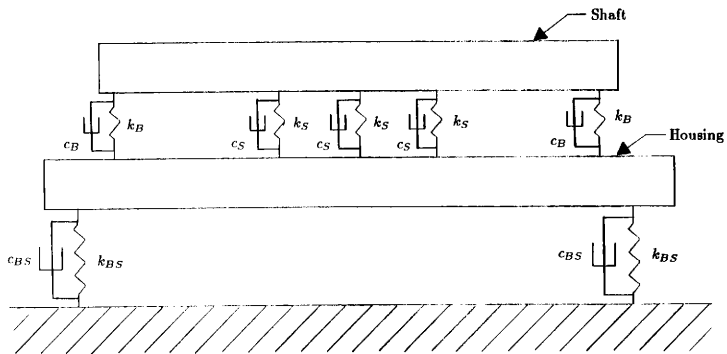
Figure 15. Schematic of flexible rotating shaft with a flexible nonrotating housing.

The technique used in this analysis is to first transfer across the shaft from the left hand end to the first bearing. The formula is

$$
\left\{ \begin{array}{c} X_S \\ V_S \\ 1 \end{array} \right\}_{B1} = [\, 9 \times 9 \,]_{n_{B1}} \, [\, 9 \times 9 \,]'_{n_{B1}-1} \cdots [\, 9 \times 9 \,]'_1 \, [\, 9 \times 18 \,] \left\{ \begin{array}{c} X_S \\ V_S \\ 1 \\ X_H \\ V_H \\ 1 \end{array} \right\}_{LHS}
\tag{25}
$$

where the 9×18 matrix has the form

$$
[\, 9 \times 18 \,] = [\, I \quad 0 \,]
\tag{26}
$$

where I represents the 9×9 identity matrix. Next, a transfer is made across the housing to the first bearing. Mathematically,

$$
\left\{ \begin{array}{c} X_H \\ V_H \\ 1 \end{array} \right\}_{B1} = [\, 9 \times 9 \,]_{m_{B1}} \, [\, 9 \times 9 \,]'_{m_{B1}-1} \cdots [\, 9 \times 9 \,]'_1 \, [\, 9 \times 18 \,] \left\{ \begin{array}{c} X_S \\ V_S \\ 1 \\ X_H \\ V_H \\ 1 \end{array} \right\}_{LHS}
\tag{27}
$$

where the 9×18 matrix has the form

$$
[\, 9 \times 18 \,] = [\, 0 \quad I \,]
\tag{28}
$$

The resultant matrices of equations (25) and (27) are both 9×18. These two equations can be combined in the form

$$
\left\{ \begin{array}{c} X_S \\ V_S \\ 1 \\ X_H \\ V_H \\ 1 \end{array} \right\}_{B1} = \left[\begin{array}{c} [\, 9 \times 18 \,]_{B1_S} \\ [\, 9 \times 18 \,]_{B1_H} \end{array} \right] \left\{ \begin{array}{c} X_S \\ V_S \\ 1 \\ X_H \\ V_H \\ 1 \end{array} \right\}_{LHS}
\tag{29}
$$

Now, to make the transfer across the bearing, the following equation is used.

$$
\left\{ \begin{array}{c} X_S \\ V_S \\ 1 \\ X_H \\ V_H \\ 1 \end{array} \right\}'_{B1} = \left[\begin{array}{cccccc} [I] & 0 & 0 & 0 & 0 & 0 \\ [K] & [I] & \{F_S\} & [-K] & 0 & 0 \\ 0 & 0 & 1 & 0 & 0 & 0 \\ 0 & 0 & 0 & [I] & 0 & 0 \\ [-K] & 0 & 0 & [K] & [I] & \{F_H\} \\ 0 & 0 & 0 & 0 & 0 & 1 \end{array} \right]_{n_{B1'}} \left\{ \begin{array}{c} X_S \\ V_S \\ 1 \\ X_H \\ V_H \\ 1 \end{array} \right\}_{B1}
\tag{30}
$$

where $[I]$ is the 4×4 identity matrix,

$$[K] = \begin{bmatrix} K_{xx} & K_{xy} & 0 & 0 \\ K_{yx} & K_{yy} & 0 & 0 \\ 0 & 0 & 0 & 0 \\ 0 & 0 & 0 & 0 \end{bmatrix}_{B1} , \tag{31}$$

the stiffness coefficients of the bearing, and 4×1 matrices $\{F_S\}$ and $\{F_H\}$ signify the weight forces of the shaft and housing, respectively. Combining equations (29) and (30) give the relationship of the displacements and forces on the right side of the bearing with those at the left hand end of the shaft and housing.

$$\left\{ \begin{array}{c} X_S \\ V_S \\ 1 \\ X_H \\ V_H \\ 1 \end{array} \right\}'_{B1} = \begin{bmatrix} 18 \times 18 \end{bmatrix}_{n_{B1'}} \begin{bmatrix} 18 \times 18 \end{bmatrix}_{B1} \left\{ \begin{array}{c} X_S \\ V_S \\ 1 \\ X_H \\ V_H \\ 1 \end{array} \right\}_{LHS} \tag{32}$$

Expressed another way, equation (32) becomes

$$\left\{ \begin{array}{c} X_S \\ V_S \\ 1 \\ X_H \\ V_H \\ 1 \end{array} \right\}'_{B1} = \begin{bmatrix} \begin{bmatrix} 9 \times 18 \end{bmatrix}_{B1'_S} \\ \begin{bmatrix} 9 \times 18 \end{bmatrix}_{B1'_H} \end{bmatrix} \left\{ \begin{array}{c} X_S \\ V_S \\ 1 \\ X_H \\ V_H \\ 1 \end{array} \right\}_{LHS} \tag{33}$$

Now, if the next connection is a seal, the transfer up to it is expressed as follows.

$$\left\{ \begin{array}{c} X_S \\ V_S \\ 1 \end{array} \right\}_{SL} = \begin{bmatrix} 9 \times 9 \end{bmatrix}_{n_{SL}} \begin{bmatrix} 9 \times 9 \end{bmatrix}'_{n_{SL}-1} \cdots \begin{bmatrix} 9 \times 18 \end{bmatrix}_{B1'_S} \left\{ \begin{array}{c} X_S \\ V_S \\ 1 \\ X_H \\ V_H \\ 1 \end{array} \right\}_{LHS} \tag{34}$$

$$\left\{ \begin{array}{c} X_H \\ V_H \\ 1 \end{array} \right\}_{SL} = \begin{bmatrix} 9 \times 9 \end{bmatrix}_{m_{SL}} \begin{bmatrix} 9 \times 9 \end{bmatrix}'_{m_{SL}-1} \cdots \begin{bmatrix} 9 \times 18 \end{bmatrix}_{B1'_H} \left\{ \begin{array}{c} X_S \\ V_S \\ 1 \\ X_H \\ V_H \\ 1 \end{array} \right\}_{LHS} \tag{35}$$

A similarity can be seen between equations (34) and (35) and equations (25) and (27). The same procedure is followed for crossing the seal as has been described for the bearing and so forth for passing over other connections.

The housing supports are easily included using the following equation,

$$\left\{ \begin{array}{c} X_H \\ V_H \\ 1 \end{array} \right\}'_{HS} = \left[\begin{array}{ccc} [I] & 0 & 0 \\ [K] & [I] & \{F_H\} \\ 0 & 0 & 1 \end{array} \right]_{n'_{HS}} \left\{ \begin{array}{c} X_H \\ V_H \\ 1 \end{array} \right\}_{HS} \tag{36}$$

where $[I]$ is the 4×4 identity matrix,

$$\{K\} = \left[\begin{array}{cccc} K_x & 0 & 0 & 0 \\ 0 & K_y & 0 & 0 \\ 0 & 0 & K_\theta & 0 \\ 0 & 0 & 0 & K_\phi \end{array} \right]_{BS}, \tag{37}$$

and $\{F_H\}$ is the same as in equation (30).

II.6 Iterative Scheme

An iterative scheme has been developed for calculating the steady state bearing eccentricities to determine the linearized bearing coefficients. This plan will first be developed for the rotor without a housing and then the effect of the housing will be discussed. Upon completion of the transfer across the length of the shaft, the final matrix will have the following form.

$$\left\{ \begin{array}{c} x \\ y \\ \theta \\ \phi \\ V_x \\ V_y \\ M_\theta \\ M_\phi \\ 1 \end{array} \right\}_N = \left[\begin{array}{ccccc} a_{11} & a_{12} & \ldots & a_{18} & a_{19} \\ a_{21} & a_{22} & \ldots & a_{28} & a_{29} \\ \vdots & \vdots & \ddots & \vdots & \vdots \\ a_{81} & a_{82} & \ldots & a_{88} & a_{89} \\ 0 & 0 & \ldots & 0 & 1 \end{array} \right]_N \left\{ \begin{array}{c} x \\ y \\ \theta \\ \phi \\ V_x \\ V_y \\ M_\theta \\ M_\phi \\ 1 \end{array} \right\}_1 \tag{38}$$

The boundary conditions are that the forces and moments at both ends of the shaft are equal to zero. Implementing these conditions results in equation (39).

$$\left\{ \begin{array}{c} 0 \\ 0 \\ 0 \\ 0 \\ 1 \end{array} \right\} = \left[\begin{array}{cccc} a_{51} & \ldots & a_{54} & a_{59} \\ a_{61} & \ldots & a_{64} & a_{69} \\ \vdots & \vdots & \ddots & \vdots \\ 0 & \ldots & 0 & 1 \end{array} \right]_N \left\{ \begin{array}{c} x \\ y \\ \theta \\ \phi \\ 1 \end{array} \right\}_1 \tag{39}$$

Rearranging terms and using simpler notation gives

$$[A]_N \{X\}_1 = -\{F_0\} \tag{40}$$

where F_0 represents the forces and moments a_{59} to a_{89}.

Inspection of equation (40) leads to the idea of a Newton-Raphson type iterative scheme to home in on the steady state bearing eccentricities based on an initial guess of the deflection at station 1. An underlying problem associated with this idea is that the objective is to find the displacements at the bearings, not at the first station. One way to get around this obstacle is to define the displacement at station one in terms of the bearing eccentricity components.

Transferring across the rotor stations up to bearing 1 gives the following matrix equation.

$$
\left\{ \begin{array}{c} x \\ y \\ \theta \\ \phi \\ V_z \\ V_y \\ M_\theta \\ M_\phi \\ 1 \end{array} \right\}_{B1}
=
\begin{bmatrix}
d_{11} & d_{12} & \ldots & d_{18} & d_{19} \\
d_{21} & d_{22} & \ldots & d_{28} & d_{29} \\
\vdots & \vdots & \ddots & \vdots & \vdots \\
d_{81} & d_{82} & \ldots & d_{88} & d_{89} \\
0 & 0 & \ldots & 0 & 1
\end{bmatrix}_{B1}
\left\{ \begin{array}{c} x \\ y \\ \theta \\ \phi \\ V_z \\ V_y \\ M_\theta \\ M_\phi \\ 1 \end{array} \right\}_{1}
\tag{41}
$$

The displacements we want are the bearing eccentricities, namely the x and y displacements of the shaft relative to the bearings at bearing stations 1 and 2.

$$
\left\{ \begin{array}{c} x \\ y \end{array} \right\}_{B1}
=
\begin{bmatrix}
d_{11} & d_{12} & d_{13} & d_{14} \\
d_{21} & d_{22} & d_{23} & d_{24}
\end{bmatrix}_{B1}
\left\{ \begin{array}{c} x \\ y \\ \theta \\ \phi \end{array} \right\}_{1}
+
\left\{ \begin{array}{c} d_{19} \\ d_{29} \end{array} \right\}_{B1}
\tag{42}
$$

Similarly for bearing two, we obtain

$$
\left\{ \begin{array}{c} x \\ y \end{array} \right\}_{B2}
=
\begin{bmatrix}
d_{11} & d_{12} & d_{13} & d_{14} \\
d_{21} & d_{22} & d_{23} & d_{24}
\end{bmatrix}_{B2}
\left\{ \begin{array}{c} x \\ y \\ \theta \\ \phi \end{array} \right\}_{1}
+
\left\{ \begin{array}{c} d_{19} \\ d_{29} \end{array} \right\}_{B2}
\tag{43}
$$

Combining equations (42) and (43) and rearranging terms results in equation (44).

$$
\begin{bmatrix}
d_{11_{B1}} & \cdots & d_{14_{B1}} \\
d_{21_{B1}} & \cdots & d_{24_{B1}} \\
d_{11_{B2}} & \cdots & d_{14_{B2}} \\
d_{21_{B2}} & \cdots & d_{24_{B2}}
\end{bmatrix}
\begin{Bmatrix} x \\ y \\ \theta \\ \phi \end{Bmatrix}_1
=
\begin{Bmatrix}
x_{B1} - d_{19_{B1}} \\
y_{B1} - d_{29_{B1}} \\
x_{B2} - d_{19_{B2}} \\
y_{B2} - d_{29_{B2}}
\end{Bmatrix}
=
\begin{Bmatrix}
x_{B1}^* \\
y_{B1}^* \\
x_{B2}^* \\
y_{B2}^*
\end{Bmatrix}
\tag{44}
$$

By inverting the 4×4 matrix and moving it to the other side, we acquire the displacements at station one in terms of the modified eccentricity components at the bearings.

$$
\begin{Bmatrix} x \\ y \\ \theta \\ \phi \end{Bmatrix}_1
=
\begin{bmatrix}
d_{11_{B1}} & \cdots & d_{14_{B1}} \\
d_{21_{B1}} & \cdots & d_{24_{B1}} \\
d_{11_{B2}} & \cdots & d_{14_{B2}} \\
d_{21_{B2}} & \cdots & d_{24_{B2}}
\end{bmatrix}^{-1}
\begin{Bmatrix}
x_{B1}^* \\
y_{B1}^* \\
x_{B2}^* \\
y_{B2}^*
\end{Bmatrix}
\tag{45}
$$

Substituting the results of equation (45) into equation (40) gives

$$
[A]_N [D]^{-1}
\begin{Bmatrix}
x_{B1}^* \\
y_{B1}^* \\
x_{B2}^* \\
y_{B2}^*
\end{Bmatrix}
+ \{ F_0 \}_N = \{ 0 \}
\tag{46}
$$

Simplifying the equation format and setting it equal to a function $\{ g_{x_B} \}$ (Gajan (1987)) renders equation (47).

$$
\{ g_{x_B} \} = [C] \{ X \}_B + \{ F \}_N
\tag{47}
$$

The solution for $\{X\}_B$ is found when $\{ g_{x_B} \} = \{0\}$. A modified Newton-Raphson iteration process will be used to find the solution. The equations for the Newton-Raphson iteration process are as follows.

$$
\begin{aligned}
\{ X \}_{B_{n+1}} &= \{ X \}_{B_n} + \{ h \}_n \\
[J]_n \{ h \}_n &= - \{ g_{x_B} \}_n
\end{aligned}
\tag{48}
$$

where,

$\{h\}_n$ is the incremental vector and

$[J]_n$ is the Jacobian matrix.

The components of the Jacobian matrix are

$$J_{ik} = \frac{\partial g_i}{\partial x_{B_k}} \tag{49}$$

There are two possible options for transferring across the bearings. One route would be to find the x and y components of the absolute bearing force F_B of equation (7) which are nonlinear functions of the eccentricity, e and attitude angle, ψ (See Figure 6). A hindrance of this course is that when you reach equation (47), $\{F\}$ turns out to be the function of the bearing eccentricities e_x and e_y, rather than $[C]$. The problem with this is that $\{F\}$ would need to be differentiated with respect to $\{X\}_B$ in order to compile the Jacobian matrix. Another option would be to look up the stiffnesses K_{xx}, K_{xy}, K_{yx}, and K_{yy} of the bearings for given eccentricities. Each of these stiffnesses are also functions of the eccentricity ratios and attitude angle, as shown in Figure 9, as well as each of the bearings geometry and oil viscosity. Assuming at least a little error in the linearization of K, it would appear that using the nonlinear force components directly would be somewhat more accurate than calculating the stiffness coefficients. However, if the stiffness coefficients are used, the matrix $[C]$ rather than matrix $\{F\}$ of equation (47) would end up as the function of the bearing displacements. $[C]$ then becomes the Jacobian matrix of equation (48) which leads to an efficient iteration process.

Convergence problems have been experienced when the stiffnesses have been used to calculate both the Jacobian and the function g_{x_B}. Therefore it has been decided to use the benefits of both options. A transfer across the shaft is first made using the x and y components of the nonlinear bearing forces. This solution is then

used to calculate the function $\{g_{x_B}\}$. Another pass is then made using the bearing stiffness coefficients. This solution is then used to calculate the Jacobian matrix $[J]_n$. The incremental vector $\{h\}_n$ can then be found using equation (48). In order to cut down on the time of computation for each pass, the transfers up to bearing 1, between bearings 1 and 2, and following bearing 2 are calculated and stored in 3 respective matrices before any iterations are done. This means that only five matrix multiplications are needed for each pass regardless of how many stations are needed to define the pump.

The iterative scheme for calculating the bearing eccentricities with the housing included follows the same general pattern as for that without. The final transfer equation will take the form of equation (50). Again, the boundary conditions are that the forces and moments at both ends are equal to zero. Applying these conditions simplifies equation (50) to (51).

$$
\begin{Bmatrix}
x_S \\
y_S \\
\theta_S \\
\phi_S \\
V_{x_S} \\
V_{y_S} \\
M_{x_S} \\
1 \\
x_H \\
y_H \\
\theta_H \\
\phi_H \\
V_{x_H} \\
V_{y_H} \\
M_{x_H} \\
M_{y_H} \\
1
\end{Bmatrix}_{RHS}
=
\begin{bmatrix}
a_{11} & a_{12} & \cdots & a_{19} & a_{1,10} & \cdots & a_{1,18} \\
\vdots & \vdots & \ddots & \vdots & \vdots & \ddots & \vdots \\
a_{81} & a_{82} & \cdots & a_{89} & a_{8,10} & \cdots & a_{8,18} \\
0 & 0 & \cdots & 1 & 0 & \cdots & 0 \\
a_{10,1} & a_{10,2} & \cdots & a_{10,9} & a_{10,10} & \cdots & a_{10,18} \\
\vdots & \vdots & \ddots & \vdots & \vdots & \ddots & \vdots \\
a_{17,1} & a_{17,2} & \cdots & a_{17,9} & a_{17,10} & \cdots & a_{17,18} \\
0 & 0 & \cdots & 0 & 0 & \cdots & 1
\end{bmatrix}
\begin{Bmatrix}
x_S \\
y_S \\
\theta_S \\
\phi_S \\
V_{x_S} \\
V_{y_S} \\
M_{x_S} \\
1 \\
x_H \\
y_H \\
\theta_H \\
\phi_H \\
V_{x_H} \\
V_{y_H} \\
M_{x_H} \\
M_{y_H} \\
1
\end{Bmatrix}_{LHS}
\tag{50}
$$

$$
\begin{Bmatrix} 0 \\ 0 \\ 0 \\ 0 \\ 0 \\ 0 \\ 0 \\ 0 \end{Bmatrix} = \begin{bmatrix} a_{51} & \cdots & a_{54} & a_{5,10} & \cdots & a_{5,13} \\ \vdots & \ddots & \vdots & \vdots & \ddots & \vdots \\ a_{81} & \cdots & a_{84} & a_{8,10} & \cdots & a_{8,13} \\ a_{14,1} & \cdots & a_{14,4} & a_{14,10} & \cdots & a_{14,13} \\ \vdots & \ddots & \vdots & \vdots & \ddots & \vdots \\ a_{17,1} & \cdots & a_{17,4} & a_{17,10} & \cdots & a_{17,13} \end{bmatrix} \begin{Bmatrix} x_S \\ y_S \\ \theta_S \\ \phi_S \\ x_H \\ y_H \\ \theta_H \\ \phi_H \end{Bmatrix}_{LHS} +
$$

$$
\begin{Bmatrix} a_{59} \\ \vdots \\ a_{89} \\ a_{14,9} \\ \vdots \\ a_{17,9} \end{Bmatrix} + \begin{Bmatrix} a_{5,18} \\ \vdots \\ a_{8,18} \\ a_{14,18} \\ \vdots \\ a_{17,18} \end{Bmatrix}
\tag{51}
$$

Rearranging terms and using simpler notation gives equation (52).

$$
[A] \begin{Bmatrix} X_S \\ X_H \end{Bmatrix} = - \begin{Bmatrix} F_{0S} \\ F_{0H} \end{Bmatrix}
\tag{52}
$$

Using the same basic procedure as before, the left hand side displacements are found in terms of the displacement at the bearings. First, the x and y components of the bearing displacement are found for bearing 1.

$$
\begin{Bmatrix} x_S \\ y_S \\ x_H \\ y_H \end{Bmatrix}_{B1} = \begin{bmatrix} d_{11} & \cdots & d_{14} & d_{1,10} & \cdots & d_{1,13} \\ d_{21} & \cdots & d_{24} & d_{2,10} & \cdots & d_{2,13} \\ d_{10,1} & \cdots & d_{10,4} & d_{10,10} & \cdots & d_{10,13} \\ d_{11,1} & \cdots & d_{11,4} & d_{11,10} & \cdots & d_{11,13} \end{bmatrix}_{B1} \begin{Bmatrix} x_S \\ y_S \\ \theta_S \\ \phi_S \\ x_H \\ y_H \\ \theta_H \\ \phi_H \end{Bmatrix}_{LHS} + \begin{Bmatrix} x_{0S} \\ y_{0S} \\ x_{0H} \\ y_{0H} \end{Bmatrix}_{B1}
\tag{53}
$$

Similarly for bearing 2,

$$
\begin{Bmatrix} x_S \\ y_S \\ x_H \\ y_H \end{Bmatrix}_{B2} = \begin{bmatrix} d_{11} & \cdots & d_{14} & d_{1,10} & \cdots & d_{1,13} \\ d_{21} & \cdots & d_{24} & d_{2,10} & \cdots & d_{2,13} \\ d_{10,1} & \cdots & d_{10,4} & d_{10,10} & \cdots & d_{10,13} \\ d_{11,1} & \cdots & d_{11,4} & d_{11,10} & \cdots & d_{11,13} \end{bmatrix}_{B2} \begin{Bmatrix} x_S \\ y_S \\ \theta_S \\ \phi_S \\ x_H \\ y_H \\ \theta_H \\ \phi_H \end{Bmatrix}_{LHS} + \begin{Bmatrix} x_{0S} \\ y_{0S} \\ x_{0H} \\ y_{0H} \end{Bmatrix}_{B2}
\tag{54}
$$

Combining equations (53) and (54) and rearranging terms results in equation (55).

$$
\begin{bmatrix} D_{B1} \\ D_{B2} \end{bmatrix}
\begin{Bmatrix} x_S \\ y_S \\ \theta_S \\ \phi_S \\ x_H \\ y_H \\ \theta_H \\ \phi_H \end{Bmatrix}_{LHS}
=
\begin{Bmatrix} x_{S_{B1}} - x_{0S_{B1}} \\ y_{S_{B1}} - y_{0S_{B1}} \\ x_{H_{B1}} - x_{0H_{B1}} \\ y_{H_{B1}} - y_{0H_{B1}} \\ x_{S_{B2}} - x_{0S_{B2}} \\ y_{S_{B2}} - y_{0S_{B2}} \\ x_{H_{B2}} - x_{0H_{B2}} \\ y_{H_{B2}} - y_{0H_{B2}} \end{Bmatrix}
=
\begin{Bmatrix} x^*_{S_{B1}} \\ y^*_{S_{B1}} \\ x^*_{H_{B1}} \\ y^*_{H_{B1}} \\ x^*_{S_{B2}} \\ y^*_{S_{B2}} \\ x^*_{H_{B2}} \\ y^*_{H_{B2}} \end{Bmatrix}
\tag{55}
$$

By inverting the 8 × 8 matrix, and moving it to the other side, the displacements at the left hand side are found in terms of the x and y displacements at the bearings.

$$
\begin{Bmatrix} x_S \\ y_S \\ \theta_S \\ \phi_S \\ x_H \\ y_H \\ \theta_H \\ \phi_H \end{Bmatrix}_{LHS}
= [\,D\,]^{-1}
\begin{Bmatrix} x^*_{S_{B1}} \\ y^*_{S_{B1}} \\ x^*_{H_{B1}} \\ y^*_{H_{B1}} \\ x^*_{S_{B2}} \\ y^*_{S_{B2}} \\ x^*_{H_{B2}} \\ y^*_{H_{B2}} \end{Bmatrix}
\tag{56}
$$

Substituting equation (56) into equation (52) gives

$$
[A]\,[D]^{-1}
\begin{Bmatrix} x^*_{S_{B1}} \\ y^*_{S_{B1}} \\ x^*_{H_{B1}} \\ y^*_{H_{B1}} \\ x^*_{S_{B2}} \\ y^*_{S_{B2}} \\ x^*_{H_{B2}} \\ y^*_{H_{B2}} \end{Bmatrix}
+ \{\,F_0\,\} = \{\,0\,\}
\tag{57}
$$

The same modified Newton-Raphson iterative scheme is used here to find the x and y displacements at the bearings. The eccentricity components are solved using the following equations.

$$
e_{x_{B1}} = x_{S_{B1}} - x_{H_{B1}}
$$

$$
e_{y_{B1}} = y_{S_{B1}} - y_{H_{B1}}
$$

$$
e_{x_{B2}} = x_{S_{B2}} - x_{H_{B2}}
$$

$$
e_{y_{B2}} = y_{S_{B2}} - y_{H_{B2}}
$$

$$\tag{58}$$

It has been found that convergence generally occurs within 50 iterations. Initial guesses in each quadrant have been tested using a simple model and each converged to the same eccentricities. Convergence problems have been experienced for cases at low speeds where the ratio of the eccentricity to the clearance is close to unity.

CHAPTER III

THEORETICAL DEVELOPMENT (DYNAMIC)

The formulation of the transfer matrices for the dynamic analysis is basically the same as that for the static analysis as derived in chapter II. The main difference is that the inertia and damping terms must now be considered at the lumped mass stations and the static terms W_x and W_y are neglected. Referring to Figure 16, the transfer equations are derived for the y–z plane across the point mass. Summing the forces in the y_n direction and the moments in the ϕ_n direction, we obtain

$$\sum F_{y_n} = m_n \ddot{y}_n \Rightarrow V'_{y_n} - V_{y_n} + \Gamma_{y_n} = m_n \ddot{y}_n$$

$$\sum M_{\phi_n} = J_{T_n} \ddot{\phi}_n + \Omega \dot{\theta}_n J_{P_n} \Rightarrow M'_{\phi_n} - M_{\phi_n} + \Gamma_{\phi_n} = J_{T_n} \ddot{\phi}_n + \Omega \dot{\theta}_n J_{P_n}$$

(59)

Rearranging terms results in the following equations.

$$V'_{y_n} = m_n \ddot{y}_n + V_{y_n} - \Gamma_{y_n}$$

$$M'_{\phi_n} = J_{T_n} \ddot{\phi}_n + \Omega \dot{\theta}_n J_{P_n} + M_{\phi_n} - \Gamma_{\phi_n}$$

(60)

Similarly, referring to Figure 17, the transfer equations are found for the x-z plane across the lumped mass.

$$V'_{x_n} = m_n \ddot{x}_n + V_{x_n} - \Gamma_{x_n}$$

$$M'_{\theta_n} = J_{T_n} \ddot{\theta}_n - \Omega \dot{\phi}_n J_{P_n} + M_{\theta_n} - \Gamma_{\theta_n}$$

(61)
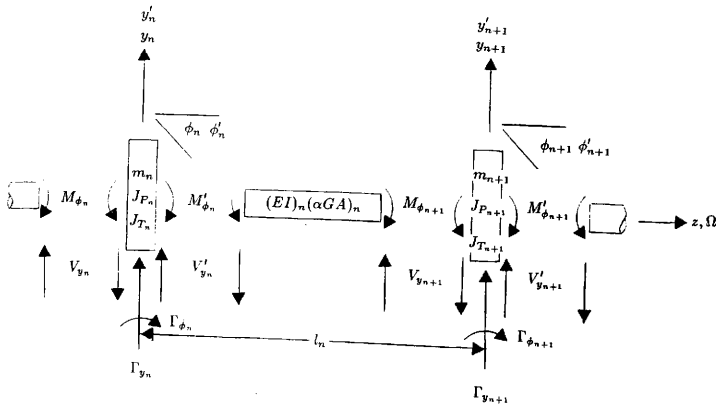
Figure 16.   Discrete shaft model for dynamic analysis in y–z plane.
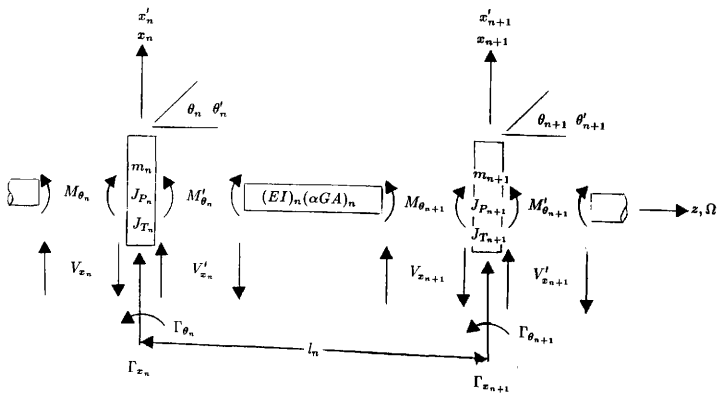
Figure 17.   Discrete shaft model for dynamic analysis in x-z plane.

For the dynamic analysis, complex notation is used, and assuming harmonic motion, the displacements and forces are

$$x_n = Re\{\bar{x}_n e^{st}\}$$

$$y_n = Re\{\bar{y}_n e^{st}\}$$

$$\theta_n = Re\{\bar{\theta}_n e^{st}\}$$

$$\phi_n = Re\{\bar{\phi}_n e^{st}\}$$

$$V_{x_n} = Re\{\bar{V}_{x_n} e^{st}\}$$

$$V_{y_n} = Re\{\bar{V}_{y_n} e^{st}\}$$

$$M_{\theta_n} = Re\{\bar{M}_{\theta_n} e^{st}\}$$

$$M_{\phi_n} = Re\{\bar{M}_{\phi_n} e^{st}\},$$

(62)

and the complex frequency s is denoted as

$$s = \lambda + i\omega \tag{63}$$

where λ is the damping exponent and ω is the damped natural frequency (Lund (1973)). The logarithmic decrement δ is calculated as

$$\delta = -\frac{2\pi\lambda}{\omega} \tag{64}$$

and gives an indication of the stability of a particular mode. When δ is negative, the mode is considered unstable, while if δ is greater than 1, the mode is deemed well damped (Lund (1973)).

. Since the static terms are not considered in the dynamic analysis, Γ now expresses the forces and moments due to the stiffness, damping, and inertia terms of the seals as follows,

$$\Gamma_{z_n} = -K_{xx}x - K_{xy}y - K_{x\theta}\theta - K_{x\phi}\phi$$
$$- C_{xx}\dot{x} - C_{xy}\dot{y} - C_{x\theta}\dot{\theta} - C_{x\phi}\dot{\phi}$$
$$- M_{xx}\ddot{x} - M_{xy}\ddot{y} - M_{x\theta}\ddot{\theta} - M_{x\phi}\ddot{\phi}$$

$$\Gamma_{y_n} = -K_{yx}x - K_{yy}y - K_{y\theta}\theta - K_{y\phi}\phi$$
$$- C_{yx}\dot{x} - C_{yy}\dot{y} - C_{y\theta}\dot{\theta} - C_{y\phi}\dot{\phi}$$
$$- M_{yx}\ddot{x} - M_{yy}\ddot{y} - M_{y\theta}\ddot{\theta} - M_{y\phi}\ddot{\phi}$$

$$\Gamma_{\theta_n} = -K_{\theta x}x - K_{\theta y}y - K_{\theta\theta}\theta - K_{\theta\phi}\phi$$
$$- C_{\theta x}\dot{x} - C_{\theta y}\dot{y} - C_{\theta\theta}\dot{\theta} - C_{\theta\phi}\dot{\phi}$$
$$- M_{\theta x}\ddot{x} - M_{\theta y}\ddot{y} - M_{\theta\theta}\ddot{\theta} - M_{\theta\phi}\ddot{\phi}$$

$$\Gamma_{\phi_n} = -K_{\phi x}x - K_{\phi y}y - K_{\phi\theta}\theta - K_{\phi\phi}\phi$$
$$- C_{\phi x}\dot{x} - C_{\phi y}\dot{y} - C_{\phi\theta}\dot{\theta} - C_{\phi\phi}\dot{\phi}$$
$$- M_{\phi x}\ddot{x} - M_{\phi y}\ddot{y} - M_{\phi\theta}\ddot{\theta} - M_{\phi\phi}\ddot{\phi}$$

$$(65)$$

and the stiffness and damping terms of the bearings as shown below.

$$\Gamma_{z_n} = -K_{xx}x - K_{xy}y - C_{xx}\dot{x} - C_{xy}\dot{y}$$
$$\Gamma_{y_n} = -K_{yx}x - K_{yy}y - C_{yx}\dot{x} - C_{yy}\dot{y}$$

$$(66)$$

Equation (65) can now be substituted into equations (59) - (61) and expressed in matrix notation as

$$
\left\{ \begin{array}{c} V_x \\ V_y \\ M_\theta \\ M_\phi \end{array} \right\}_n' = \left\{ \begin{array}{c} V_x \\ V_y \\ M_\theta \\ M_\phi \end{array} \right\}_n + \left[\begin{array}{cccc} s^2 m & 0 & 0 & 0 \\ 0 & s^2 m & 0 & 0 \\ 0 & 0 & s^2 J_T & -s\Omega J_P \\ 0 & 0 & s\Omega J_P & s^2 J_T \end{array} \right] \left\{ \begin{array}{c} x \\ y \\ \theta \\ \phi \end{array} \right\}_n
$$
$$
+ \left[\begin{array}{cccc} s^2 M_{xx} & s^2 M_{xy} & s^2 M_{x\theta} & s^2 M_{x\phi} \\ s^2 M_{yx} & s^2 M_{yy} & s^2 M_{y\theta} & s^2 M_{y\phi} \\ s^2 M_{\theta x} & s^2 M_{\theta y} & s^2 M_{\theta\theta} & s^2 M_{\theta\phi} \\ s^2 M_{\phi x} & s^2 M_{\phi y} & s^2 M_{\phi\theta} & s^2 M_{\phi\phi} \end{array} \right]_n \left\{ \begin{array}{c} x \\ y \\ \theta \\ \phi \end{array} \right\}_n
$$
$$
+ \left[\begin{array}{cccc} sC_{xx} & sC_{xy} & sC_{x\theta} & sC_{x\phi} \\ sC_{yx} & sC_{yy} & sC_{y\theta} & sC_{y\phi} \\ sC_{\theta x} & sC_{\theta y} & sC_{\theta\theta} & sC_{\theta\phi} \\ sC_{\phi x} & sC_{\phi y} & sC_{\phi\theta} & sC_{\phi\phi} \end{array} \right]_n \left\{ \begin{array}{c} x \\ y \\ \theta \\ \phi \end{array} \right\}_n
$$
$$
+ \left[\begin{array}{cccc} K_{xx} & K_{xy} & K_{x\theta} & K_{x\phi} \\ K_{yx} & K_{yy} & K_{y\theta} & K_{y\phi} \\ K_{\theta x} & K_{\theta y} & K_{\theta\theta} & K_{\theta\phi} \\ K_{\phi x} & K_{\phi y} & K_{\phi\theta} & K_{\phi\phi} \end{array} \right]_n \left\{ \begin{array}{c} x \\ y \\ \theta \\ \phi \end{array} \right\}_n
\tag{67}
$$

for a seal station and equation (66) can be substituted into the same equations and expressed in matrix notation as

$$
\left\{ \begin{array}{c} V_x \\ V_y \\ M_\theta \\ M_\phi \end{array} \right\}_n' = \left\{ \begin{array}{c} V_x \\ V_y \\ M_\theta \\ M_\phi \end{array} \right\}_n + \left[\begin{array}{cccc} s^2 m & 0 & 0 & 0 \\ 0 & s^2 m & 0 & 0 \\ 0 & 0 & s^2 J_T & -s\Omega J_P \\ 0 & 0 & s\Omega J_P & s^2 J_T \end{array} \right] \left\{ \begin{array}{c} x \\ y \\ \theta \\ \phi \end{array} \right\}_n
$$
$$
+ \left[\begin{array}{cccc} sC_{xx} + K_{xx} & sC_{xy} + K_{xy} & 0 & 0 \\ sC_{yx} + K_{yx} & sC_{yy} - K_{yy} & 0 & 0 \\ 0 & 0 & 0 & 0 \\ 0 & 0 & 0 & 0 \end{array} \right] \left\{ \begin{array}{c} x \\ y \\ \theta \\ \phi \end{array} \right\}_n
\tag{68}
$$

for a bearing station.

The displacements across the lumped mass as well as the transfer across the massless beam are the same as for the static case (see equations (3)-(6)).

III.1   Critical Speed Calculations

        The final equation for the one spool case will have the following form where the 8×8 matrix is full of polynomials (Murphy (1984)).

$$
\left\{
\begin{array}{c}
x \\
y \\
\theta \\
\phi \\
V_x \\
V_y \\
M_\theta \\
M_\phi
\end{array}
\right\}_N
=
\left[
\begin{array}{cc}
D_{11} & D_{12} \\
D_{21} & D_{22}
\end{array}
\right]_N
\left\{
\begin{array}{c}
x \\
y \\
\theta \\
\phi \\
V_x \\
V_y \\
M_\theta \\
M_\phi
\end{array}
\right\}_1
\tag{69}
$$

The boundary conditions for this analysis are that the forces and moments on both ends of the shaft are zero. Applying these conditions produces equation (70).

$$
\left\{
\begin{array}{c}
0 \\
0 \\
0 \\
0
\end{array}
\right\}
= [\, D_{21} \,]_N
\left\{
\begin{array}{c}
x \\
y \\
\theta \\
\phi
\end{array}
\right\}_1
\tag{70}
$$

For the non-trivial solution, the determinant of $[D_{21}]_N$ must be equal to zero. Expanding the determinant results in a polynomial of degree $8 * N + 2$. The roots of this polynomial are the complex eigenvalues described in the previous section.

$$
s = \lambda + i\omega
\tag{71}
$$

The solution is obtained using a 3–stage algorithm using quadratic iteration developed by Jenkins and Traub (1970) implemented in the routine RPOLY (Jenkins (1975)).

III.2   Modified Ricatti Technique

        Horner and Pilkey (1978) described a new transfer matrix technique for analyzing structures called the Riccati transfer matrix method. The Ricatti transformation "converts a numerically unstable two-point boundary value problem into a numerically stable initial value problem" (Horner and Pilkey (1978)). Songyuan

(1985) used this method to increase the efficiency of the Murphy-Vance technique for calculating the damped critical speeds, stability, and mode shapes of rotor-bearing systems. This strategy is formulated as follows (Songyuan (1985)).

First, in order to keep the size of the equations small in the following explanation, it is necessary to define two matrix variables.

$$\{X\} = \left\{\begin{array}{c} x \\ y \\ \theta \\ \phi \end{array}\right\} \text{, and } \{V\} = \left\{\begin{array}{c} V_x \\ V_y \\ M_\theta \\ M_\phi \end{array}\right\} \tag{72}$$

The transfers across a lumped mass and a beam element from left to right can be expressed as

$$\left\{\begin{array}{c} X \\ V \end{array}\right\}_i' = \left[\begin{array}{cc} I & 0 \\ K & I \end{array}\right]_i \left\{\begin{array}{c} X \\ V \end{array}\right\}_i \tag{73}$$

$$\left\{\begin{array}{c} X \\ V \end{array}\right\}_{i+1} = \left[\begin{array}{cc} L & B \\ 0 & L^T \end{array}\right]_i \left\{\begin{array}{c} X \\ V \end{array}\right\}_i' \tag{74}$$

Expanding equations (73) and (74) give

$$V_i' = K_i X_i + V_i \tag{75}$$

$$X_i' = X_i \tag{76}$$

$$V_{i+1} = L_i^T V_i' \tag{77}$$

$$X_{i+1} = L_i X_i' + B_i V_i' \tag{78}$$

Next, define

$$V_i = Q_i X_i \tag{79}$$

$$V_i' = Q_i' X_i' \tag{80}$$

Substituting equation (79) into equation (75) gives

$$V_i' = (K_i + Q_i) X_i \tag{81}$$

Taking this equation, along with equations (76) and (80), it can be seen that

$$Q_i' = Q_i + K_i \tag{82}$$

Now, placing equation (80) into (78) gives

$$X_{i+1} = (L_i + B_i Q_i') X_i' \tag{83}$$

or

$$X_i' = (L_i + B_i Q_i')^{-1} X_{i+1} \tag{84}$$

Using this equation in A.9 and substituting into equation (77) renders

$$V_{i+1} = L_i^T Q_i' (L_i + B_i Q_i')^{-1} X_{i+1} \tag{85}$$

Considering this equation and (79), it can be observed that

$$Q_{i+1} = L_i^T Q_i' (L_i + B_i Q_i')^{-1} \tag{86}$$

Equations (82) and (86) are the recursive relationships for Q_i' and Q_{i+1} described in Horner and Pilkey's paper (1978). Inverting a matrix in the midst of the Murphy-Vance technique is no easy task and would greatly decrease the efficiency if it had to be done at each station as it would be using equation (86). Songyuan (1985) developed a strategy by which no inversion is necessary.

Combining equations (82) and (86) gives

$$Q_i' = L_{i-1}^T Q_{i-1}' (L_{i-1} + B_{i-1} Q_{i-1}')^{-1} + K_i \tag{87}$$

Now define

$$T_{i-1} = L_{i-1} + B_{i-1}Q'_{i-1} \tag{88}$$

and substitute into equation (87) yielding

$$Q'_i = L_{i-1}^T Q'_{i-1} T_{i-1}^{-1} + K_i \tag{89}$$

Next define

$$R_i = \sum_{j=1}^{i-1} T_j = T_{i-1}T_{i-2}\ldots T_1 \tag{90}$$

and

$$P_i = Q'_i R_i \tag{91}$$

Multiplying equation (89) into (90)A.19 gives

$$P_i = L_{i-1}^T Q'_{i-1} T_{i-1}^{-1} R_i + K_i R_i$$

$$= L_{i-1}^T Q'_{i-1} T_{i-1}^{-1} T_{i-1}T_{i-2}\ldots T_1 + K_i R_i$$

$$= L_{i-1}^T Q'_{i-1} R_{i-1} + K_i R_i \tag{92}$$

or

$$P_i = L_{i-1}^T P_{i-1} + K_i R_i \tag{93}$$

Multiplying equation (88) into R_{i-1} renders

$$T_{i-1}R_{i-1} = L_{i-1}R_{i-1} + B_{i-1}Q'_{i-1}R_{i-1} \tag{94}$$

or

$$R_i = L_{i-1}R_{i-1} + B_{i-1}P_{i-1} \tag{95}$$

Equations (93) and (95) are now the recursive relationships for P_i and R_i. Considering equations (75), (76), and (80), it can be seen that

$$Q'_1 = K_1 \tag{96}$$

In order to keep equation (90) meaningful, start with R_1 equal to the identity matrix. It follows from this and equation (96) that P_1 equals K_1.

This technique can be extended to include the housing. The equations will first be set up across a connection station, either a bearing or a seal. The transfer across the lumped mass and beam element can be expressed as follows.

$$\left\{ \begin{array}{c} X_S \\ X_H \\ V_S \\ V_H \end{array} \right\}'_i = \left[\begin{array}{cccc} I & 0 & 0 & 0 \\ 0 & I & 0 & 0 \\ m_S + K & -K & I & 0 \\ -K & m_H + K & 0 & I \end{array} \right]_i \left\{ \begin{array}{c} X_S \\ X_H \\ V_S \\ V_H \end{array} \right\}_i \tag{97}$$

$$\left\{ \begin{array}{c} X_S \\ X_H \\ V_S \\ V_H \end{array} \right\}_{i+1} = \left[\begin{array}{cccc} L_S & 0 & B_S & 0 \\ 0 & L_H & 0 & B_H \\ 0 & 0 & L_S^T & 0 \\ 0 & 0 & 0 & L_H^T \end{array} \right]_i \left\{ \begin{array}{c} X_S \\ X_H \\ V_S \\ V_H \end{array} \right\}'_i \tag{98}$$

If it is defined that

$$\{ X \} = \left\{ \begin{array}{c} X_S \\ X_H \end{array} \right\}, and \ \{ V \} = \left\{ \begin{array}{c} V_S \\ V_H \end{array} \right\} \tag{99}$$

then equations (97) and (98) can be represented by (73) and (74), respectively. The previous explanation now holds for the present situation except that the matrix variables now depict 8×8 matrices instead of 4×4 and the vector variables now portray

8×1 vectors instead of 4×1. The recursive relationships for R_i and P_i are now

$$\begin{bmatrix} R_{11} & R_{12} \\ R_{21} & R_{22} \end{bmatrix}_i = \begin{bmatrix} L_S & 0 \\ 0 & L_H \end{bmatrix}_{i-1} \begin{bmatrix} R_{11} & R_{12} \\ R_{21} & R_{22} \end{bmatrix}_{i-1}$$

$$+ \begin{bmatrix} B_S & 0 \\ 0 & B_H \end{bmatrix}_{i-1} \begin{bmatrix} P_{11} & P_{12} \\ P_{21} & P_{22} \end{bmatrix}_{i-1}$$

$$= \begin{bmatrix} L_S R_{11} & L_S R_{12} \\ L_H R_{21} & L_H R_{22} \end{bmatrix}_{i-1} + \begin{bmatrix} H_S P_{11} & B_S P_{12} \\ B_H P_{21} & B_H P_{22} \end{bmatrix}_{i-1} \qquad (100)$$

$$\begin{bmatrix} P_{11} & P_{12} \\ P_{21} & P_{22} \end{bmatrix}_i = \begin{bmatrix} L_S^T & 0 \\ 0 & L_H^T \end{bmatrix}_{i-1} \begin{bmatrix} P_{11} & P_{12} \\ P_{21} & P_{22} \end{bmatrix}_{i-1}$$

$$+ \begin{bmatrix} m_S + K & -K \\ -K & m_H + K \end{bmatrix}_i \begin{bmatrix} R_{11} & R_{12} \\ R_{21} & R_{22} \end{bmatrix}_i$$

$$= \begin{bmatrix} L_S^T P_{11} & L_S^T P_{12} \\ L_H^T P_{21} & L_H^T P_{22} \end{bmatrix}_{i-1}$$

$$+ \begin{bmatrix} (m_S + K)R_{11} - K R_{21} & (m_S + K)R_{12} - K R_{22} \\ -K R_{11} + (m_H + K)R_{21} & -K R_{12} + (m_H + K)R_{22} \end{bmatrix}_i \quad (101)$$

For transferring across a portion of the shaft and housing up to a connection, equation (100) is the same and (101) becomes

$$\begin{bmatrix} P_{11} & P_{12} \\ P_{21} & P_{22} \end{bmatrix}_i = \begin{bmatrix} L_S^T P_{11} & L_S^T P_{12} \\ L_H^T P_{21} & L_H^T P_{22} \end{bmatrix}_{i-1} + \begin{bmatrix} m_S R_{11} & m_S R_{12} \\ m_H R_{21} & m_H R_{22} \end{bmatrix}_i \qquad (102)$$

It can be seen that the top halves of equations (100) and (102) have no housing terms and the bottom halves contain no shaft terms. Therefore, the top halves of these equations can be used to transfer across the shaft up to and following any connection. Similarly, the bottom halves can be used to transfer across the housing up to and following any connection. In order to cross a connection, equation (100) is found up to the connection for the shaft and housing. Equation (101) can now be calculated and used to cross over the seal or bearing station. Starting the transfer, R_1 is again set to the identity, while

$$P_1 = \begin{bmatrix} m_S & 0 \\ 0 & m_H \end{bmatrix}_1 \qquad (103)$$

if the first station is not a connection. Otherwise,

$$P_1 = \begin{bmatrix} m_S + K & -K \\ -K & m_H + K \end{bmatrix}_1 \tag{104}$$

III.3 Scaling Technique

In order to combat problems with numerical overflow and underflow, as well as speed up the time of execution, the scaling and condensation procedure described in Murphy (1984) has also been used for this project. A brief description of the procedure is given for clarity. The first step is to scale the polynomial by making the following substitution

$$s = f\bar{s} \tag{105}$$

where f is an arbitrary constant. Using this equation, the unscaled polynomial

$$P = a_0 + a_1 s^1 + a_2 s^2 + a_3 s^3 + \ldots + a_n s^n \tag{106}$$

becomes

$$P = a_0 + a_1 f \bar{s}^1 + a_2 f \bar{s}^2 + a_3 f \bar{s}^3 + \ldots + a_n f \bar{s}^n \tag{107}$$

or

$$P = \bar{a}_0 + \bar{a}_1 \bar{s}^1 + \bar{a}_2 \bar{s}^2 + \bar{a}_3 \bar{s}^3 + \ldots + \bar{a}_n \bar{s}^n \tag{108}$$

The coefficient f is chosen to try to make all the coefficients $\bar{a}_1 \ldots \bar{a}_n$ as close to $\bar{a}_0$ as possible. This way when all the coefficients are divided by $\bar{a}_0$, they are all as near unity as feasible, thus diminishing the probability of numerical underflow and overflow.

Another consequence of this scaling procedure is that if f is chosen as the highest magnitude of s that we are interested in, then the higher order terms of the polynomial can be neglected. This can be seen by considering equation (105), where if f is the largest magnitude of the eigenvalue

$$|s| = \sqrt{\lambda^2 + \omega^2}$$

of interest, then all $|\bar{s}|$'s of interest will be less than one. Therefore, if the higher order coefficients of equation (108) are much smaller than the lower order coefficients,

$$\bar{a}_j << \bar{a}_i \ , j > i$$

then the product of the roots and coefficients are even smaller.

$$\bar{a}_j \bar{s}^j <<< \bar{a}_i \bar{s}^i \tag{109}$$

Thus, the higher order terms can be neglected. Murphy developed an algorithm by which these higher terms can be eliminated as the transfer is made along the shaft, thereby greatly speeding up the time of execution without losing any accuracy.

III.4   Guyan Reduction for Two–Spool Case

The final equation for the two spool case will have the following form,

$$
\begin{Bmatrix}
x_S \\
y_S \\
\theta_S \\
\phi_S \\
V_{x_S} \\
V_{y_S} \\
M_{\theta_S} \\
M_{\phi_S} \\
x_H \\
y_H \\
\theta_H \\
\phi_H \\
V_{x_H} \\
V_{y_H} \\
M_{\theta_H} \\
M_{\phi_H}
\end{Bmatrix}_{RHS}
=
\begin{bmatrix}
D_{11} & D_{12} & \ldots & D_{18} \\
D_{21} & D_{22} & \ldots & D_{28} \\
\vdots & \vdots & \ddots & \vdots \\
D_{81} & D_{82} & \ldots & D_{88}
\end{bmatrix}
\begin{Bmatrix}
x_S \\
y_S \\
\theta_S \\
\phi_S \\
V_{x_S} \\
V_{y_S} \\
M_{\theta_S} \\
M_{\phi_S} \\
x_H \\
y_H \\
\theta_H \\
\phi_H \\
V_{x_H} \\
V_{y_H} \\
M_{\theta_H} \\
M_{\phi_H}
\end{Bmatrix}_{LHS}
\tag{110}
$$

with each D_{ii} a 2×2 matrix. As with the one spool case, the boundary conditions are that the forces and moments at both ends of the shaft and housing are zero. Applying these conditions gives

$$\begin{Bmatrix} 0 \\ 0 \\ 0 \\ 0 \end{Bmatrix} = \begin{bmatrix} D_{31} & D_{32} & D_{35} & D_{36} \\ D_{41} & D_{42} & D_{45} & D_{46} \\ D_{71} & D_{72} & D_{75} & D_{76} \\ D_{81} & D_{82} & D_{85} & D_{86} \end{bmatrix} \begin{Bmatrix} X_S \\ \Theta_S \\ X_H \\ \Theta_H \end{Bmatrix}_{LHS} \tag{111}$$

For the non-trivial solution, the determinant of the 8×8 matrix must be equal to zero. The most time consuming aspect of Murphy's method is in calculating the determinant of the matrix in equation (70). For the one spool case, the determinant is for a 4×4 matrix. For the two spool case, the matrix is doubled in size. In calculating determinants the standard way, $n! - 1$ additions and/or subtractions are needed, and $(n - 1) * n!$ multiplications are needed (Kolman (1986)). For a 4×4 matrix, this results in 23 summations and 72 products, while for an 8×8 matrix, 40319 additions and 282240 multiplications are required. These numbers do not even take into account that we are dealing with matrices full of huge polynomials, but the relative size can be seen.

In order to lower the number of multiplications and additions for the two spool case, the Guyan reduction technique (Guyan (1965)) is used to reduce the size of the final matrix to a 4×4. Equation (111) is rewritten as

$$\begin{Bmatrix} 0 \\ 0 \\ 0 \\ 0 \end{Bmatrix} = \begin{bmatrix} D_{31} & D_{35} & D_{32} & D_{36} \\ D_{41} & D_{45} & D_{42} & D_{46} \\ D_{71} & D_{75} & D_{72} & D_{76} \\ D_{81} & D_{85} & D_{82} & D_{86} \end{bmatrix} \begin{Bmatrix} X_S \\ X_H \\ \Theta_S \\ \Theta_H \end{Bmatrix}_{LHS} , \tag{112}$$

or more simply,

$$\begin{Bmatrix} 0 \\ 0 \end{Bmatrix} = \begin{bmatrix} B_{11} & B_{12} \\ B_{21} & B_{22} \end{bmatrix} \begin{Bmatrix} X \\ \Theta \end{Bmatrix} , \tag{113}$$

where each B_{ii} is a 4×4 matrix.

Equation (113) can be represented by the two formulas

$$[B_{11}] \{X\} + [B_{12}] \{\Theta\} = \{0\} \tag{114}$$

$$[B_{21}] \{X\} + [B_{22}] \{\Theta\} = \{0\} \tag{115}$$

Using equation (115), the angular displacement of the shaft and housing can be put in terms of the radial displacement of the shaft and housing.

$$\{\Theta\} = -[B_{22}]^{-1} [B_{21}] \{X\} \tag{116}$$

Substituting this into equation (114) gives

$$[B_{11}] \{X\} - [B_{12}] [B_{22}]^{-1} [B_{21}] \{X\} = \{0\} \tag{117}$$

or

$$\left[[B_{11}] - [B_{12}] [B_{22}]^{-1} [B_{21}] \right] \{X\} = \{0\} \tag{118}$$

Now, the non-trivial solution is found when the determinant of the 4×4 matrix of equation (118) is solved. Using this technique requires 250 additions and/or subtractions and 320 multiplications without taking into account the polynomial factor. This is a reduction of two orders of magnitude for additions and three orders of magnitude for the number of multiplications in finding the eigenvalues, i.e., damped natural frequencies and damping exponents.

A difficulty lies in the calculation of the inverse of the 4×4 matrix $[B_{22}]$ of equation (118). The method used in the calculation of the inverse is

$$[B_{22}]^{-1} = \frac{adj[B_{22}]}{det[B_{22}]}$$

where $adj[B_{22}]$ is the adjoint of $[B_{22}]$ and $det[B_{22}]$ is the polynomial determinant of $[B_{22}]$ of some degree m. This denominator polynomial was then multiplied into the matrix $[B_{11}]$ of equation (118) in order to put the whole equation over a common denominator. Since the right hand side of the equation is $\{0\}$, the denominator was then merely crossed out of the equation. Now when the determinant is calculated, the polynomial obtained is $3m$ orders greater than what is required for the system, thus producing $3m$ extra roots. These extra roots are actually the roots for the polynomial determinant of $[B_{22}]$.

An analysis has been performed in order to determine the range of roots that can be divided out without destroying the accuracy of the computed eigenvalues. The model is a simply supported stacked steel beam system as shown in Figure 18. The inner and outer connections have stiffnesses in the x and y directions of 10E16 lb/in^2. These large stiffnesses are used in order to decouple the beam's effect on each other. The lower beam represents a housing with an outside radius of 1 inch, inside radius of

0.7 inches, and length of 24 inches. The upper beam portrays a solid rotor of radius 0.5 inches and length 24 inches.

The first five natural frequencies of each beam are calculated as a single spool rotor using PATH and are compared with theoretical values computed using Harris and Crede (1976) constants for a simple hinged–hinged beam model. Results are tabulated in Table 1.

The only roots that need to be divided out are those less than or equal to the maximum frequency of interest. Therefore, using the scale factor f described in the previous section, the number of roots divided out is steadily increased. Table 2 displays the eigenvalues computed using scale factors of 210,000 rpm and 330,000 rpm along with the number of roots divided out. Using a scale factor of 210,000 rpm, sixty denominator roots are divided out. The eigenvalues calculated are exact up to the cutoff frequency which has an error of 0.1%. Employing a scale factor of 330,000 rpm, 84 denominator roots are divided out. This results in a maximum error of 17.5% for the first housing eigenvalue and an error of 9.7% for the second rotor eigenvalue. The other values match well with the single–spool values, though with an additional eigenvalue computed in the ninth slot. Based on this analysis, PATH gives a warning message if more than 70 denominator roots need to be purged.

III.5   Mode Shape Calculations

The mode shapes are calculated by first finding the relative displacements at the far left station. Rewriting equation (70),

$$\begin{bmatrix} C_{11} & C_{12} & C_{13} & C_{14} \\ C_{21} & C_{22} & C_{23} & C_{24} \\ C_{31} & C_{32} & C_{33} & C_{44} \\ C_{41} & C_{42} & C_{43} & C_{44} \end{bmatrix}_N \begin{Bmatrix} x \\ y \\ \theta \\ \phi \end{Bmatrix}_1 = \begin{Bmatrix} 0 \\ 0 \\ 0 \\ 0 \end{Bmatrix} \qquad (119)$$
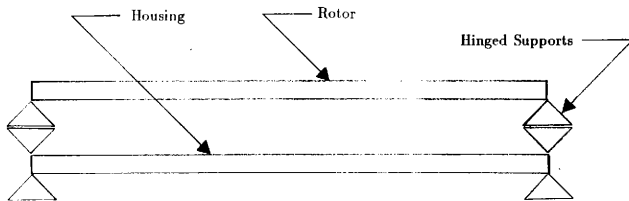
Figure 18. Simply supported stacked beam system.

Table 1. Natural Frequencies using Single Spool Model (rad/sec)

Rotor		Housing	
Theory	PATH (25 stations)	Theory	Path (14 stations)
863.5	862.5	2108.	2096.
3456.	3428.	8437.	8248.
7778.	7689.	18988.	18075.
13824.	13559.	33748.	31027.
21610.	20965.	52757.	46455.

Table 2. Eigenvalue Accuracy Comparison (rad/sec)

$f = 210,000 rpm$	$f = 330,000 rpm$	single–spool
862.5	862.6	862.5
2096.	2463.	2096.
3428.	3771.	3428.
7689.	7669.	7689.
8248.	8269.	8248.
13559.	13559.	13559.
18075.	18075.	18075.
20995.	20968.	20965.
-	29676.	-
-	31020.	31027.
60 roots	84 roots	

and setting x_1 to $1. + i0$ results in the following set of three simultaneous equations.

$$\begin{bmatrix} C_{22} & C_{23} & C_{24} \\ C_{32} & C_{33} & C_{44} \\ C_{42} & C_{43} & C_{44} \end{bmatrix}_N \begin{Bmatrix} y \\ \theta \\ \phi \end{Bmatrix}_1 = - \begin{Bmatrix} C_{21} \\ C_{31} \\ C_{41} \end{Bmatrix} \tag{120}$$

Equation (120) can now be solved for the modal displacements y_1, θ_1, and ϕ_1 corresponding to a particular eigenvalue. A transfer is again made across the shaft using

these values and the same eigenvalue to find the modal displacements at each station. The other mode shapes are found in the same manner using the other complex eigenvalues.

It should be kept in mind that the elements in the 4×4 matrix of equation (119) are polynomials of sometimes large degree n. An efficient strategy of evaluating these polynomials is Horner's rule (Forsythe, et al. (1977)), depicted in the following equation.

$$P(s) = a_{n+1} + s(a_n + s(a_{n-1} + s(\ldots(a_2 + a_1 s)\ldots))) \qquad (121)$$

If damping is included in the model, the modal displacements x, y, θ, and ϕ will be complex. Letting

$$\tilde{x}_i = x_{ri} + i x_{ci}$$
$$\tilde{y}_i = y_{ri} + i y_{ci} \qquad (122)$$

then

$$x_i = x_{ri} \cos \omega_d t - x_{ci} \sin \omega_d t$$
$$y_i = y_{ri} \cos \omega_d t - y_{ci} \sin \omega_d t \qquad (123)$$

which represents an ellipse in the x-y plane (Barrett, et al. (1976)). The mode shapes are therefore represented by the semi-major and semi-minor axes, a and b, of the ellipse, and the orientation angle ψ as shown in Figure 19 (Barrett, et al. (1976)).

$$a_i = [\, 0.5(x_{ri}^2 + x_{ci}^2 + y_{ri}^2 + y_{ci}^2)$$
$$+ \sqrt{0.25(x_{ri}^2 + x_{ci}^2 - y_{ri}^2 - y_{ci}^2)^2 + (x_{ri}y_{ri} + x_{ci}y_{ci})^2} \,]^{\frac{1}{2}}$$
$$b_i = \frac{x_{ri}y_{ri} - x_{ci}y_{ci}}{a_i} \qquad (124)$$
$$\psi_i = \frac{1}{2} \tan^{-1}[\, \frac{2(x_{ri}y_{ri} + x_{ci}y_{ci})}{(x_{ri}^2 + x_{ci}^2 - y_{ri}^2 - y_{ci}^2)} \,]$$

The mode shapes for the housing are calculated in basically the same manner except that equation (119) would be a rewrite of equation (111) instead of (70).

III.6   Response to Imbalance

The solution for the imbalance response of a flexible rotor using transfer matrices has been explained by Lund and Orcutt (1967) and more extensively by Kleespies (1986). Considering Figures 20 and 21, and summing forces in the x and y directions for the nth lumped mass station gives

$$\sum F_{y_n} = m\ddot{y} \Rightarrow V'_{y_n} - V_{y_n} + \Gamma_{y_n} + m\omega^2 e_n \sin(\omega t + \phi) = m\ddot{y}$$

$$\sum F_{z_n} = m\ddot{x} \Rightarrow V'_{z_n} - V_{z_n} + \Gamma_{z_n} + m\omega^2 e_n \cos(\omega t + \phi) = m\ddot{x}$$

$$(125)$$

or in complex notation

$$\bar{V}'_{y_n} = -m\omega^2 \bar{y} + \bar{V}_{y_n} - \bar{\Gamma}_{y_n} - m\omega^2 e_n (\cos\alpha_n + i\sin\alpha_n)$$

$$\bar{V}'_{z_n} = -m\omega^2 \bar{x} + \bar{V}_{z_n} - \bar{\Gamma}_{z_n} - m\omega^2 e_n (\sin\alpha_n - i\cos\alpha_n)$$

$$(126)$$

where e_n is the CG eccentricity for the nth station and α is given as the offset CG angle from some specific line of reference. The CG angle α is used to differentiate orientations of imbalances along the shaft. The other equations for the moments, displacements, and forces across the lumped mass and massless beam are the same as for the previously mentioned dynamic analysis. Now, though, the transfer matrix is of order 9×9 for the one spool case and 17×17 with the housing included.

For the one spool case, the final equation will look like

$$\begin{Bmatrix} x \\ y \\ \theta \\ \phi \\ V_x \\ V_y \\ M_\theta \\ M_\phi \\ 1 \end{Bmatrix}_N = \begin{bmatrix} C_{11} & C_{12} & \dots & C_{19} \\ \vdots & \vdots & \ddots & \vdots \\ C_{81} & C_{82} & \dots & C_{89} \\ 0 & 0 & \dots & 1 \end{bmatrix}_N \begin{Bmatrix} x \\ y \\ \theta \\ \phi \\ V_x \\ V_y \\ M_\theta \\ M_\phi \\ 1 \end{Bmatrix}_1 \qquad (127)$$
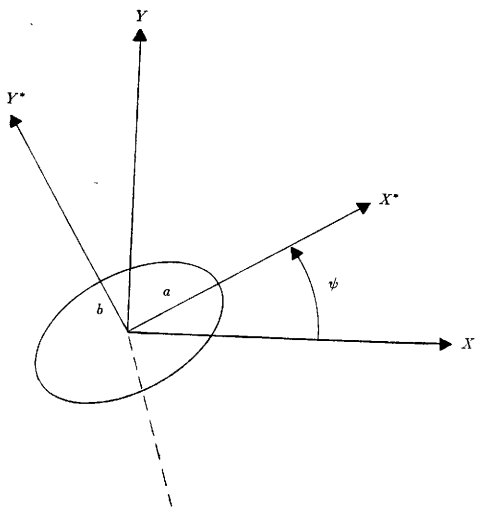
Figure 19.   Elliptical orbit schematic.
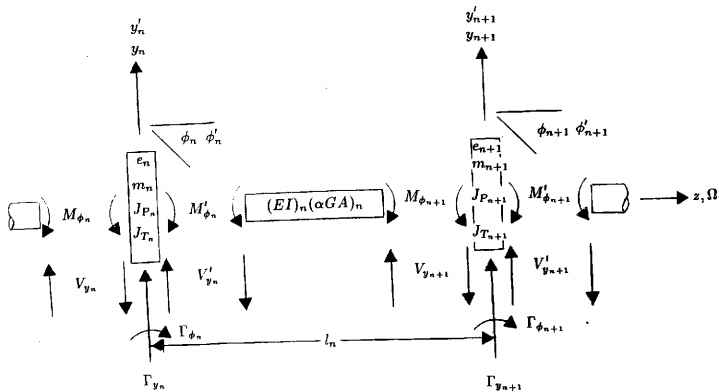
Figure 20.   Discrete shaft model for imbalance analysis in y–z plane.
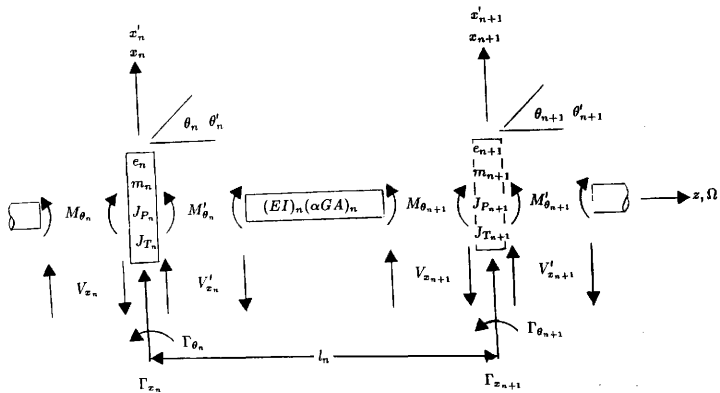
Figure 21. Discrete shaft model for imbalance analysis in x–z plane.

Applying the boundary conditions of zero forces and moments at both ends of the shaft give

$$\begin{Bmatrix} 0 \\ 0 \\ 0 \\ 0 \end{Bmatrix} = \begin{bmatrix} C_{51} & C_{52} & C_{53} & C_{54} \\ C_{61} & C_{62} & C_{63} & C_{64} \\ C_{71} & C_{72} & C_{73} & C_{74} \\ C_{81} & C_{82} & C_{83} & C_{84} \end{bmatrix}_N \begin{Bmatrix} x \\ y \\ \theta \\ \phi \end{Bmatrix}_1 + \begin{Bmatrix} C_{59} \\ C_{69} \\ C_{79} \\ C_{89} \end{Bmatrix}_N \tag{128}$$

or

$$\begin{bmatrix} C_{51} & C_{52} & C_{53} & C_{54} \\ C_{61} & C_{62} & C_{63} & C_{64} \\ C_{71} & C_{72} & C_{73} & C_{74} \\ C_{81} & C_{82} & C_{83} & C_{84} \end{bmatrix}_N \begin{Bmatrix} x \\ y \\ \theta \\ \phi \end{Bmatrix}_1 = - \begin{Bmatrix} C_{59} \\ C_{69} \\ C_{79} \\ C_{89} \end{Bmatrix}_N \tag{129}$$

which is a set of four simultaneous equations. Equation (129) can be solved for the displacements at station 1 and these values can be used to transfer across the shaft again to find the displacements at all the other stations. The values of the displacements are complex and are represented in the same manner as the mode shapes of section 3.2. The response with the housing included is found in the same manner, except the matrices are larger.

Murphy described in his dissertation a method by which the boundary conditions at the left end of the rotor

$$V_{x_1} = V_{y_1} = M_{\theta_1} = M_{\phi_1} = 0$$

could be taken into account at the beginning of the transfer, thus saving a great deal of computation time. His algorithm has been modified here for the imbalance response. First, rewrite the final system transfer matrix of equation (127) as

$$\begin{bmatrix} [UL] & \{UR\} \\ [LL] & \{LR\} \\ 0 & 1 \end{bmatrix}_N = \begin{bmatrix} [UL] & [UM] & \{UR\} \\ [LL] & [LM] & \{LR\} \\ 0 & 0 & 1 \end{bmatrix}_N \begin{bmatrix} [I] & 0 \\ 0 & 0 \\ 0 & 1 \end{bmatrix} \tag{130}$$

where $[UL]$, $[LL]$, $[UM]$, and $[LM]$ are 4×4 submatrices, $\{UR\}$ and $\{LR\}$ represent 4×1 vectors, $[I]$ is the 4×4 identity matrix, and 1 is the 1×1 identity matrix.

Equation (130) can be rewritten as

$$\begin{bmatrix} [UL] & \{UR\} \\ [LL] & \{LR\} \\ 0 & 1 \end{bmatrix}_N = [\ ]_N [\ ]_{N-1} \cdots [\ ]_2 [\ ]_1 \begin{bmatrix} [U] \\ \{D\} \\ i \end{bmatrix} \qquad (131)$$

where the little matrices $[\ ]_N [\ ]_{N-1} \cdots [\ ]_2 [\ ]_1$ signify the transfer through the stations along the rotor. When multiplying across, start with $[U] = [I]$ and $[D] = 0$. When the 9×9 matrix of station 1 is multiplied into the 9×5 matrix, it will produce another 9×5 matrix. This sequence is then repeated until the left hand side of equation (131) is constructed. Equation (129) is then the same as

$$[\,LL\,]_N \begin{Bmatrix} x \\ y \\ \theta \\ \phi \end{Bmatrix}_1 = -[\,LR\,]_N \qquad (132)$$

The two-spool case can be represented in the same manner. First, the final system transfer matrix is represented by

$$\begin{bmatrix} UL_1 & UM_1 & UM_{R1} \\ LL_1 & LM_1 & LM_{R1} \\ 0 & 1 & 0 \\ UL_2 & UM_2 & UM_{R2} \\ LL_2 & LM_2 & LM_{R2} \end{bmatrix}_{RHS} =$$

$$\begin{bmatrix} UL_1 & UM_{L1} & UM_1 & UM_{R1} & UR_1 \\ LL_1 & LM_{L1} & LM_1 & LM_{R1} & LR_1 \\ 0 & 0 & 1 & 0 & 0 \\ UL_2 & UM_{L2} & UM_2 & UM_{R2} & UR_2 \\ LL_2 & LM_{L2} & LM_2 & LM_{R2} & LR_2 \end{bmatrix}_{RHS} \begin{bmatrix} I & 0 & 0 \\ 0 & 0 & 0 \\ 0 & 1 & 0 \\ 0 & 0 & I \\ 0 & 0 & 0 \end{bmatrix} \qquad (133)$$

where UM_1, LM_1, UM_2, and LM_2 are 4×1 matrices, I is the 4×4 identity matrix, 1 is the 1×1 identity matrix, and the rest are 4×4 matrices. The upper 9×9 portion of the large matrix of equation (133) is the same as that of equation (130). Since the housing does not rotate, it does not need the extra column for a mass imbalance. Equation (134) corresponds to equation (132) with a housing.

$$\begin{bmatrix} LL_1 & LM_{R1} \\ LL_2 & LM_{R2} \end{bmatrix}_{RHS} \begin{Bmatrix} x_S \\ y_S \\ \theta_S \\ \phi_S \\ x_H \\ y_H \\ \theta_H \\ \phi_H \end{Bmatrix}_{LHS} = -\begin{bmatrix} LM_1 \\ LM_2 \end{bmatrix}_{RHS} \qquad (134)$$

CHAPTER IV

PROGRAM VERIFICATION

Most of the options available for the one spool case are also available in Gajan's program APDS (Analysis of Pump Dynamic Systems). Therefore, a comparison has been made using his program and thesis to verify this program. A time comparison is also made.

IV.1 Static Equilibrium Verification

Figure 22 (Gajan (1987)) shows a 3-bearing shaft with two disks previously modelled by Nikolajsen (1978), and by Gajan (1987) as a 2-bearing shaft with a midspan seal. The model also includes seal (bearing) misalignment and bearing support flexibility. The same model used by Gajan has been analyzed using the transfer matrix program and the 3 results are compared below in Table 3.

The results for the eccentricity ratio match fairly well for all three programs. The differences between APDS and PATH could be due to APDS adding mass for the bearing supports while PATH does not. PATH takes the bearing support mass into account with the housing option. Another possibility is that APDS uses a finite element distributed model for the shaft while PATH uses a transfer matrix lumped mass model. Nikolajsen's disparity is "considered to be primarily due to replacing a nonlinear bearing with a linear seal at the center station" (Gajan (1987)).
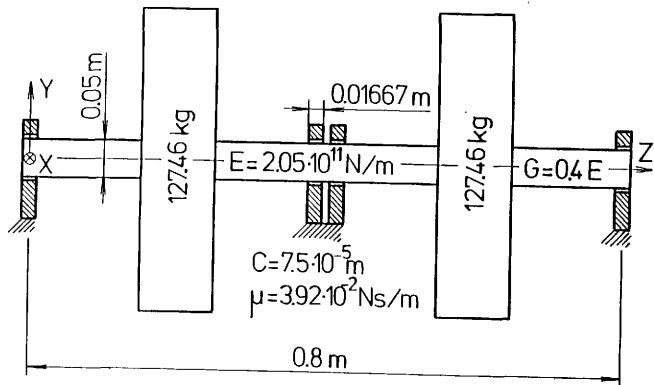
Figure 22. Three bearing shaft with two disks.

Table 3. Equilibrium Comparison

	Nikolajsen	APDS	PATH
Ecc. Ratio			
x-comp.	.442	.436	.424
y-comp.	.609	.585	.613
Total	.752	.731	.746

IV.2   Dynamic Verification - Single Spool

In Gajan's thesis, he analyzed an eleven stage centrifugal pump built by Pacific Pumps and previously analyzed by Engineering Dynamics Incorporated (EDI). Figure 23 (Gajan (1987)) is a schematic of the analyzed pump. A natural frequency calculation has been made for the pump and the results are compared in Table 4 with EDI's analysis, Gajan's analysis, and the current analysis using program PATH.

As can be seen, the two programs APDS and PATH compare almost exactly. The biggest difference is the time of execution, where PATH is approximately one order of magnitude faster than APDS. During this run, each program also calculated the first six precessional mode shapes and all modes for the real roots. The precessional modes are shown in Figures 24, 25, and 26.

A six case study was also carried out by Gajan (1987) in order to discern the effects of the extra stiffness, damping, and inertia seal coefficients and the static analysis. For this project, four cases are carried out and compared to results from APDS. Case 1 uses 2×2 stiffness and damping coefficient matrices for the seals and bearings. Case 2 extends case 1 by adding a 2×2 inertia coefficient matrix for the
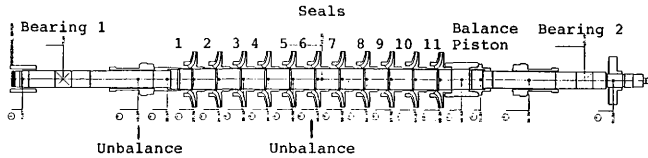
Figure 23. Eleven stage centrifugal pump.

Table 4. Natural Frequency Calculations for an 11 Stage Pump

	EDI	APDS	PATH
Natural Frequency	3959.	3994.	3994.
Log Decrement	-1.8	-1.72	-1.73
Natural Frequency	4997.	5081.	5081.
Log Decrement	3.53	3.62	3.61
Natural Frequency	5007.	5049.	5047.
Log Decrement	1.1	1.11	1.11
Natural Frequency	–	5491.	5494.
Log Decrement	–	14.2	14.2
Natural Frequency	9304.	9530.	9513.
Log Decrement	.97	.98	.98
Natural Frequency	9777.	9902.	9884.
Log Decrement	.58	.65	.65
CPU Time		9:59.84	1:10.64

seals. Case 3 enlarges the seal stiffness, damping and inertia coefficient matrices to 4×4's, thus adding moment effects of the seals. Case 4 is the same as 3 with a static analysis for determining the bearing coefficients.

Campbell diagrams are used to contrast the four cases as displayed in Figures 27, 28, 29, and 30. These diagrams are plots of the damped natural frequencies versus the running speed. The log decrements are shown for data points for every 1000 rpm running speed. A line, $y = x$, is also shown on each plot. Wherever this line crosses the mode line, the speed represents a potential critical speed. If the log decrement is greater than one, the mode is considered well damped. If the log decrement is negative, the mode is unstable. Usually each mode will consist of a

MODE SHAPE PLOT

EDI TEST CASE
GAJAN THESIS, APPENDIX III, PG 74
RUNNING SPEED =   0.0000E+00 RPM
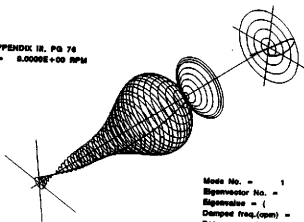
Mode No. =   1
Eigenvector No. =   1
Eigenvalue = (114.860   418.279)
Damped freq.(cpm) =   3994.289
Rotor speed (rpm) =   0.0000
UNSTABLE MODE

MODE SHAPE PLOT

EDI TEST CASE
GAJAN THESIS, APPENDIX III, PG 75
RUNNING SPEED =   0.0000E+00 RPM
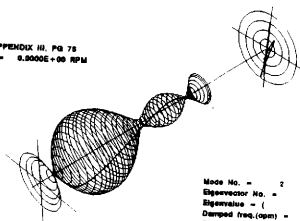
Mode No. =   2
Eigenvector No. =   2
Eigenvalue = (-93.270   528.321)
Damped freq.(cpm) =   5046.090
Rotor speed (rpm) =   0.0000
STABLE MODE

Figure 24.   EDI test case precessional modes 1 and 2.

MODE SHAPE PLOT

EDI TEST CASE
GAJAN THESIS, APPENDIX III, PG 76
RUNNING SPEED =   0.0000E+00 RPM

Mode No. =   3
Eigenvector No. =   3
Eigenvalue = (-308.055   531.987)
Damped freq.(cpm) =   5079.913
Rotor speed (rpm) =   0.0000
STABLE MODE

MODE SHAPE PLOT

EDI TEST CASE
GAJAN THESIS, APPENDIX III, PG 76
RUNNING SPEED =   0.0000E+00 RPM

Mode No. =   4
Eigenvector No. =   4
Eigenvalue = (-1300.164   576.121)
Damped freq.(cpm) =   5501.546
Rotor speed (rpm) =   0.0000
STABLE MODE

Figure 25.   EDI test case precessional modes 3 and 4.
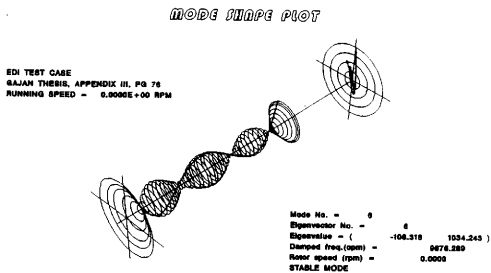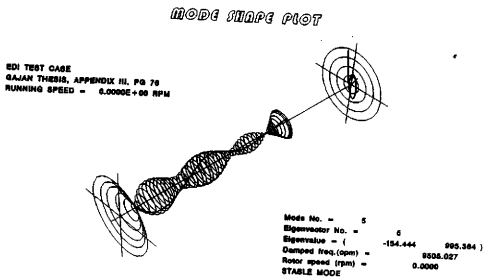
Figure 26. EDI test case precessional modes 5 and 6.

forward precessional and a backward precessional mode, identified on the diagrams by the letters 'F' and 'B', respectively (Lund (1973)). Table 5 discloses the potential critical speeds and log decrements for each case.

Table 5. Critical Speeds and Log Decrements

	Critical Speed	Log Decrement
Case 1		
	4943.	.79
	4926.	2.6
Case 2		
	1461.	9.7
	2689.	8.1
	4690.	.82
	4656.	2.5
Case 3		
	940.	6.4
	1228.	7.9
	5003.	.99
	5266.	2.4
Case 4		
	5016.	1.0
	5350.	2.4

Mode shapes for the four test cases have been plotted and are shown in Figure 31 for a shaft speed of 5000 rpm. This speed is chosen since it is the approximate critical speed for each case as displayed in Table 5. Plots are taken for the forward whirl mode closest to the running speed. For the response to imbalance, two one ounce-inch unbalances are placed 90 degrees out of phase at station numbers 5 and 19 as in Gajan's thesis. Figure 32 displays the displacement of station 19 versus

CAMPBELL DIAGRAM
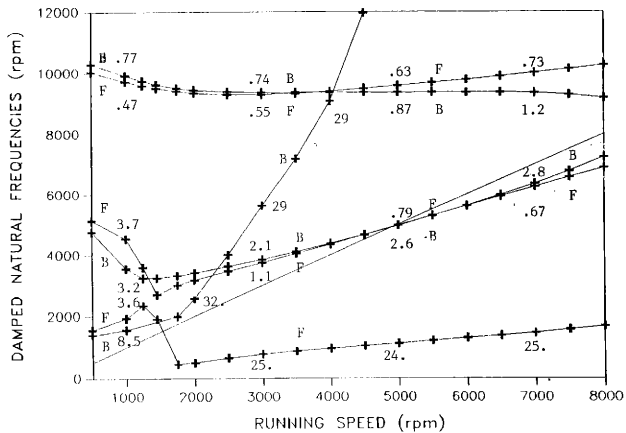
CASE 1

Figure 27. Campbell diagram — case 1.

Figure 28. Campbell diagram — case 2.
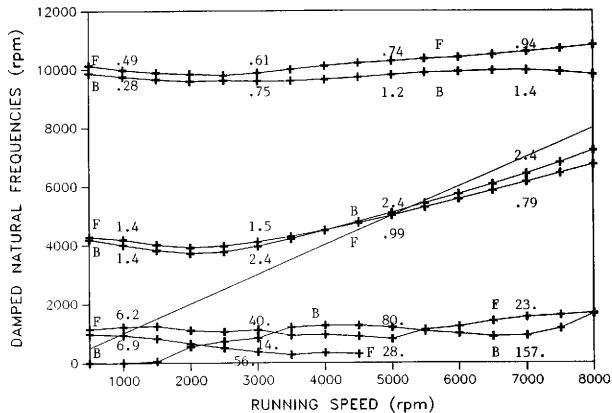
Figure 29. Campbell diagram — case 3.

CAMPBELL DIAGRAM
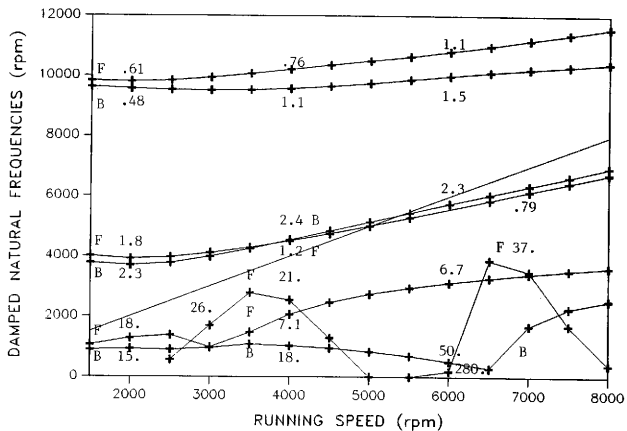
Case 4

Figure 30. Campbell diagram — case 4.

the running speed. Station 19 is one of the stations where an unbalance is located. Figures 33 and 34 exhibit the reactions of the bearings to the imbalance versus the running speed.

Case 1 was computed using APDS and the values computed match PATH nearly perfectly. A Campbell Diagram has also been calculated for case 3 using APDS. It is shown in Figure 35. The numbers computed did not exactly match those computed using PATH. The reason for this discrepancy is not understood, but could be caused by the different methods used to account for the inertia coefficients. PATH uses a lumped mass transfer matrix model, while APDS uses a finite element distributed mass model.

IV.3   Dynamic Verification - Rotor with Flexible Housing

In order to verify the correctness of the pump housing option, an analysis has been made of a simple rotor. The model is of a Centritech lab rotor on damped asymmetric bearings defined and analyzed in the JAZZ user's manual (Murphy and Vance (1982)). Two cases have been analyzed. The first analysis is with a near mass-less housing and supports designed to produce the same stiffness used by Murphy when put in series. This is done by aligning the intershaft bearings with the bearing supports and giving them stiffness and damping coefficients that are twice the magnitude of the coefficients used in the JAZZ analysis. Figure 36 shows schematics of the two models. As shown, the housing has been modeled to follow the shape of the rotor as its diameter changes. Eigenvalues calculated for this system are compared
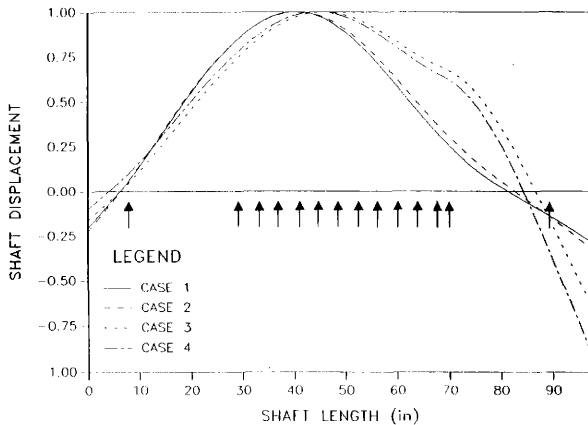
Figure 31. Mode shapes — 5000 rpm.

RESPONSE TO IMBALANCE

Station 19 Displacement vs. Speed

LEGEND

—— CASE 1
– – CASE 2
·· – CASE 3
—·· CASE 4

DISPLACEMENT (mils)

0.08
0.07
0.06
0.05
0.04
0.03
0.02
0.01
0.00

RUNNING SPEED (rpm)

1000 2000 3000 4000 5000 6000 7000 8000
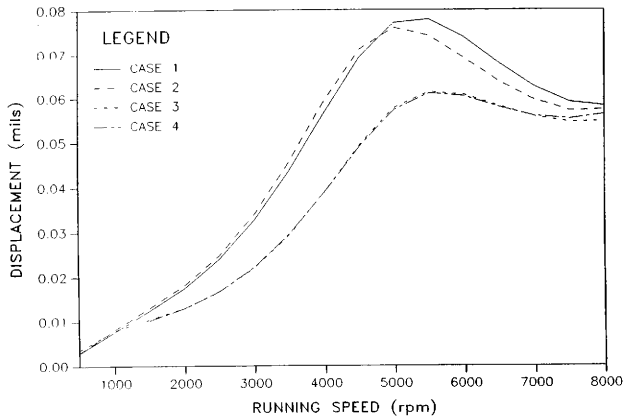
Figure 32.   Station 19 response to imbalance.

RESPONSE TO IMBALANCE

Left Bearing Reaction vs. Speed

LEGEND
—— CASE 1
— — CASE 2
· · · CASE 3
—·— CASE 4

BEARING REACTION (lbs)

RUNNING SPEED (rpm)
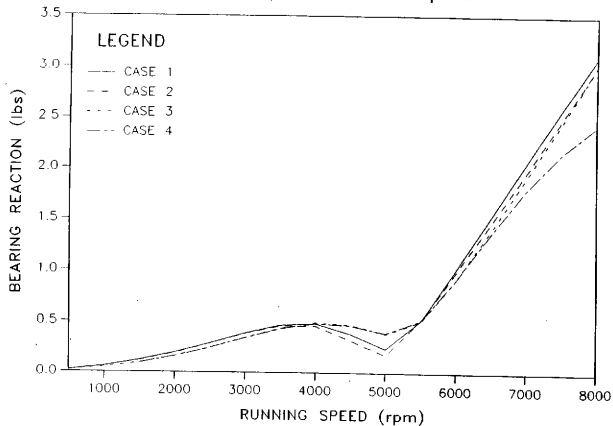
Figure 33. Left bearing reaction to imbalance.

RESPONSE TO IMBALANCE

Right Bearing Reaction vs. Speed
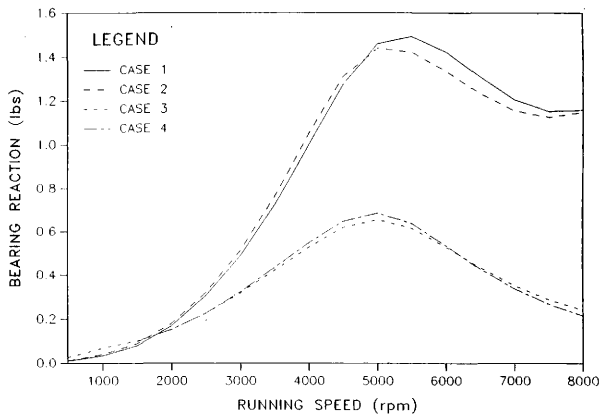
Figure 34. Right bearing reaction to imbalance.
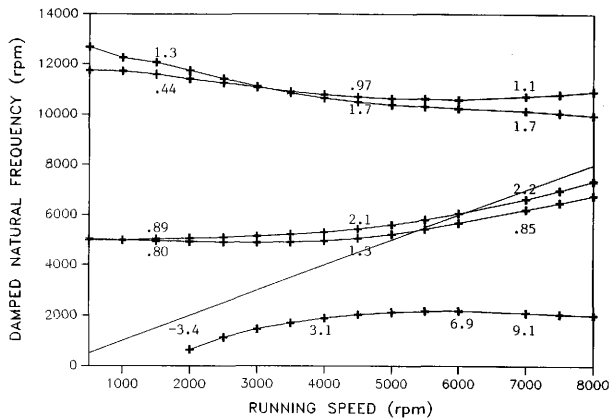
Figure 35. Campbell diagram - Case 3 using program APDS.

with Murphy's without the housing. The second analysis is made with a steel flexible housing and is compared with values generated using STAB2V2 (Li and Gunter (1978)), a linear stability analysis program for dual rotor systems. Both cases are with the rotor running at a speed of 4688 rpm.

Table 6 displays the values generated with the first run. PATH values match frequencies generated using JAZZ with a maximum error of 0.9%.

The values corresponding to the second analysis are shown in Table 7. The mode shapes for the rotor and housing are displayed in Figures 37, 38, 39, 40, 41, 42, 43, and 44 along with the corresponding mode plots for the rotor as computed using JAZZ. The eigenvalues computed using each program match each other within a maximum difference of 1.9%. Comparing Table 6 with Table 7, it would appear that the 4th and 5th frequencies result from the inclusion of the housing. The mode shapes for these frequencies, as displayed in Figures 40 and 41 lend support to this notion. The desirability of using the Murphy–Vance polynomial technique is affirmed here by the existence of the second eigenvalue computed using PATH, which is missed using STAB2V2. These modes appear reasonable and the rotor modes corresponding to the eigenvalues computed for the single spool model match the two dimensional mode plots from Murphy and Vance (1982). PATH's flexible housing option is now considered verified.
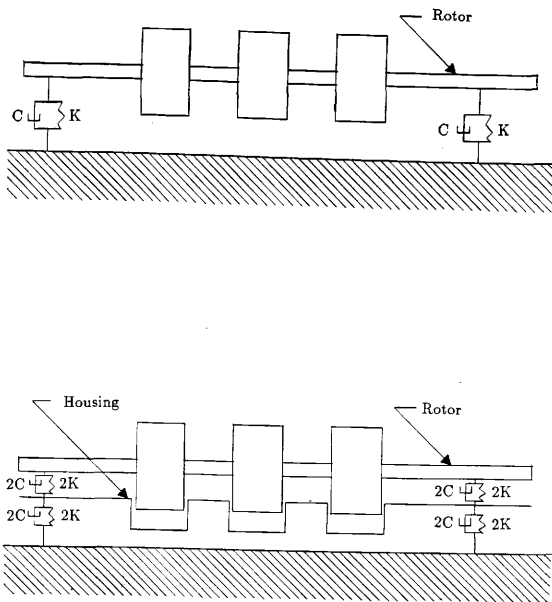
Figure 36. Centritech lab rotor on damped asymmetric bearings with and without a housing.

Table 6. Natural Frequency Comparison with Near Massless Flexible Housing

JAZZ		PATH	
Log. Dec.	Nat'l Freq. (rpm)	Log. Dec.	Nat'l Freq. (rpm)
0.548	1860.8	0.550	1860.0
0.139	1933.2	0.138	1932.4
0.333	7497.1	0.334	7506.7
0.351	8056.8	0.352	8062.6
0.258	15617.	0.259	15660.
0.203	17568.	0.205	17607.

Table 7. Natural Frequency Comparison with Steel Flexible Housing

STAB2V2		PATH	
Log. Dec.	Nat'l Freq. (rpm)	Log. Dec.	Nat'l Freq. (rpm)
0.557	1859.	0.559	1865.
-	-	0.140	1936.
0.332	7499.	0.334	7567.
0.355	8054.	0.359	8145.
0.095	8741.	0.096	8748.
0.236	8773.	0.238	8780.
0.259	15625.	0.262	15857.
0.203	17567.	0.209	17907.
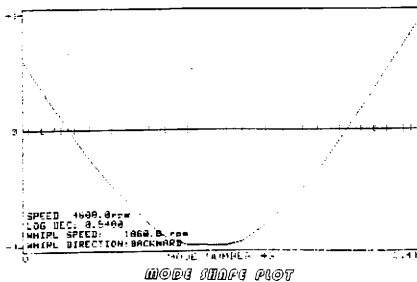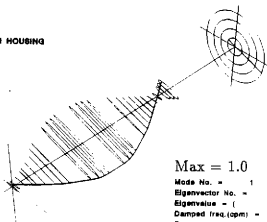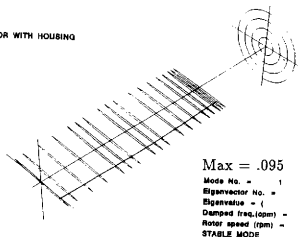
Figure 37. Centritech lab rotor with flexible housing model mode 1.
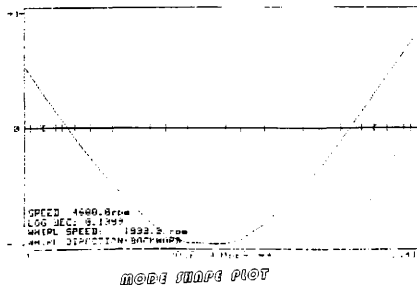
MODE SHAPE PLOT

CENTRITECH ROTOR WITH HOUSING
ROTOR MODE

Max = 1.0

Mode No. =   2
Eigenvector No. =   2
Eigenvalue = (-4.508   202.766)
Damped freq.(cpm) =   1936.289
Rotor speed (rpm) =   4688.0000
STABLE MODE

MODE SHAPE PLOT

CENTRITECH ROTOR WITH HOUSING
HOUSING MODE

Max = .037
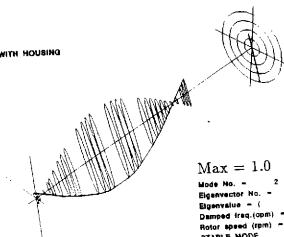
Mode No. =   2
Eigenvector No. =   2
Eigenvalue = (-4.508   202.766)
Damped freq.(cpm) =   1936.289
Rotor speed (rpm) =   4688.0000
STABLE MODE
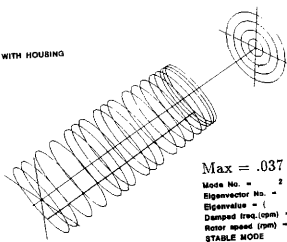
Figure 38.   Centritech lab rotor with flexible housing model mode 2.
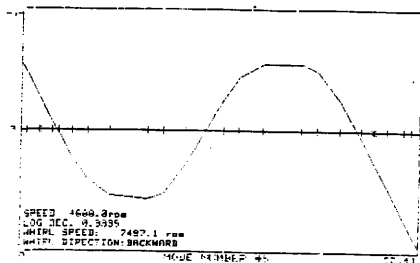
SPEED: 4688.0rpm
LOG DEC: 0.3935
WHIRL SPEED: 7497.1 rpm
WHIRL DIRECTION: BACKWARD

MODE NUMBER 4.

CENTRITECH ROTOR WITH HOUSING
ROTOR MODE

Max = 1.0

Mode No. =   3
Eigenvector No. =   3
Eigenvalue =   (-42.141   792.373)
Damped freq. (cpm) =   7586.601
Rotor speed (rpm) =   4888.0000
STABLE MODE

CENTRITECH ROTOR WITH HOUSING
HOUSING MODE

Max = .18
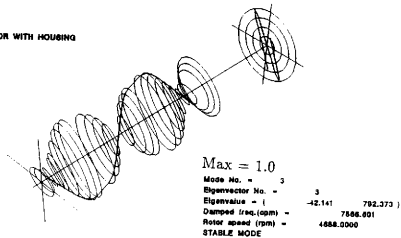
Mode No. =   3
Eigenvector No. =   3
Eigenvalue =   (-42.141   792.373)
Damped freq. (cpm) =   7586.601
Rotor speed (rpm) =   4888.0000
STABLE MODE
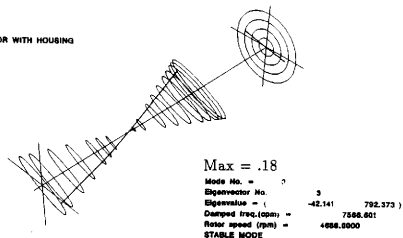
Figure 39.   Centritech lab rotor with flexible housing model mode 3.

CENTRITECH ROTOR WITH HOUSING
ROTOR MODE

Max = 1.0

Mode No. =   4
Eigenvector No. =   4
Eigenvalue = (-46.664   852.8)
Damped freq.(cpm) =   8144.501
Rotor speed (rpm) =   4666.0000
STABLE MODE

CENTRITECH ROTOR WITH HOUSING
HOUSING MODE

Max = .19

Mode No. =   4
Eigenvector No. =   4
Eigenvalue = (-46.664   852.866)
Damped freq.(cpm) =   8144.501
Rotor speed (rpm) =   4666.0000
STABLE MODE
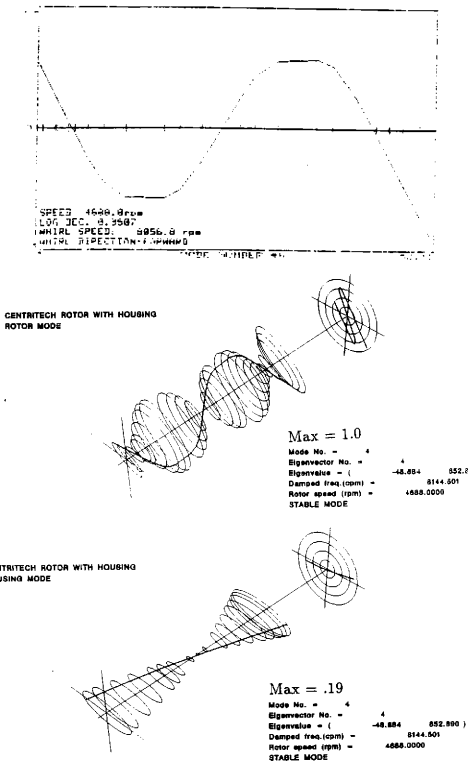
Figure 40.   Centritech lab rotor with flexible housing model mode 4.

CENTRITECH ROTOR WITH HOUSING
ROTOR MODE
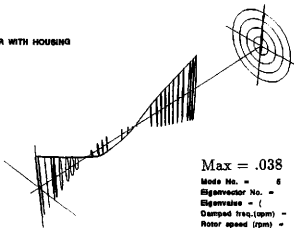
Max = .038

Mode No. = 5
Eigenvector No. = 5
Eigenvalue = (-13.935   916.086)
Damped freq.(cpm) = 8747.973
Rotor speed (rpm) = 4688.0000
STABLE MODE

CENTRITECH ROTOR WITH HOUSING
HOUSING MODE
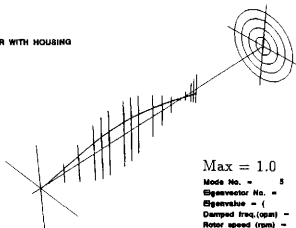
Max = 1.0

Mode No. = 5
Eigenvector No. = 5
Eigenvalue = (-13.935   916.086)
Damped freq.(cpm) = 8747.973
Rotor speed (rpm) = 4688.0000
STABLE MODE

Figure 41.   Centritech lab rotor with flexible housing model mode 5.

CENTRITECH ROTOR WITH HOUSING
ROTOR MODE   6
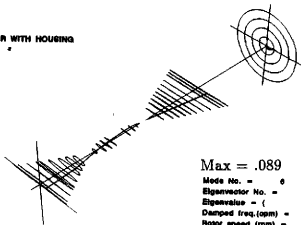
Max = .089

Mode No. =   6
Eigenvector No. =   6
Eigenvalue = (-34.791   919.447)
Damped freq.(rpm) =   8780.089
Rotor speed (rpm) =   4658.0000
STABLE MODE

CENTRITECH ROTOR WITH HOUSING
HOUSING MODE
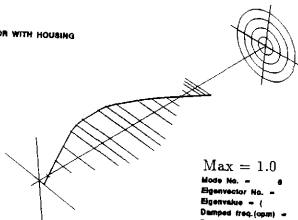
Max = 1.0

Mode No. =   6
Eigenvector No. =   6
Eigenvalue = (-34.791   919.447)
Damped freq.(rpm) =   8780.089
Rotor speed (rpm) =   4658.0000
STABLE MODE

Figure 42.   Centritech lab rotor with flexible housing model mode 6.
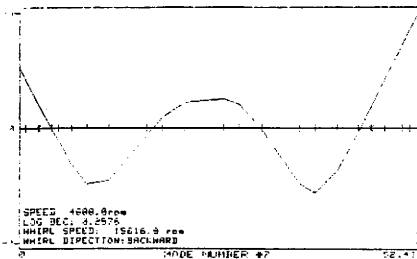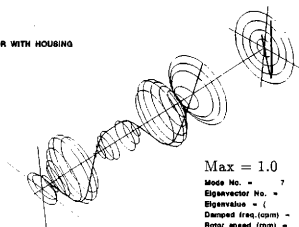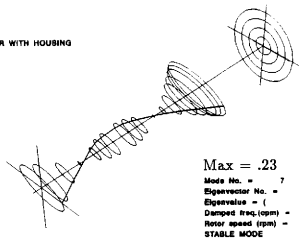
Figure 43. Centritech lab rotor with flexible housing model mode 7.

SPEED 4688.0rpm
LOG DEC. 3.2826
WHIRL SPEED: 17567.9 rpm
WHIRL DIRECTION:FORWARD

MODE NUMBER 4H   52.4:

CENTRITECH ROTOR WITH HOUSING
ROTOR MODE

Max = 1.0

Mode No. =   8
Eigenvector No. =   8
Eigenvalue = (-61.921   1869.267)
Damped freq.(cpm) =   17550.188
Rotor speed (rpm) =   4688.0000
STABLE MODE

CENTRITECH ROTOR WITH HOUSING
HOUSING MODE

Max = .17

Mode No. =   8
Eigenvector No. =   8
Eigenvalue = (-61.921   1869.267)
Damped freq.(cpm) =   17550.188
Rotor speed (rpm) =   4688.0000
STABLE MODE

Figure 44.   Centritech lab rotor with flexible housing model mode 8.

CHAPTER V

EFFECTS OF PUMP HOUSING

An analysis is now described that shows the effects of the vertical pump housing on the natural frequencies and modes of the system. An investigation is first made of the system without the housing, and the results are then compared with an analysis of the system including the housing. Johnston Pump has graciously provided a vertical pump model for use in showing the effects of modelling the flexible housing. The pump is a three stage vertical water pump with a running speed of 1770 rpm. It is driven by a 100 H.P. motor and pumps 1400/1700 gallons per minute with a total head of 165/135 feet. A schematic of the pump model is shown in Figure 45. The dark circle blots indicate lumped mass locations.

Johnston Pump was unable to provide the damping and stiffness coefficients for the bearings. These coefficients have therefore come from other sources as follows. The coefficients for the bottom sump bronze bearing and three impeller bronze bearings were calculated using a computer program called JOURNAL written by Earles (1987) which matched published data presented by Allaire, et al. (1975) and Lund (1965). The coefficients for the next three rubber bearings located along the column pipe were interpolated from data provided in a paper by Hiroshi and Hirohisa (1989).

Campbell diagrams for the pump with and without the housing are shown in Figures 46, 47, and 48. From the analysis without the housing, nine damped natural frequency run lines are computed lower than the running speed of 1770 rpm. An
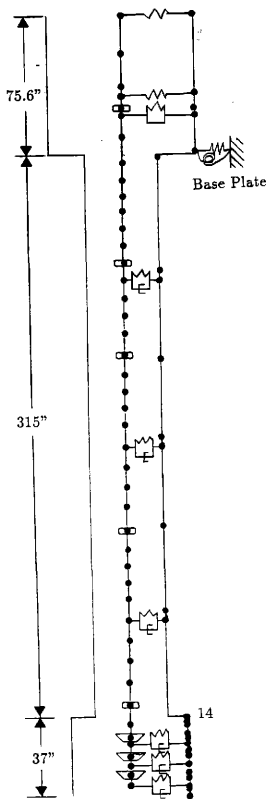
Figure 45. Modelling schematic of Johnston vertical pump.

interesting phenomenom is the large window shown in Figure 47 near the running speed. According to this analysis, there are no critical speeds near the running speed of 1770 rpm. Figures 49, 50, and 51 display the first six modes computed with the rotor rotating at 1770 rpm.

Figure 48 displays the Campbell diagram for the pump with the housing. Eigenvalues were calculated for running speeds from 200 rpm to 2000 rpm in 200 rpm increments. It appears from the plots that the program PATH missed some roots. A scale factor of 3400 rpm was used for this analysis, but nevertheless 90 denominator roots were divided out for each speed. Dividing out this many roots probably resulted in numerical error before the eigenvalues of interest were even begun to be computed as discussed in section III.4. The difference in the Campbell diagrams with and without the housing seem to comfirm this, as does the fact that mode shapes corresponding to roots with the housing included were unable to be computed due to numerical overflow. It appears that the greatest effect of including the housing is in raising the natural frequencies of the system. This also contradicts what would normally be expected since the foundation of case 1 is the flexible housing in case 2. The overall stiffness of the system is now lower in case 2 than in case 1, which should imply lower natural frequencies or at least more natural frequencies in the lower frequency range as in Figure 47.

Though the objective of this chapter is to describe the effects of including the housing in the model, the apparent numerical instability of this particular model prevents this. The deduction is that the pump modelled with the housing included is too large to be analyzed using the Guyan reduction technique implemented in PATH.

CAMPBELL DIAGRAM

Johnston Pump ... without housing
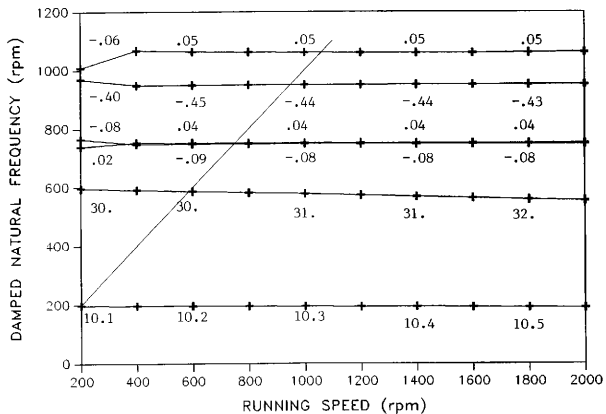
Figure 46. Campbell Diagram for first six modes of Johnston pump model without the housing.

CAMPBELL DIAGRAM

Johnston Pump ... without housing
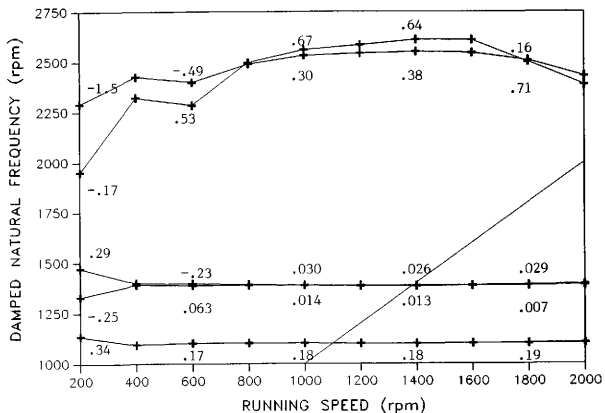
Figure 47. Campbell Diagram for modes seven–eleven of Johnston pump model without the housing.

CAMPBELL DIAGRAM

Johnston Pump ... with housing
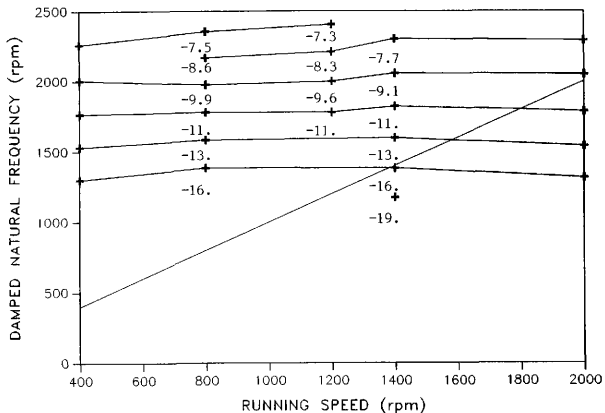
Figure 48. Campbell Diagram for Johnston pump model with the housing included.

MODE SHAPE PLOT

Johnston Pump
without housing
Speed = 1770 rpm
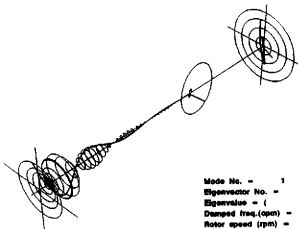
Mode No. =   1
Eigenvector No. =   1
Eigenvalue = (-33.819   20.095)
Damped freq.(cpm) =   191.839
Rotor speed (rpm) =   1770.0000
STABLE MODE

MODE SHAPE PLOT

Johnston Pump
without housing
Speed = 1770 rpm
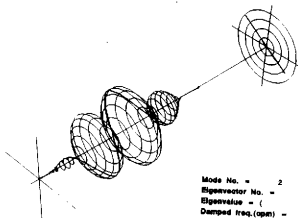
Mode No. =   2
Eigenvector No. =   2
Eigenvalue = (-0.453   78.703)
Damped freq.(cpm) =   751.552
Rotor speed (rpm) =   1770.0000
STABLE MODE

Figure 49.   First and second mode shapes for vertical pump without housing.

MODE SHAPE PLOT

Johnston Pump
without housing
Speed = 1770 rpm

Mode No. =   3
Eigenvector No. =
Eigenvalue = (-9.846   111.196   )
Damped freq.(cpm) =   1091.855
Rotor speed (rpm) =   1770.0000
STABLE MODE

MODE SHAPE PLOT

Johnston Pump
without housing
Speed = 1770 rpm

Mode No. =   4
Eigenvector No. =
Eigenvalue = (-9.440   115.348   )
Damped freq.(cpm) =   1101.496
Rotor speed (rpm) =   1770.0000
STABLE MODE
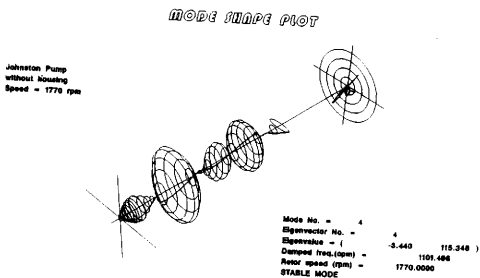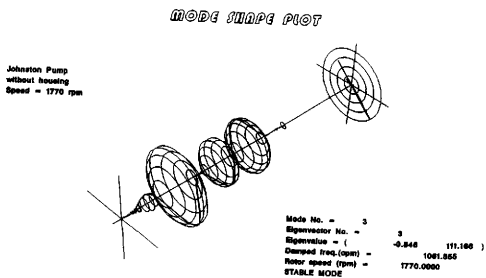
Figure 50.   Third and fourth mode shapes for vertical pump without housing.
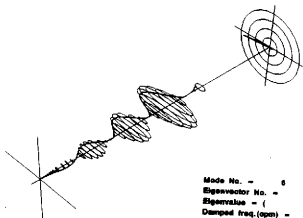
Figure 51. Fifth and sixth mode shapes for vertical pump without housing.

CHAPTER VI

CONCLUSIONS AND DISCUSSION

An efficient program has been developed for use in analyzing multi–stage centrifugal pumps with or without a housing. Some of the more positive features of the program are its speed, the ability to include the housing in the model, and the flexibility of being used interactively for single speed analyses or in batch for multiple speed runs. The accuracy of PATH has been demonstrated by comparison to the finite element program APDS. The desirability of using the polynomial approach has also been shown with the Centritech model by computing an eigenvalue missed using the standard Lund–type method.

As with any engineering project, additional improvements need to be considered. Problems with long rotors have been shown in the analysis of the vertical water pump. Lund and Wang (1986) described a method by which the Riccati method could be applied to the analysis of long shafts on a flexible foundation. This method would need to be modified for use with the Murphy–Vance polynomial approach. L'Antigua (1989) described a method by which shell elements could be combined with the transfer matrix approach in rotordynamic analysis. This method was shown to be especially useful for transferring across conical sections of the model. Another improvement would be to define an approach by which the housing could be efficiently modelled using the polynomial method without having to take the inverse of any matrices.

REFERENCES

Agostinelli, A., Nobles, D., and Mockridge, C.R., 1960, "An Experimental Investigation of Radial Thrust in Centrifugal Pumps", *Journal of Engineering for Power*, Vol. 82, April, pp 120–126

Allaire, P.E., Nicholas, J.C., Barrett, L.E., Gunter, E.J., 1975, "Bearing Characteristics and Stability for Finite Bearings", *University of Virginia report No. ME-543-121-75*, Charlottesville, VA, March

Barrett, L.E., Gunter, E.J., Allaire, P.E., 1976, "The Stability of Rotor–Bearing Systems Using Transfer Functions", *Report No. UVA/464761/ME76/133*, University of Virginia, Charlottesville, VA, Dec.

Bohm, R.T., 1966, "Tame Menace of Turbine Vibration", *SAE Journal*, Vol. 74, No. 2, Feb., pp 44–48

Chamieh, D.S., Acosta, A.J., Brennen, C.E., Caughey, T.K., and Franz, R., 1982, "Experimental Measurements of Hydrodynamic Stiffness Matrices for a Centrifugal Pump Impeller", *Proceedings of NASA/ARO Workshop on Rotordynamic Instability Problems in High Performance Turbomachinery*, NASA CP–2250, pp 382–398

Chamieh, D.S., 1983, "Forces on a Whirling Centrifugal Pump - Theory and Experiments", *PhD Dissertation*, Division of Engineering and Applied Science, California Institute of Technology

Chang, C.M., Braun, F.W., 1987, "Solving the Vibration Problem of a Vertical Multistage Cryogenic Pump", *4th International Pump Symposium*, Houston, TX, Texas A&M University, pp 85–94

Childs, D., 1981, "Rotordynamic Moment Coefficients for Finite–Length Turbulent Seals", *Proceedings IFTOMM Conference on Rotordynamic Problems in Power Plants*, Rome, Italy, Sept., pp 368–376

Cornman, R.E., 1986, "Analytical and Experimental Techniques for Solving Pump Structural Resonance Problems", *Proceedings of the 3rd International Pump Symposium*, Mechanical Engineering Dept., Texas A&M University, pp 27–32

Dicmas, J.L., 1987, *Vertical Turbine, Mixed Flow, and Propeller Pumps*, McGraw-Hill Book Co., New York, NY

Domm, H., Hergt, P., 1970, "Radial Forces on Impeller of Volute Casing Pumps", *Flow Research on Blading* (L.S. Dzung, ed.), Elsevier Pub. Co., The Netherlands, pp 305–321

Earles, L.L., 1987, "JOURNAL.FOR: A Computer Program to Determine Bearing Coefficients for Finite Length Journal Bearings",*MEEN 639 Class Project for Dr. J.M. Vance*, Texas A&M University

Forsythe, G.E., Malcolm, M.A., Moler, C.B., 1977, *Computer Methods for Mathematical Computations*, Prentice–Hall, Englewood Cliffs, NJ

Gajan, Richard, 1987, "The Development of a Rotordynamics Computer Code to Analyze Multi-Stage Centrifugal Pumps", *M.S. Thesis*, Texas A&M University, College Station, TX

Guyan, R.J., 1965, "Reduction of Stiffness and Mass Matrices",*AIAA Journal*, Vol. 3, No. 2, Feb., pg. 380

Harris, C.M., Crede, C.E., 1976, *Shock and Vibration Handbook*, 2nd Ed., McGraw–Hill Book Co., New York, NY

Hibner, D.H., 1975, "Dynamic Response of Viscous–Damped Multi-Shaft Jet Engines", *Journal of Aircraft*, Vol. 12, No. 4, April, pp 305–312

Hinata, T., Kanemitsu, Y., Nagamatsu, A., Okuma, M., 1985, "Computer Aided Vibration Analysis of Vertical Shaft Pumps by Component Mode Synthesis Method", *ASME Paper No. 85–DET–178*

Hiroshi, S., Hirohisa, T., 1989, "Dry–Start Submerged Bearing for Vertical Pumps", *6th International Pump Symposium*, Houston, TX, Texas A&M University

Horner, G.C., Pilkey, W.D., 1978, "The Riccati Transfer Matrix Method", *Journal of Mechanical Design*, Vol. 100, April, pp 297–302

Iversen, H.W., Rolling, R.E., Carlson, J.J., 1960, "Volute Pressure Distribution, Radial Force on the Impeller and Volute Mixing Losses of a Radial Flow Centrifugal Pump", *Journal of Engineering for Power*, Vol. 82, pp 136–144

Jenkins, M.A., Traub, J.F., 1970, "A Three–Stage Algorithm for Real Polynomials Using Quadratic Iteration", *SIAM Journal of Numerical Analysis*, Vol. 7, No. 4, Dec., pp 545–566

Jenkins, M.A., 1975, "Algorithm 493: Zeros of a Real Polynomial", *ACM Transactions on Mathematical Software*, Vol. 1, No. 2, June, pp 178–189

Jery, B., Franz, R., 1982, "Stiffness Matrices for the Rocketdyne Diffuser Volute", *Report No. e249.1*, California Institute of Technology, Div. of Eng. and Appl. Sci., October

Jery, A., Acosta, A.J., Brennen, C.E., Caughey, T.K., 1984, "Hydrodynamic Impeller Stiffness, Damping, and Inertia in the Rotordynamics of Centrifugal Flow Pumps", *Proceedings of Workshop on Rotordynamic Instability Problems in High-Performance Turbomachinery*, Texas A&M University, College Station, TX, NASA CP-2338

Kleespies, H.S., 1986, "Calculation of Rotordynamic Unbalance Response Including Torque and Cross-Coupled Stiffness and Damping Effects", *M.S. Thesis*, Texas A&M University, College Station, TX

Koenig, E.C., 1961, "Analysis for Calculating Lateral Vibration Characteristics of Rotating Systems With Any Number of Flexible Supports: Part 1 - The Method of Analysis", *Journal of Applied Mechanics*, Vol. 28, Dec., pp 585–590

Kolman, Bernard, 1986, *Elementary Linear Algebra*, 4th Ed., Macmillan Publishing Co., New York, NY

L'Antigua, E.A., 1989, "Rotordynamic Analysis with Shell Elements for the Transfer Matrix Method", *M.S. Thesis*, Texas A&M University, College Station, TX

Leckie, F., Pestel,E., 1960, "Transfer-Matrix Fundamentals", *International Journal of Mechanical Science*, Vol. 2, pp 137–167

Lee, J.M., Pak, C.G., Lee, H.S., 1985, "Vibration Analysis of an Idealized Vertical Pump Model", *ASME Paper No. 85-DET-165*

Li, D.F., Gunter, E.J., 1978, "Linear Stability Analysis of Dual-Rotor Systems", *Report No. UVA/528140/MAE78/113*, University of Virginia, Charlottesville, VA, Sept.

Lund, J.W., 1965, "Rotor-Bearing Dynamics Design Technology, Part III: Design Handbook for Fluid-Film Type Bearings", *Technical Report AFAPL-TR-64-45*, Airforce Aero Propulsion Lab., Wright Patterson AFB, May

Lund, J.W., Orcutt, F.K., 1967, "Calculations and Experiments on the Unbalance Response of a Flexible Rotor", *Journal of Engineering for Industry*, Nov., pp 785–796

Lund, J.W., 1973, "Stability and Damped Critical Speeds of a Flexible Rotor in Fluid-Film Bearings", *1973 ASME Design Technology Conference*, No. 73-DET-103, Cincinnati, OH, Sept. 9–12

Lund, J.W., Wang, Z., 1986, "Application of the Riccati Method to Rotor Dynamic Analysis of Long Shafts on a Flexible Foundation", *Journal of Vibrations, Acoustics, Stress, and Reliability in Design*, Vol. 108, Apr., pp 177–181

Murphy, B.T., Vance, J.M., 1982, "JAZZ: A Computer Program for Stability and Critical Speed Analysis of Rotating Machinery", Texas A&M University, Dec., pp 23–36

Murphy, B.T., Vance, J.M., 1983, "An Improved Method for Calculating Critical Speeds and Rotordynamic Stability of Turbomachinery", *Journal of Engineering for Power*, Vol. 105, July, pp 591–595

Murphy, B.T., 1984, "Eigenvalues of Rotating Machinery", *PhD Dissertation*, Texas A&M University, College Station, TX

Myklestad, N.O., 1944, "A New Method of Calculating Natural Modes of Uncoupled Bending Vibrations of Airplane Wings and Other Types of Beams", *Journal of the Aeronautical Sciences*, Vol. 11, No. 2, April, pp 153–162

Nelson, H.D., et al., 1981, "Transient Response of Rotor-Bearing Systems Using Component Mode Synthesis - Part I Mathematical Model - Part II Digital Computer Manual for Program ARDS - Part III Example Analyses", *Reports Prepared for NASA Lewis*, Arizona State University

Nelson, H.D., Meacham, W.L., 1982, "Transient Response of Rotor-Bearing Systems Using Component Mode Synthesis - Part IV Mathematical Development (Multi-Shaft Systems) - Part V Digital Computer Manual for Program ARDS (Multi-Shaft Systems)", *Reports Prepared for NASA Lewis*, Arizona State University

Nikolajsen, J.L., 1978, "Modeling and Control of Rotor-Bearing Systems", *PhD Dissertation*, Sussex University, Sussex, U.K.

Nikolajsen, J.L., Kelly, J.H., 1989, "The Effect of Bearing Misalignment on Rotor Stability", Submitted to *Journal of Tribology*, January 16

Pilkey, W., Chang, P.Y., 1971, "Avoiding Iterative Searches to Find Critical Speeds of Rotating Shafts With the Transfer Matrix Method", *ASME Paper No. 71-VIBR-53*

Prohl, M.A., 1945, "A General Method for Calculating Critical Speeds of Flexible Rotors", *Journal of Applied Mechanics*, Vol. 12

Smith, D.R., Woodward, G.M., 1988, "Vibration Analysis of Vertical Pumps", *Sound and Vibration*, June, pp 24–30

Songyuan, Lu, 1985, "A Method for Calculating Damped Critical Speeds and Stability of Rotor–Bearing Systems", *ASME Paper No. 85–Det–116*

Steidel, R. F., 1979, *An Introduction to Mechanical Vibrations*, John Wiley & Sons, 2nd Ed., New York, NY

Vance, J.M., 1988, *Rotordynamics of Turbomachinery*, John Wiley & Sons, U.S.A.

Woodcock, J.S., 1971, "Dynamic Characteristics of a Journal Bearing Oil–Film", *D. Phil. Thesis*, University of Sussex, Sussex, U.K.

Supplementary Sources Consulted

Moore, A.W., Sens, H., (ed.), 1954, *The Vertical Pump by Johnston*, Johnston Pump Co., Pasadena, CA

Nikolajsen, J.L., Gajan, R.J., 1988, "A New Computer Program for Pump Rotor-dynamic Analysis", *Proceedings of 5th International Pump Users Symposium*, Houston, TX, May

APPENDIX A

INPUT DATA FOR EQUILIBRIUM ANALYSIS VERIFICATION

Gajan (1987) The system of units used is kilogram, meter, second

Shaft Material Properties

Density	7.76E3	(kg/m^3)
Elastic Modulus	2.05E11	(N/m^2)
Shear Modulus	.82E11	(N/m^2)

Shaft Description

Element Number	Length (m)	Outer Radius (m)
1	.2	.025
2	.2	.025
3	.2	.025
4	.2	.025

Concentrated Masses

Station Number	Concentrated Mass (kg)	Diametral Mom. of I. $(kg * m^2)$	Polar Mom. of I. $(kg * m^2)$
2	127.46	0.0	0.0
4	127.46	0.0	0.0

Bearing Description (both bearings)

Bearing 1 station number	1	
Bearing 2 station number	5	
Oil Viscosity	3.93E-2	$(N * s/m^2)$
Bearing Length	1.667E-2	(m)
Bearing Diameter	5.0E-2	(m)
Bearing Radial Clearance	7.5E-5	(m)

Bearing Sommerfeld Number and Attitude Angle

Eccentricity Ratio	Sommerfeld Number	Attitude Angle (rad)
0.0	1.0E15	1.57
0.1	8.9526	1.41
0.2	4.07	1.31
0.3	2.453	1.19
0.4	1.5335	1.08
0.5	.9551	.96
0.6	.563	.838
0.7	.2966	.715
0.8	.125	.558
0.9	.03	.401
1.0	.87E-9	1.0E-9

Bearing Dimensionless Stiffness Coefficients

Eccentricity Ratio	K_{xx}	K_{xy}	K_{yx}	K_{yy}
0.0	2.5	26.	-26.	1.0
0.1	2.4	9.56	-9.49	1.161
0.2	2.38	4.52	-5.50	1.32
0.3	2.33	2.7	-4.33	1.61
0.4	2.26	1.69	-3.92	2.0
0.5	2.19	1.0	-3.87	2.63
0.6	2.12	.54	-4.025	3.54
0.7	2.037	0.0	-4.48	4.98
0.8	2.033	-.563	-5.37	7.42
0.9	2.163	-1.55	-7.68	14.62
1.0	2.4	-3.0	-14.0	35.0

Bearing Dimensionless Damping Coefficients

Eccentricity Ratio	C_{xx}	C_{xy}	C_{yx}	C_{yy}
0.0	40.0	-2.3	-.9	40.0
0.1	22.65	-2.35	-1.43	18.88
0.2	11.75	-2.42	-2.61	10.57
0.3	7.59	-2.45	-2.90	7.97
0.4	5.52	-2.48	-2.99	6.95
0.5	4.12	-2.51	-3.01	6.67
0.6	2.98	-2.48	-2.95	6.9
0.7	2.36	-2.58	-3.03	7.6
0.8	1.92	-2.87	-3.32	9.28
0.9	1.55	-3.58	-3.96	14.19
1.0	1.15	-4.0	-4.90	25.0

Bearing Support Coefficients

Bearing	K_x (N/m)	K_y (N/m)	C_x $(N*s/m)$	C_y $(N*s/m)$
1	8.33E06	8.33E06	0.0	0.0
2	8.33E06	8.33E06	0.0	0.0

Seal Stiffness
Speed = 4000 rpm

Station Number	K_{xx} (N/m)	K_{xy} (N/m)	K_{yx} (N/m)	K_{yy} (N/m)
3	1.366E7	1.812E7	-1.812E7	1.366E7

Seal Damping
Speed = 4000 rpm

Station Number	C_{xx} $(N*s/m)$	C_{xy} $(N*s/m)$	C_{yx} $(N*s/m)$	C_{yy} $(N*s/m)$
3	9.1E4	3.6E4	-3.6E4	9.1E4

Seal Misalignments

Station	X (m)	Y (m)	ϕ (rad)	θ (rad)
3	0.0	-3.686E-4	0.0	0.0

APPENDIX B

INPUT DATA FOR EDI COMPARISON

Gajan (1987) The system of units used is pound, inch, second

Shaft Material Properties

Density	.7764E-3	$(lb * s^2/in^4)$
Elastic Modulus	30.E6	(lb/in^2)
Shear Modulus	.82E11	(lb/in^2)

Concentrated Masses

Station Number	Concentrated Mass $(lb * s^2/in)$	Diametral Mom. of I. $(lb * s^2 * in)$	Polar Mom. of I. $(lb * s^2 * in)$
1	.05564	.14383	.2963
5	.015528	0.0	0.0
9	.040217	.108	.21580
11	.02976	.1056	.211
13	.031056	.109	.218
15	.031056	.109	.218
17	.031056	.109	.218
19	.031056	.109	.218
21	.031056	.109	.218
23	.029500	.1056	.211
25	.031056	.109	.218
27	.030800	.1079	.2158
29	.029762	.1056	.211
30	.037525	0.0	0.0
31	.010691	0.0	0.0
32	.015528	0.0	0.0
35	.035481	0.0	0.0
37	.004558	0.0	0.0

Shaft Description

Element Number	Length (m)	Outer Radius (m)
1	1.44	1.19
2	1.185	1.213
3	5.1875	1.25
4	13.125	1.2525
5	3.25	1.2550
6	1.3750	1.4975
7	1.5625	1.50
8	1.4380	1.50
9	2.3150	1.50
10	1.4380	1.50
11	2.3130	1.50
12	1.4380	1.50
13	2.3130	1.50
14	1.4380	1.50
15	2.3130	1.50
16	1.4380	1.50
17	2.3130	1.50
18	1.4380	1.50
19	2.3130	1.50
20	1.4380	1.50
21	2.3130	1.50
22	1.4380	1.50
23	2.3130	1.50
24	1.4380	1.50
25	2.3130	1.50
26	1.4380	1.50
27	2.3130	1.50
28	1.4380	1.50
29	2.1245	1.50
30	3.6225	1.50
31	2.3750	1.255
32	13.0	1.25
33	3.25	1.25
34	1.5	1.0
35	4.25	1.0
36	1.1250	.394

Support Stiffness

Station Number	K_{xx} (lb/in)	K_{xy} (lb/in)	K_{yx} (lb/in)	K_{yy} (lb/in)
4	.29200E6	0.0	0.0	.41400E6
9	12590.	7950.	-7950.	12590.
11	11170.	5620.	-5620.	11170.
13	11240.	5630.	-5630.	11240.
15	11280.	5660.	-5660.	11280.
17	11310.	5680.	-5680.	11310.
19	11350.	5710.	-5710.	11350.
21	11390.	5740.	-5740.	11390.
23	11420.	5770.	-5770.	11420.
25	11500.	5800.	-5800.	11500.
27	11490.	5820.	-5820.	11490.
29	5840.	7770.	-7770.	5840.
30	-82400.	.15360E6	-.15360E6	-82400.
33	.29200E6	0.0	0.0	.41400E6

Support Damping

Station Number	C_{xx} (lb*s/in)	C_{xy} (lb*s/in)	C_{yx} (lb*s/in)	C_{yy} (lb*s/in)
4	609.	0.0	0.0	609.
9	30.4	0.0	0.0	30.4
11	25.4	0.0	0.0	25.4
13	25.4	0.0	0.0	25.4
15	25.4	0.0	0.0	25.4
17	25.4	0.0	0.0	25.4
19	25.4	0.0	0.0	25.4
21	25.4	0.0	0.0	25.4
23	25.4	0.0	0.0	25.4
25	25.4	0.0	0.0	25.4
27	25.4	0.0	0.0	25.4
29	16.0	0.0	0.0	16.0
30	253.	0.0	0.0	253.
33	609.3	0.0	0.0	609.3

APPENDIX C

INPUT DATA FOR EDI CASE ONE

Gajan (1987) The system of units used is pound, inch, second

Shaft Material Properties

Density	.7764E-3	$(lb * s^2/in^4)$
Elastic Modulus	30.E6	(lb/in^2)
Shear Modulus	.82E11	(lb/in^2)

Concentrated Masses

Station Number	Concentrated Mass $(lb * s^2/in)$	Diametral Mom. of I. $(lb * s^2 * in)$	Polar Mom. of I. $(lb * s^2 * in)$
1	.05564	.14383	.2963
5	.015528	0.0	0.0
9	.040217	.108	.21580
11	.02976	.1056	.211
13	.031056	.109	.218
15	.031056	.109	.218
17	.031056	.109	.218
19	.031056	.109	.218
21	.031056	.109	.218
23	.029500	.1056	.211
25	.031056	.109	.218
27	.030800	.1079	.2158
29	.029762	.1056	.211
30	.037525	0.0	0.0
31	.010691	0.0	0.0
32	.015528	0.0	0.0
35	.035481	0.0	0.0
37	.004558	0.0	0.0

Shaft Description

Element Number	Length (*in*)	Outer Radius (*in*)
1	1.44	1.19
2	1.185	1.213
3	5.1875	1.25
4	13.125	1.2525
5	3.25	1.2550
6	1.3750	1.4975
7	1.5625	1.50
8	1.4380	1.50
9	2.3150	1.50
10	1.4380	1.50
11	2.3130	1.50
12	1.4380	1.50
13	2.3130	1.50
14	1.4380	1.50
15	2.3130	1.50
16	1.4380	1.50
17	2.3130	1.50
18	1.4380	1.50
19	2.3130	1.50
20	1.4380	1.50
21	2.3130	1.50
22	1.4380	1.50
23	2.3130	1.50
24	1.4380	1.50
25	2.3130	1.50
26	1.4380	1.50
27	2.3130	1.50
28	1.4380	1.50
29	2.1245	1.50
30	3.6225	1.50
31	2.3750	1.255
32	13.0	1.25
33	3.25	1.25
34	1.5	1.0
35	4.25	1.0
36	1.1250	.394

Bearing Description (both bearings)

Bearing 1 station number	4	
Bearing 2 station number	33	
Oil Viscosity	2.0E-6	$(lb * s/in^2)$
Bearing Length	1.0	(in)
Bearing Diameter	2.5	(in)
Bearing Radial Clearance	.003	(in)

Bearing Stiffness Coefficients

Speed (rpm)	K_{xx} (lb/in)	K_{xy} (lb/in)	K_{yx} (lb/in)	K_{yy} (lb/in)
500	10000.	0.0	0.0	.8E6
1000	12330.	0.0	0.0	.74E6
1500	15000.	0.0	0.0	.62E6
2000	17900.	0.0	0.0	.573E6
2500	19500.	0.0	0.0	.55E6
3000	21000.	0.0	0.0	.524E6
3500	23200.	0.0	0.0	.48E6
4000	25280.	0.0	0.0	.450E6
4500	27430.	0.0	0.0	.428E6
5000	29600.	0.0	0.0	.407E6
5500	31000.	0.0	0.0	.38E6
6000	34000.	0.0	0.0	.37E6
6500	36000.	0.0	0.0	.355E6
7000	36000.	0.0	0.0	.345E6
7500	38500.	0.0	0.0	.344E6
8000	41900.	0.0	0.0	.342E6

Bearing Damping Coefficients

Speed (rpm)	C_{xx} (lb * s/in)	C_{xy} (lb * s/in)	C_{yx} (lb * s/in)	C_{yy} (lb * s/in)
500.	280.	0.0	0.0	7500.
1000.	280.	0.0	0.0	7240.
1500.	280.	0.0	0.0	4500.
2000.	280.	0.0	0.0	2100.
2500.	280.	0.0	0.0	1800.
3000.	280.	0.0	0.0	1470.
3500.	280.	0.0	0.0	1220.
4000.	280.	0.0	0.0	1120.
4500.	280.	0.0	0.0	1020.
5000.	280.	0.0	0.0	910.
5500.	280.	0.0	0.0	840.
6000.	280.	0.0	0.0	700.
6500.	280.	0.0	0.0	669.
7000.	280.	0.0	0.0	620.
7500.	280.	0.0	0.0	550.
8000.	280.	0.0	0.0	500.

Seal Descriptions

Seal Number	Station
1	9
2	11
3	13
4	15
5	17
6	19
7	21
8	23
9	25
10	27
11	29
12	30

Seal Stiffness Input

Part 1   Speed = 1100 rpm

Seal Number	K_{xx} (lb/in)	K_{xy} (lb/in)	$K_{x\phi}$ (lb/rad)	$K_{x\theta}$ (lb/rad)
1	686.	263.	0.0	0.0
2	481.	194.	0.0	0.0
3	483.	195.	0.0	0.0
4	483.	196.	0.0	0.0
5	487.	197.	0.0	0.0
6	489.	198.	0.0	0.0
7	493.	199.	0.0	0.0
8	496.	200.	0.0	0.0
9	499.	201.	0.0	0.0
10	503.	202.	0.0	0.0
11	348.	175.	0.0	0.0
12	11834.	9622.	0.0	0.0

Part 2   Speed = 1100 rpm

Seal Number	$K_{\phi x}$ (lb)	$K_{\phi y}$ (lb)	$K_{\phi\phi}$ $(lb*in/rad)$	$K_{\phi\theta}$ $(lb*in/rad)$
1	0.0	0.0	0.0	0.0
2	0.0	0.0	0.0	0.0
3	0.0	0.0	0.0	0.0
4	0.0	0.0	0.0	0.0
5	0.0	0.0	0.0	0.0
6	0.0	0.0	0.0	0.0
7	0.0	0.0	0.0	0.0
8	0.0	0.0	0.0	0.0
9	0.0	0.0	0.0	0.0
10	0.0	0.0	0.0	0.0
11	0.0	0.0	0.0	0.0
12	0.0	0.0	0.0	0.0

Seal Damping Input

Part 1   Speed = 1100 rpm

Seal Number	C_{xx} $(lb*s/in)$	C_{xy} $(lb*s/in)$	$C_{x\phi}$ $(lb*s/rad)$	$C_{x\theta}$ $(lb*s/rad)$
1	3.93	.311	0.0	0.0
2	3.13	.276	0.0	0.0
3	3.14	.279	0.0	0.0
4	3.15	.282	0.0	0.0
5	3.16	.285	0.0	0.0
6	3.17	.288	0.0	0.0
7	3.18	.291	0.0	0.0
8	3.19	.294	0.0	0.0
9	3.20	.297	0.0	0.0
10	3.21	.3	0.0	0.0
11	2.04	.19	0.0	0.0
12	246.	33.25	0.0	0.0

Part 2   Speed = 1100 rpm

Seal Number	$C_{\phi x}$ $(lb*s)$	$C_{\phi y}$ $(lb*s)$	$C_{\phi\phi}$ $(\frac{lb*s*in}{rad})$	$C_{\phi\theta}$ $(\frac{lb*s*in}{rad})$
1	0.0	0.0	0.0	0.0
2	0.0	0.0	0.0	0.0
3	0.0	0.0	0.0	0.0
4	0.0	0.0	0.0	0.0
5	0.0	0.0	0.0	0.0
6	0.0	0.0	0.0	0.0
7	0.0	0.0	0.0	0.0
8	0.0	0.0	0.0	0.0
9	0.0	0.0	0.0	0.0
10	0.0	0.0	0.0	0.0
11	0.0	0.0	0.0	0.0
12	0.0	0.0	0.0	0.0

Seal Inertia Input
Part 1   Speed = 1100 rpm

Seal Number	M_{xx} $(lb*s^2/in)$	M_{xy} $(lb*s^2/in)$	$M_{x\phi}$ $(lb*s^2/rad)$	$M_{x\theta}$ $(lb*s^2/rad)$
1	0.0	0.0	0.0	0.0
2	0.0	0.0	0.0	0.0
3	0.0	0.0	0.0	0.0
4	0.0	0.0	0.0	0.0
5	0.0	0.0	0.0	0.0
6	0.0	0.0	0.0	0.0
7	0.0	0.0	0.0	0.0
8	0.0	0.0	0.0	0.0
9	0.0	0.0	0.0	0.0
10	0.0	0.0	0.0	0.0
11	0.0	0.0	0.0	0.0
12	0.0	0.0	0.0	0.0

Part 2   Speed = 1100 rpm

Seal Number	$M_{\phi x}$ $(lb*s^2)$	$M_{\phi y}$ $(lb*s^2)$	$M_{\phi\phi}$ $(\frac{lb*s^2*in}{rad})$	$M_{\phi\theta}$ $(\frac{lb*s^2*in}{rad})$
1	0.0	0.0	0.0	0.0
2	0.0	0.0	0.0	0.0
3	0.0	0.0	0.0	0.0
4	0.0	0.0	0.0	0.0
5	0.0	0.0	0.0	0.0
6	0.0	0.0	0.0	0.0
7	0.0	0.0	0.0	0.0
8	0.0	0.0	0.0	0.0
9	0.0	0.0	0.0	0.0
10	0.0	0.0	0.0	0.0
11	0.0	0.0	0.0	0.0
12	0.0	0.0	0.0	0.0

Seal Stiffness Input

Part 1   Speed = 3300 rpm

Seal Number	K_{xx} (lb/in)	K_{xy} (lb/in)	$K_{x\phi}$ (lb/rad)	$K_{x\theta}$ (lb/rad)
1	5948.	2544.	0.0	0.0
2	4810.	2078.	0.0	0.0
3	4830.	2085.	0.0	0.0
4	4840.	2095.	0.0	0.0
5	4870.	2105.	0.0	0.0
6	4890.	2106.	0.0	0.0
7	4930.	2108.	0.0	0.0
8	4960.	2112.	0.0	0.0
9	4990.	2117.	0.0	0.0
10	5008.	2120.	0.0	0.0
11	3672.	1854.	0.0	0.0
12	.125E6	71134.	0.0	0.0

Part 2   Speed = 3300 rpm

Seal Number	$K_{\phi x}$ (lb)	$K_{\phi y}$ (lb)	$K_{\phi\phi}$ (lb * in/rad)	$K_{\phi\theta}$ (lb * in/rad)
1	0.0	0.0	0.0	0.0
2	0.0	0.0	0.0	0.0
3	0.0	0.0	0.0	0.0
4	0.0	0.0	0.0	0.0
5	0.0	0.0	0.0	0.0
6	0.0	0.0	0.0	0.0
7	0.0	0.0	0.0	0.0
8	0.0	0.0	0.0	0.0
9	0.0	0.0	0.0	0.0
10	0.0	0.0	0.0	0.0
11	0.0	0.0	0.0	0.0
12	0.0	0.0	0.0	0.0

Seal Damping Input

Part 1   Speed = 3300 rpm

Seal Number	C_{xx} $(lb*s/in)$	C_{xy} $(lb*s/in)$	$C_{x\phi}$ $(lb*s/rad)$	$C_{x\theta}$ $(lb*s/rad)$
1	12.64	.79	0.0	0.0
2	10.81	.69	0.0	0.0
3	10.83	.70	0.0	0.0
4	10.85	.70	0.0	0.0
5	10.87	.71	0.0	0.0
6	10.90	.71	0.0	0.0
7	10.92	.72	0.0	0.0
8	10.94	.72	0.0	0.0
9	10.96	.73	0.0	0.0
10	11.0	.74	0.0	0.0
11	7.3	.47	0.0	0.0
12	686.	97.1	0.0	0.0

Part 2   Speed = 3300 rpm

Seal Number	$C_{\phi x}$ $(lb*s)$	$C_{\phi y}$ $(lb*s)$	$C_{\phi\phi}$ $\left(\frac{lb*s*in}{rad}\right)$	$C_{\phi\theta}$ $\left(\frac{lb*s*in}{rad}\right)$
1	0.0	0.0	0.0	0.0
2	0.0	0.0	0.0	0.0
3	0.0	0.0	0.0	0.0
4	0.0	0.0	0.0	0.0
5	0.0	0.0	0.0	0.0
6	0.0	0.0	0.0	0.0
7	0.0	0.0	0.0	0.0
8	0.0	0.0	0.0	0.0
9	0.0	0.0	0.0	0.0
10	0.0	0.0	0.0	0.0
11	0.0	0.0	0.0	0.0
12	0.0	0.0	0.0	0.0

Seal Inertia Input
Part 1   Speed = 3300 rpm

Seal Number	M_{xx} ($lb * s^2/in$)	M_{xy} ($lb * s^2/in$)	$M_{x\phi}$ ($lb * s^2/rad$)	$M_{x\theta}$ ($lb * s^2/rad$)
1	0.0	0.0	0.0	0.0
2	0.0	0.0	0.0	0.0
3	0.0	0.0	0.0	0.0
4	0.0	0.0	0.0	0.0
5	0.0	0.0	0.0	0.0
6	0.0	0.0	0.0	0.0
7	0.0	0.0	0.0	0.0
8	0.0	0.0	0.0	0.0
9	0.0	0.0	0.0	0.0
10	0.0	0.0	0.0	0.0
11	0.0	0.0	0.0	0.0
12	0.0	0.0	0.0	0.0

Part 2   Speed = 3300 rpm

Seal Number	$M_{\phi x}$ ($lb * s^2$)	$M_{\phi y}$ ($lb * s^2$)	$M_{\phi\phi}$ ($\frac{lb*s^2*in}{rad}$)	$M_{\phi\theta}$ ($\frac{lb*s^2*in}{rad}$)
1	0.0	0.0	0.0	0.0
2	0.0	0.0	0.0	0.0
3	0.0	0.0	0.0	0.0
4	0.0	0.0	0.0	0.0
5	0.0	0.0	0.0	0.0
6	0.0	0.0	0.0	0.0
7	0.0	0.0	0.0	0.0
8	0.0	0.0	0.0	0.0
9	0.0	0.0	0.0	0.0
10	0.0	0.0	0.0	0.0
11	0.0	0.0	0.0	0.0
12	0.0	0.0	0.0	0.0

Seal Stiffness Input

Part 1   Speed = 6600 rpm

Seal Number	K_{xx} (lb/in)	K_{xy} (lb/in)	$K_{x\phi}$ (lb/rad)	$K_{x\theta}$ (lb/rad)
1	23116.	10716.	0.0	0.0
2	18810.	8776.	0.0	0.0
3	18910.	8786.	0.0	0.0
4	19010.	8796.	0.0	0.0
5	19110.	8806.	0.0	0.0
6	19210.	8816.	0.0	0.0
7	19250.	8826.	0.0	0.0
8	19310.	8846.	0.0	0.0
9	19390.	8866.	0.0	0.0
10	19440.	8893.	0.0	0.0
11	14134.	7726.	0.0	0.0
12	.55E6	.255E6	0.0	0.0

Part 2   Speed = 6600 rpm

Seal Number	$K_{\phi x}$ (lb)	$K_{\phi y}$ (lb)	$K_{\phi\phi}$ (lb * in/rad)	$K_{\phi\theta}$ (lb * in/rad)
1	0.0	0.0	0.0	0.0
2	0.0	0.0	0.0	0.0
3	0.0	0.0	0.0	0.0
4	0.0	0.0	0.0	0.0
5	0.0	0.0	0.0	0.0
6	0.0	0.0	0.0	0.0
7	0.0	0.0	0.0	0.0
8	0.0	0.0	0.0	0.0
9	0.0	0.0	0.0	0.0
10	0.0	0.0	0.0	0.0
11	0.0	0.0	0.0	0.0
12	0.0	0.0	0.0	0.0

Seal Damping Input

Part 1   Speed = 6600 rpm

Seal Number	C_{xx} $(lb*s/in)$	C_{xy} $(lb*s/in)$	$C_{x\phi}$ $(lb*s/rad)$	$C_{x\theta}$ $(lb*s/rad)$
1	26.7	1.35	0.0	0.0
2	22.92	1.19	0.0	0.0
3	22.99	1.2	0.0	0.0
4	23.03	1.21	0.0	0.0
5	23.06	1.22	0.0	0.0
6	23.08	1.23	0.0	0.0
7	23.10	1.24	0.0	0.0
8	23.12	1.25	0.0	0.0
9	23.14	1.26	0.0	0.0
10	23.16	1.28	0.0	0.0
11	15.36	.813	0.0	0.0
12	1320.	190.	0.0	0.0

Part 2   Speed = 6600 rpm

Seal Number	$C_{\phi x}$ $(lb*s)$	$C_{\phi y}$ $(lb*s)$	$C_{\phi\phi}$ $(\frac{lb*s*in}{rad})$	$C_{\phi\theta}$ $(\frac{lb*s*in}{rad})$
1	0.0	0.0	0.0	0.0
2	0.0	0.0	0.0	0.0
3	0.0	0.0	0.0	0.0
4	0.0	0.0	0.0	0.0
5	0.0	0.0	0.0	0.0
6	0.0	0.0	0.0	0.0
7	0.0	0.0	0.0	0.0
8	0.0	0.0	0.0	0.0
9	0.0	0.0	0.0	0.0
10	0.0	0.0	0.0	0.0
11	0.0	0.0	0.0	0.0
12	0.0	0.0	0.0	0.0

Seal Inertia Input

Part 1   Speed = 6600 rpm

Seal Number	M_{xx} $(lb*s^2/in)$	M_{xy} $(lb*s^2/in)$	$M_{x\phi}$ $(lb*s^2/rad)$	$M_{x\theta}$ $(lb*s^2/rad)$
1	0.0	0.0	0.0	0.0
2	0.0	0.0	0.0	0.0
3	0.0	0.0	0.0	0.0
4	0.0	0.0	0.0	0.0
5	0.0	0.0	0.0	0.0
6	0.0	0.0	0.0	0.0
7	0.0	0.0	0.0	0.0
8	0.0	0.0	0.0	0.0
9	0.0	0.0	0.0	0.0
10	0.0	0.0	0.0	0.0
11	0.0	0.0	0.0	0.0
12	0.0	0.0	0.0	0.0

Part 2   Speed = 6600 rpm

Seal Number	$M_{\phi x}$ $(lb*s^2)$	$M_{\phi y}$ $(lb*s^2)$	$M_{\phi\phi}$ $(\frac{lb*s^2*in}{rad})$	$M_{\phi\theta}$ $(\frac{lb*s^2*in}{rad})$
1	0.0	0.0	0.0	0.0
2	0.0	0.0	0.0	0.0
3	0.0	0.0	0.0	0.0
4	0.0	0.0	0.0	0.0
5	0.0	0.0	0.0	0.0
6	0.0	0.0	0.0	0.0
7	0.0	0.0	0.0	0.0
8	0.0	0.0	0.0	0.0
9	0.0	0.0	0.0	0.0
10	0.0	0.0	0.0	0.0
11	0.0	0.0	0.0	0.0
12	0.0	0.0	0.0	0.0

APPENDIX D

INPUT DATA FOR EDI CASE TWO

Gajan (1987) The system of units used is pound, inch, second

Shaft Material Properties

Density	.7764E-3	$(lb * s^2/in^4)$
Elastic Modulus	30.E6	(lb/in^2)
Shear Modulus	.82E11	(lb/in^2)

Concentrated Masses

Station Number	Concentrated Mass $(lb * s^2/in)$	Diametral Mom. of I. $(lb * s^2 * in)$	Polar Mom. of I. $(lb * s^2 * in)$
1	.05564	.14383	.2963
5	.015528	0.0	0.0
9	.040217	.108	.21580
11	.02976	.1056	.211
13	.031056	.109	.218
15	.031056	.109	.218
17	.031056	.109	.218
19	.031056	.109	.218
21	.031056	.109	.218
23	.029500	.1056	.211
25	.031056	.109	.218
27	.030800	.1079	.2158
29	.029762	.1056	.211
30	.037525	0.0	0.0
31	.010691	0.0	0.0
32	.015528	0.0	0.0
35	.035481	0.0	0.0
37	.004558	0.0	0.0

Shaft Description

Element Number	Length (in)	Outer Radius (in)
1	1.44	1.19
2	1.185	1.213
3	5.1875	1.25
4	13.125	1.2525
5	3.25	1.2550
6	1.3750	1.4975
7	1.5625	1.50
8	1.4380	1.50
9	2.3150	1.50
10	1.4380	1.50
11	2.3130	1.50
12	1.4380	1.50
13	2.3130	1.50
14	1.4380	1.50
15	2.3130	1.50
16	1.4380	1.50
17	2.3130	1.50
18	1.4380	1.50
19	2.3130	1.50
20	1.4380	1.50
21	2.3130	1.50
22	1.4380	1.50
23	2.3130	1.50
24	1.4380	1.50
25	2.3130	1.50
26	1.4380	1.50
27	2.3130	1.50
28	1.4380	1.50
29	2.1245	1.50
30	3.6225	1.50
31	2.3750	1.255
32	13.0	1.25
33	3.25	1.25
34	1.5	1.0
35	4.25	1.0
36	1.1250	.394

Bearing Description (both bearings)

Bearing 1 station number	4	
Bearing 2 station number	33	
Oil Viscosity	2.0E-6	$(lb*s/in^2)$
Bearing Length	1.0	(in)
Bearing Diameter	2.5	(in)
Bearing Radial Clearance	.003	(in)

Bearing Stiffness Coefficients

Speed (rpm)	K_{xx} (lb/in)	K_{xy} (lb/in)	K_{yx} (lb/in)	K_{yy} (lb/in)
500	10000.	0.0	0.0	.8E6
1000	12330.	0.0	0.0	.74E6
1500	15000.	0.0	0.0	.62E6
2000	17900.	0.0	0.0	.573E6
2500	19500.	0.0	0.0	.55E6
3000	21000.	0.0	0.0	.524E6
3500	23200.	0.0	0.0	.48E6
4000	25280.	0.0	0.0	.450E6
4500	27430.	0.0	0.0	.428E6
5000	29600.	0.0	0.0	.407E6
5500	31000.	0.0	0.0	.38E6
6000	34000.	0.0	0.0	.37E6
6500	36000.	0.0	0.0	.355E6
7000	36000.	0.0	0.0	.345E6
7500	38500.	0.0	0.0	.344E6
8000	41900.	0.0	0.0	.342E6

Bearing Damping Coefficients

Speed (rpm)	C_{xx} (lb*s/in)	C_{xy} (lb*s/in)	C_{yx} (lb*s/in)	C_{yy} (lb*s/in)
500.	280.	0.0	0.0	7500.
1000.	280.	0.0	0.0	7240.
1500.	280.	0.0	0.0	4500.
2000.	280.	0.0	0.0	2100.
2500.	280.	0.0	0.0	1800.
3000.	280.	0.0	0.0	1470.
3500.	280.	0.0	0.0	1220.
4000.	280.	0.0	0.0	1120.
4500.	280.	0.0	0.0	1020.
5000.	280.	0.0	0.0	910.
5500.	280.	0.0	0.0	840.
6000.	280.	0.0	0.0	700.
6500.	280.	0.0	0.0	669.
7000.	280.	0.0	0.0	620.
7500.	280.	0.0	0.0	550.
8000.	280.	0.0	0.0	500.

Seal Descriptions

Seal Number	Station
1	9
2	11
3	13
4	15
5	17
6	19
7	21
8	23
9	25
10	27
11	29
12	30

Seal Stiffness Input

Part 1   Speed = 1100 rpm

Seal Number	K_{xx} (lb/in)	K_{xy} (lb/in)	$K_{x\phi}$ (lb/rad)	$K_{x\theta}$ (lb/rad)
1	686.	263.	0.0	0.0
2	481.	194.	0.0	0.0
3	483.	195.	0.0	0.0
4	483.	196.	0.0	0.0
5	487.	197.	0.0	0.0
6	489.	198.	0.0	0.0
7	493.	199.	0.0	0.0
8	496.	200.	0.0	0.0
9	499.	201.	0.0	0.0
10	503.	202.	0.0	0.0
11	348.	175.	0.0	0.0
12	11834.	9622.	0.0	0.0

Part 2   Speed = 1100 rpm

Seal Number	$K_{\phi z}$ (lb)	$K_{\phi y}$ (lb)	$K_{\phi\phi}$ (lb*in/rad)	$K_{\phi\theta}$ (lb*in/rad)
1	0.0	0.0	0.0	0.0
2	0.0	0.0	0.0	0.0
3	0.0	0.0	0.0	0.0
4	0.0	0.0	0.0	0.0
5	0.0	0.0	0.0	0.0
6	0.0	0.0	0.0	0.0
7	0.0	0.0	0.0	0.0
8	0.0	0.0	0.0	0.0
9	0.0	0.0	0.0	0.0
10	0.0	0.0	0.0	0.0
11	0.0	0.0	0.0	0.0
12	0.0	0.0	0.0	0.0

Seal Damping Input

Part 1   Speed = 1100 rpm

Seal Number	C_{xx} $(lb*s/in)$	C_{xy} $(lb*s/in)$	$C_{x\phi}$ $(lb*s/rad)$	$C_{x\theta}$ $(lb*s/rad)$
1	3.93	.311	0.0	0.0
2	3.13	.276	0.0	0.0
3	3.14	.279	0.0	0.0
4	3.15	.282	0.0	0.0
5	3.16	.285	0.0	0.0
6	3.17	.288	0.0	0.0
7	3.18	.291	0.0	0.0
8	3.19	.294	0.0	0.0
9	3.20	.297	0.0	0.0
10	3.21	.3	0.0	0.0
11	2.04	.19	0.0	0.0
12	246.	33.25	0.0	0.0

Part 2   Speed = 1100 rpm

Seal Number	$C_{\phi x}$ $(lb*s)$	$C_{\phi y}$ $(lb*s)$	$C_{\phi\phi}$ $(\frac{lb*s*in}{rad})$	$C_{\phi\theta}$ $(\frac{lb*s*in}{rad})$
1	0.0	0.0	0.0	0.0
2	0.0	0.0	0.0	0.0
3	0.0	0.0	0.0	0.0
4	0.0	0.0	0.0	0.0
5	0.0	0.0	0.0	0.0
6	0.0	0.0	0.0	0.0
7	0.0	0.0	0.0	0.0
8	0.0	0.0	0.0	0.0
9	0.0	0.0	0.0	0.0
10	0.0	0.0	0.0	0.0
11	0.0	0.0	0.0	0.0
12	0.0	0.0	0.0	0.0

Seal Inertia Input

Part 1   Speed = 1100 rpm

Seal Number	M_{xx} $(lb * s^2/in)$	M_{xy} $(lb * s^2/in)$	$M_{x\phi}$ $(lb * s^2/rad)$	$M_{x\theta}$ $(lb * s^2/rad)$
1	0.003	0.0	0.0	0.0
2	0.002	0.0	0.0	0.0
3	0.002	0.0	0.0	0.0
4	0.002	0.0	0.0	0.0
5	0.002	0.0	0.0	0.0
6	0.002	0.0	0.0	0.0
7	0.002	0.0	0.0	0.0
8	0.002	0.0	0.0	0.0
9	0.002	0.0	0.0	0.0
10	0.002	0.0	0.0	0.0
11	0.0015	0.00003	0.0	0.0
12	0.3156	-.0032	0.0	0.0

Part 2   Speed = 1100 rpm

Seal Number	$M_{\phi x}$ $(lb * s^2)$	$M_{\phi y}$ $(lb * s^2)$	$M_{\phi\phi}$ $(\frac{lb*s^2*in}{rad})$	$M_{\phi\theta}$ $(\frac{lb*s^2*in}{rad})$
1	0.0	0.0	0.0	0.0
2	0.0	0.0	0.0	0.0
3	0.0	0.0	0.0	0.0
4	0.0	0.0	0.0	0.0
5	0.0	0.0	0.0	0.0
6	0.0	0.0	0.0	0.0
7	0.0	0.0	0.0	0.0
8	0.0	0.0	0.0	0.0
9	0.0	0.0	0.0	0.0
10	0.0	0.0	0.0	0.0
11	0.0	0.0	0.0	0.0
12	0.0	0.0	0.0	0.0

Seal Stiffness Input

Part 1   Speed = 3300 rpm

Seal Number	K_{xx} (lb/in)	K_{xy} (lb/in)	$K_{x\phi}$ (lb/rad)	$K_{x\theta}$ (lb/rad)
1	5948.	2544.	0.0	0.0
2	4810.	2078.	0.0	0.0
3	4830.	2085.	0.0	0.0
4	4840.	2095.	0.0	0.0
5	4870.	2105.	0.0	0.0
6	4890.	2106.	0.0	0.0
7	4930.	2108.	0.0	0.0
8	4960.	2112.	0.0	0.0
9	4990.	2117.	0.0	0.0
10	5008.	2120.	0.0	0.0
11	3672.	1854.	0.0	0.0
12	.125E6	71134.	0.0	0.0

Part 2   Speed = 3300 rpm

Seal Number	$K_{\phi x}$ (lb)	$K_{\phi y}$ (lb)	$K_{\phi\phi}$ ($lb*in/rad$)	$K_{\phi\theta}$ ($lb*in/rad$)
1	0.0	0.0	0.0	0.0
2	0.0	0.0	0.0	0.0
3	0.0	0.0	0.0	0.0
4	0.0	0.0	0.0	0.0
5	0.0	0.0	0.0	0.0
6	0.0	0.0	0.0	0.0
7	0.0	0.0	0.0	0.0
8	0.0	0.0	0.0	0.0
9	0.0	0.0	0.0	0.0
10	0.0	0.0	0.0	0.0
11	0.0	0.0	0.0	0.0
12	0.0	0.0	0.0	0.0

Seal Damping Input
Part 1 Speed = 3300 rpm

Seal Number	C_{zz} ($lb*s/in$)	C_{zy} ($lb*s/in$)	$C_{z\phi}$ ($lb*s/rad$)	$C_{z\theta}$ ($lb*s/rad$)
1	12.64	.79	0.0	0.0
2	10.81	.69	0.0	0.0
3	10.83	.70	0.0	0.0
4	10.85	.70	0.0	0.0
5	10.87	.71	0.0	0.0
6	10.90	.71	0.0	0.0
7	10.92	.72	0.0	0.0
8	10.94	.72	0.0	0.0
9	10.96	.73	0.0	0.0
10	11.0	.74	0.0	0.0
11	7.3	.47	0.0	0.0
12	686.	97.1	0.0	0.0

Part 2 Speed = 3300 rpm

Seal Number	$C_{\phi z}$ ($lb*s$)	$C_{\phi y}$ ($lb*s$)	$C_{\phi\phi}$ ($\frac{lb*s*in}{rad}$)	$C_{\phi\theta}$ ($\frac{lb*s*in}{rad}$)
1	0.0	0.0	0.0	0.0
2	0.0	0.0	0.0	0.0
3	0.0	0.0	0.0	0.0
4	0.0	0.0	0.0	0.0
5	0.0	0.0	0.0	0.0
6	0.0	0.0	0.0	0.0
7	0.0	0.0	0.0	0.0
8	0.0	0.0	0.0	0.0
9	0.0	0.0	0.0	0.0
10	0.0	0.0	0.0	0.0
11	0.0	0.0	0.0	0.0
12	0.0	0.0	0.0	0.0

Seal Inertia Input
Part 1   Speed = 3300 rpm

Seal Number	M_{xx} $(lb*s^2/in)$	M_{xy} $(lb*s^2/in)$	$M_{x\phi}$ $(lb*s^2/rad)$	$M_{x\theta}$ $(lb*s^2/rad)$
1	0.003	0.0	0.0	0.0
2	0.003	0.0	0.0	0.0
3	0.003	0.0	0.0	0.0
4	0.003	0.0	0.0	0.0
5	0.003	0.0	0.0	0.0
6	0.003	0.0	0.0	0.0
7	0.003	0.0	0.0	0.0
8	0.003	0.0	0.0	0.0
9	0.003	0.0	0.0	0.0
10	0.003	0.0	0.0	0.0
11	0.002	0.0	0.0	0.0
12	0.316	0.003	0.0	0.0

Part 2   Speed = 3300 rpm

Seal Number	$M_{\phi x}$ $(lb*s^4)$	$M_{\phi y}$ $(lb*s^2)$	$M_{\phi\phi}$ $(\frac{lb*s^2*in}{rad})$	$M_{\phi\theta}$ $(\frac{lb*s^2*in}{rad})$
1	0.0	0.0	0.0	0.0
2	0.0	0.0	0.0	0.0
3	0.0	0.0	0.0	0.0
4	0.0	0.0	0.0	0.0
5	0.0	0.0	0.0	0.0
6	0.0	0.0	0.0	0.0
7	0.0	0.0	0.0	0.0
8	0.0	0.0	0.0	0.0
9	0.0	0.0	0.0	0.0
10	0.0	0.0	0.0	0.0
11	0.0	0.0	0.0	0.0
12	0.0	0.0	0.0	0.0

Seal Stiffness Input

Part 1   Speed = 6600 rpm

Seal Number	K_{xx} (lb/in)	K_{xy} (lb/in)	$K_{x\phi}$ (lb/rad)	$K_{x\theta}$ (lb/rad)
1	23116.	10716.	0.0	0.0
2	18810.	8776.	0.0	0.0
3	18910.	8786.	0.0	0.0
4	19010.	8796.	0.0	0.0
5	19110.	8806.	0.0	0.0
6	19210.	8816.	0.0	0.0
7	19250.	8826.	0.0	0.0
8	19310.	8846.	0.0	0.0
9	19390.	8866.	0.0	0.0
10	19440.	8893.	0.0	0.0
11	14134.	7726.	0.0	0.0
12	.55E6	.255E6	0.0	0.0

Part 2   Speed = 6600 rpm

Seal Number	$K_{\phi x}$ (lb)	$K_{\phi y}$ (lb)	$K_{\phi\phi}$ ($lb*in/rad$)	$K_{\phi\theta}$ ($lb*in/rad$)
1	0.0	0.0	0.0	0.0
2	0.0	0.0	0.0	0.0
3	0.0	0.0	0.0	0.0
4	0.0	0.0	0.0	0.0
5	0.0	0.0	0.0	0.0
6	0.0	0.0	0.0	0.0
7	0.0	0.0	0.0	0.0
8	0.0	0.0	0.0	0.0
9	0.0	0.0	0.0	0.0
10	0.0	0.0	0.0	0.0
11	0.0	0.0	0.0	0.0
12	0.0	0.0	0.0	0.0

Seal Damping Input

Part 1   Speed = 6600 rpm

Seal Number	C_{xx} (lb * s/in)	C_{xy} (lb * s/in)	$C_{x\phi}$ (lb * s/rad)	$C_{x\theta}$ (lb * s/rad)
1	26.7	1.35	0.0	0.0
2	22.92	1.19	0.0	0.0
3	22.99	1.2	0.0	0.0
4	23.03	1.21	0.0	0.0
5	23.06	1.22	0.0	0.0
6	23.08	1.23	0.0	0.0
7	23.10	1.24	0.0	0.0
8	23.12	1.25	0.0	0.0
9	23.14	1.26	0.0	0.0
10	23.16	1.28	0.0	0.0
11	15.36	.813	0.0	0.0
12	1320.	190.	0.0	0.0

Part 2   Speed = 6600 rpm

Seal Number	$C_{\phi x}$ (lb * s)	$C_{\phi y}$ (lb * s)	$C_{\phi\phi}$ ($\frac{lb*s*in}{rad}$)	$C_{\phi\theta}$ ($\frac{lb*s*in}{rad}$)
1	0.0	0.0	0.0	0.0
2	0.0	0.0	0.0	0.0
3	0.0	0.0	0.0	0.0
4	0.0	0.0	0.0	0.0
5	0.0	0.0	0.0	0.0
6	0.0	0.0	0.0	0.0
7	0.0	0.0	0.0	0.0
8	0.0	0.0	0.0	0.0
9	0.0	0.0	0.0	0.0
10	0.0	0.0	0.0	0.0
11	0.0	0.0	0.0	0.0
12	0.0	0.0	0.0	0.0

Seal Inertia Input

Part 1   Speed = 6600 rpm

Seal Number	M_{xx} $(lb*s^2/in)$	M_{xy} $(lb*s^2/in)$	$M_{x\phi}$ $(lb*s^2/rad)$	$M_{x\theta}$ $(lb*s^2/rad)$
1	0.002	0.0	0.0	0.0
2	0.002	0.0	0.0	0.0
3	0.002	0.0	0.0	0.0
4	0.002	0.0	0.0	0.0
5	0.002	0.0	0.0	0.0
6	0.002	0.0	0.0	0.0
7	0.002	0.0	0.0	0.0
8	0.002	0.0	0.0	0.0
9	0.002	0.0	0.0	0.0
10	0.002	0.0	0.0	0.0
11	0.001	0.0	0.0	0.0
12	0.316	0.0	0.0	0.0

Part 2   Speed = 6600 rpm

Seal Number	$M_{\phi x}$ $(lb*s^2)$	$M_{\phi y}$ $(lb*s^2)$	$M_{\phi\phi}$ $(\frac{lb*s^2*in}{rad})$	$M_{\phi\theta}$ $(\frac{lb*s^2*in}{rad})$
1	0.0	0.0	0.0	0.0
2	0.0	0.0	0.0	0.0
3	0.0	0.0	0.0	0.0
4	0.0	0.0	0.0	0.0
5	0.0	0.0	0.0	0.0
6	0.0	0.0	0.0	0.0
7	0.0	0.0	0.0	0.0
8	0.0	0.0	0.0	0.0
9	0.0	0.0	0.0	0.0
10	0.0	0.0	0.0	0.0
11	0.0	0.0	0.0	0.0
12	0.0	0.0	0.0	0.0

APPENDIX E

INPUT DATA FOR EDI CASE THREE

Gajan (1987) The system of units used is pound, inch, second

Shaft Material Properties

Density	.7764E-3	$(lb * s^2/in^4)$
Elastic Modulus	30.E6	(lb/in^2)
Shear Modulus	.82E11	(lb/in^2)

Concentrated Masses

Station Number	Concentrated Mass $(lb * s^2/in)$	Diametral Mom. of I. $(lb * s^2 * in)$	Polar Mom. of I. $(lb * s^2 * in)$
1	.05564	.14383	.2963
5	.015528	0.0	0.0
9	.040217	.108	.21580
11	.02976	.1056	.211
13	.031056	.109	.218
15	.031056	.109	.218
17	.031056	.109	.218
19	.031056	.109	.218
21	.031056	.109	.218
23	.029500	.1056	.211
25	.031056	.109	.218
27	.030800	.1079	.2158
29	.029762	.1056	.211
30	.037525	0.0	0.0
31	.010691	0.0	0.0
32	.015528	0.0	0.0
35	.035481	0.0	0.0
37	.004558	0.0	0.0

Shaft Description

Element Number	Length (in)	Outer Radius (in)
1	1.44	1.19
2	1.185	1.213
3	5.1875	1.25
4	13.125	1.2525
5	3.25	1.2550
6	1.3750	1.4975
7	1.5625	1.50
8	1.4380	1.50
9	2.3150	1.50
10	1.4380	1.50
11	2.3130	1.50
12	1.4380	1.50
13	2.3130	1.50
14	1.4380	1.50
15	2.3130	1.50
16	1.4380	1.50
17	2.3130	1.50
18	1.4380	1.50
19	2.3130	1.50
20	1.4380	1.50
21	2.3130	1.50
22	1.4380	1.50
23	2.3130	1.50
24	1.4380	1.50
25	2.3130	1.50
26	1.4380	1.50
27	2.3130	1.50
28	1.4380	1.50
29	2.1245	1.50
30	3.6225	1.50
31	2.3750	1.255
32	13.0	1.25
33	3.25	1.25
34	1.5	1.0
35	4.25	1.0
36	1.1250	.394

Bearing Description (both bearings)

Bearing 1 station number	4	
Bearing 2 station number	33	
Oil Viscosity	2.0E-6	$(lb * s/in^2)$
Bearing Length	1.0	(in)
Bearing Diameter	2.5	(in)
Bearing Radial Clearance	.003	(in)

Bearing Stiffness Coefficients

Speed (rpm)	K_{zz} (lb/in)	K_{zy} (lb/in)	K_{yz} (lb/in)	K_{yy} (lb/in)
500	10000.	0.0	0.0	.8E6
1000	12330.	0.0	0.0	.74E6
1500	15000.	0.0	0.0	.62E6
2000	17900.	0.0	0.0	.573E6
2500	19500.	0.0	0.0	.55E6
3000	21000.	0.0	0.0	.524E6
3500	23200.	0.0	0.0	.48E6
4000	25280.	0.0	0.0	.450E6
4500	27430.	0.0	0.0	.428E6
5000	29600.	0.0	0.0	.407E6
5500	31000.	0.0	0.0	.38E6
6000	34000.	0.0	0.0	.37E6
6500	36000.	0.0	0.0	.355E6
7000	36000.	0.0	0.0	.345E6
7500	38500.	0.0	0.0	.344E6
8000	41900.	0.0	0.0	.342E6

Bearing Damping Coefficients

Speed (rpm)	C_{xx} (lb * s/in)	C_{xy} (lb * s/in)	C_{yx} (lb * s/in)	C_{yy} (lb * s/in)
500.	280.	0.0	0.0	7500.
1000.	280.	0.0	0.0	7240.
1500.	280.	0.0	0.0	4500.
2000.	280.	0.0	0.0	2100.
2500.	280.	0.0	0.0	1800.
3000.	280.	0.0	0.0	1470.
3500.	280.	0.0	0.0	1220.
4000.	280.	0.0	0.0	1120.
4500.	280.	0.0	0.0	1020.
5000.	280.	0.0	0.0	910.
5500.	280.	0.0	0.0	840.
6000.	280.	0.0	0.0	700.
6500.	280.	0.0	0.0	669.
7000.	280.	0.0	0.0	620.
7500.	280.	0.0	0.0	550.
8000.	280.	0.0	0.0	500.

Seal Descriptions

Seal Number	Station
1	9
2	11
3	13
4	15
5	17
6	19
7	21
8	23
9	25
10	27
11	29
12	30

Seal Stiffness Input

Part 1   Speed = 1100 rpm

Seal Number	K_{xx} (lb/in)	K_{xy} (lb/in)	$K_{x\phi}$ (lb/rad)	$K_{x\theta}$ (lb/rad)
1	686.	263.	-1600.	1600.
2	481.	194.	-1120.	1120.
3	483.	195.	-1123.	1123.
4	483.	196.	-1126.	1126.
5	487.	197.	-1129.	1129.
6	489.	198.	-1132.	1132.
7	493.	199.	-1135.	1135.
8	496.	200.	-1139.	1139.
9	499.	201.	-1146.	1146.
10	503.	202.	-1153.	1153.
11	348.	175.	-800.	800.
12	11834.	9622.	-.293E6	.293E6

Part 2   Speed = 1100 rpm

Seal Number	$K_{\phi x}$ (lb)	$K_{\phi y}$ (lb)	$K_{\phi\phi}$ (lb*in/rad)	$K_{\phi\theta}$ (lb*in/rad)
1	74.	186.	463.	48.
2	54.	129.	323.	36.
3	54.2	129.4	324.3	36.2
4	54.4	129.8	325.5	36.4
5	54.6	130.6	327.0	36.6
6	54.9	131.6	328.3	36.8
7	55.2	132.6	329.7	37.0
8	55.7	134.0	331.0	37.1
9	55.9	135.0	333.0	37.2
10	56.1	137.0	335.0	37.3
11	49.	95.	233.	30.5
12	20444.	14654.	.458E6	91398.

Seal Damping Input

Part 1   Speed = 1100 rpm

Seal Number	C_{xx} $(lb*s/in)$	C_{xy} $(lb*s/in)$	$C_{x\phi}$ $(lb*s/rad)$	$C_{x\theta}$ $(lb*s/rad)$
1	3.93	.311	.160	.160
2	3.13	.276	.137	.137
3	3.14	.279	.1375	.1375
4	3.15	.282	.138	.138
5	3.16	.285	.1385	.1385
6	3.17	.288	.1389	.1389
7	3.18	.291	.1393	.1393
8	3.19	.294	.1397	.1397
9	3.20	.297	.1399	.1399
10	3.21	.3	.141	.141
11	2.04	.19	.095	.095
12	246.2	33.25	72.	72.

Part 2   Speed = 1100 rpm

Seal Number	$C_{\phi x}$ $(lb*s)$	$C_{\phi y}$ $(lb*s)$	$C_{\phi\phi}$ $(\frac{lb*s*in}{rad})$	$C_{\phi\theta}$ $(\frac{lb*s*in}{rad})$
1	.116	1.1	.76	.057
2	.105	.876	.61	.0526
3	.1052	.879	.613	.05265
4	.1054	.882	.616	.0527
5	.1057	.885	.619	.05275
6	.1059	.888	.622	.0528
7	.1062	.891	.625	.05285
8	.1065	.893	.627	.0529
9	.1067	.895	.629	.05295
10	.107	.997	.63	.053
11	.07	.57	.4	.036
12	76.	494.	1897.	182.

Seal Inertia Input
Part 1   Speed = 1100 rpm

Seal Number	M_{xx} $(lb*s^2/in)$	M_{xy} $(lb*s^2/in)$	$M_{x\phi}$ $(lb*s^2/rad)$	$M_{x\theta}$ $(lb*s^2/rad)$
1	.003	0.0	-.002	.002
2	.002	0.0	-.001	.001
3	.002	0.0	-.001	.001
4	.002	0.0	-.001	.001
5	.002	0.0	-.001	.001
6	.002	0.0	-.001	.001
7	.002	0.0	-.001	.001
8	.002	0.0	-.001	.001
9	.002	0.0	-.001	.001
10	.002	0.0	-.001	.001
11	.0015	.00003	-.001	-.001
12	.3156	-.0032	-.7	-.7

Part 2   Speed = 1100 rpm

Seal Number	$M_{\phi x}$ $(lb*s^s)$	$M_{\phi y}$ $(lb*s^2)$	$M_{\phi\phi}$ $(\frac{lb*s^2*in}{rad})$	$M_{\phi\theta}$ $(\frac{lb*s^2*in}{rad})$
1	0.0	.0012	.001	0.0
2	0.0	.0012	.001	0.0
3	0.0	.0012	.001	0.0
4	0.0	.0012	.001	0.0
5	0.0	.0012	.001	0.0
6	0.0	.0012	.001	0.0
7	0.0	.0012	.001	0.0
8	0.0	.0012	.001	0.0
9	0.0	.0012	.001	0.0
10	0.0	.0012	.001	0.0
11	0.0	.005	.0005	0.0
12	-.007	.715	1.72	-.005

Seal Stiffness Input

Part 1   Speed = 3300 rpm

Seal Number	K_{xx} (lb/in)	K_{xy} (lb/in)	$K_{x\phi}$ (lb/rad)	$K_{x\theta}$ (lb/rad)
1	5948.	2544.	-15520.	15520.
2	4810.	2078.	-12707.	12707.
3	4830.	2085.	-12737.	12737.
4	4840.	2095.	-12747.	12747.
5	4870.	2105.	-12777.	12777.
6	4890.	2106.	-12807.	12807.
7	4930.	2108.	-12837.	12837.
8	4960.	2112.	-12867.	12867.
9	4990.	2117.	-12900.	12900.
10	5008.	2120.	-12951.	12951.
11	3672.	1854.	-9610.	9610.
12	.125E6	71134.	-.215E7	.215E7

Part 2   Speed = 3300 rpm

Seal Number	$K_{\phi x}$ (lb)	$K_{\phi y}$ (lb)	$K_{\phi\phi}$ $(lb*in/rad)$	$K_{\phi\theta}$ $(lb*in/rad)$
1	698.	1570.	4370.	442.
2	567.	1258.	3558.	366.
3	568.	1262.	3568.	367.
4	569.	1268.	3578.	368.
5	570.	1273.	3588.	369.
6	572.	1280.	3598.	371.
7	574.	1288.	3608.	373.
8	576.	1293.	3618.	374.
9	578.	1308.	3630.	375.
10	580.	1316.	3644.	377.
11	510.	966.	2703.	315.
12	.146E6	.156E6	.416E7	.751E6

Seal Damping Input
Part 1   Speed = 3300 rpm

Seal Number	C_{xx} $(lb * s/in)$	C_{xy} $(lb * s/in)$	$C_{x\phi}$ $(lb * s/rad)$	$C_{x\theta}$ $(lb * s/rad)$
1	12.64	.79	.51	.51
2	10.81	.69	.44	.44
3	10.83	.70	.44	.44
4	10.85	.70	.44	.44
5	10.87	.71	.44	.44
6	10.90	.71	.44	.44
7	10.92	.72	.44	.44
8	10.94	.72	.44	.44
9	10.96	.73	.44	.44
10	11.0	.74	.44	.44
11	7.3	.47	.31	.31
12	686.	97.1	210.	210.

Part 2   Speed = 3300 rpm

Seal Number	$C_{\phi x}$ $(lb * s)$	$C_{\phi y}$ $(lb * s)$	$C_{\phi\phi}$ $(\frac{lb*s*in}{rad})$	$C_{\phi\theta}$ $(\frac{lb*s*in}{rad})$
1	.311	3.45	2.33	.19
2	.272	2.95	2.0	.163
3	.275	2.95	2.02	.163
4	.278	2.96	2.03	.164
5	.281	2.96	2.04	.164
6	.284	2.97	2.05	.165
7	.287	2.97	2.06	.166
8	.290	2.98	2.07	.167
9	.296	2.98	2.08	.168
10	.3	3.0	2.1	.17
11	.2	2.0	1.4	.12
12	.220	1334.	5555.	524.

Seal Inertia Input
Part 1   Speed = 3300 rpm

Seal Number	M_{xx} ($lb * s^2/in$)	M_{xy} ($lb * s^2/in$)	$M_{x\phi}$ ($lb * s^2/rad$)	$M_{x\theta}$ ($lb * s^2/rad$)
1	.003	0.0	-.001	.001
2	.003	0.0	-.001	.001
3	.003	0.0	-.001	.001
4	.003	0.0	-.001	.001
5	.003	0.0	-.001	.001
6	.003	0.0	-.001	.001
7	.003	0.0	-.001	.001
8	.003	0.0	-.001	.001
9	.003	0.0	-.001	.001
10	.003	0.0	-.001	.001
11	.002	0.0	-.0008	.0008
12	.316	.003	-.7	.7

Part 2   Speed = 3300 rpm

Seal Number	$M_{\phi x}$ ($lb * s^2$)	$M_{\phi y}$ ($lb * s^2$)	$M_{\phi\phi}$ ($\frac{lb*s^2*in}{rad}$)	$M_{\phi\theta}$ ($\frac{lb*s^2*in}{rad}$)
1	0.0	.001	.0005	0.0
2	0.0	.001	.0005	0.0
3	0.0	.001	.0005	0.0
4	0.0	.001	.0005	0.0
5	0.0	.001	.0005	0.0
6	0.0	.001	.0005	0.0
7	0.0	.001	.0005	0.0
8	0.0	.001	.0005	0.0
9	0.0	.001	.0005	0.0
10	0.0	.001	.0005	0.0
11	0.0	.001	.0005	0.0
12	-.006	.70	1.726	-.0053

Seal Stiffness Input

Part 1   Speed = 6600 rpm

Seal Number	K_{xx} (lb/in)	K_{xy} (lb/in)	$K_{x\phi}$ (lb/rad)	$K_{x\theta}$ (lb/rad)
1	23116.	10716.	-65911.	65911.
2	18810.	8776.	-54222.	54222.
3	18910.	8786.	-54250.	54250.
4	19010.	8796.	-54300.	54300.
5	19110.	8806.	-54350.	54350.
6	19210.	8816.	-54400.	54400.
7	19250.	8826.	-54450.	54450.
8	19310.	8846.	-54500.	54500.
9	19390.	8866.	-54550.	54550.
10	19440.	8893.	-54625.	54625.
11	14134.	7726.	-40240.	40240.
12	.55E6	.255E6	-.886E7	.886E7

Part 2   Speed = 6600 rpm

Seal Number	$K_{\phi x}$ (lb)	$K_{\phi y}$ (lb)	$K_{\phi \phi}$ (lb * in/rad)	$K_{\phi \theta}$ (lb * in/rad)
1	2906.	6000.	18254.	1811.
2	2368.	4840.	14946.	1811.
3	2372.	4850.	14960.	1508.
4	2378.	4860.	14970.	1512.
5	2381.	4875.	14980.	1516.
6	2388.	4890.	15000.	1520.
7	2391.	4900.	15020.	1524.
8	2398.	4925.	15076.	1528.
9	2401.	4960.	15099.	1532.
10	2407.	5023.	15118.	1536.
11	2100.	3656.	11138.	1283.
12	.51E6	.687E6	.168E8	.286E8

Seal Damping Input

Part 1   Speed = 6600 rpm

Seal Number	C_{xx} $(lb*s/in)$	C_{xy} $(lb*s/in)$	$C_{x\phi}$ $(lb*s/rad)$	$C_{x\theta}$ $(lb*s/rad)$
1	26.7	1.35	1.05	1.05
2	22.92	1.19	.9	.9
3	22.99	1.2	.903	.903
4	23.03	1.21	.905	.905
5	23.06	1.22	.907	.907
6	23.08	1.23	.909	.909
7	23.10	1.24	.911	.911
8	23.12	1.25	.913	.913
9	23.14	1.26	.915	.915
10	23.16	1.28	.917	.917
11	15.36	.813	.657	.657
12	1320.	190.	408.	408.

Part 2   Speed = 6600 rpm

Seal Number	$C_{\phi x}$ $(lb*s)$	$C_{\phi y}$ $(lb*s)$	$C_{\phi\phi}$ $(\frac{lb*s*in}{rad})$	$C_{\phi\theta}$ $(\frac{lb*s*in}{rad})$
1	.56	7.2	4.72	.39
2	.49	6.2	4.12	.33
3	.5	6.2	4.13	.331
4	.5	6.2	4.13	.331
5	.5	6.2	4.13	.331
6	.5	6.2	4.13	.331
7	.5	6.2	4.13	.331
8	.5	6.2	4.13	.331
9	.5	6.2	4.13	.331
10	.52	6.25	4.15	.336
11	.35	4.15	2.75	.24
12	427.	2512.	11028.	1016.

Seal Inertia Input

Part 1   Speed = 6600 rpm

Seal Number	M_{xx} $(lb * s^2/in)$	M_{xy} $(lb * s^2/in)$	$M_{x\phi}$ $(lb * s^2/rad)$	$M_{x\theta}$ $(lb * s^2/rad)$
1	.002	0.0	-.002	.002
2	.002	0.0	-.002	.002
3	.002	0.0	-.002	.002
4	.002	0.0	-.002	.002
5	.002	0.0	-.002	.002
6	.002	0.0	-.002	.002
7	.002	0.0	-.002	.002
8	.002	0.0	-.002	.002
9	.002	0.0	-.002	.002
10	.002	0.0	-.002	.002
11	.001	0.0	-.001	.001
12	.316	0.0	-.7	.7

Part 2   Speed = 6600 rpm

Seal Number	$M_{\phi x}$ $(lb * s^3)$	$M_{\phi y}$ $(lb * s^2)$	$M_{\phi\phi}$ $(\frac{lb*s^2*in}{rad})$	$M_{\phi\theta}$ $(\frac{lb*s^2*in}{rad})$
1	0.0	.001	.0008	0.0
2	0.0	.001	.0008	0.0
3	0.0	.001	.0008	0.0
4	0.0	.001	.0008	0.0
5	0.0	.001	.0008	0.0
6	0.0	.001	.0008	0.0
7	0.0	.001	.0008	0.0
8	0.0	.001	.0008	0.0
9	0.0	.001	.0008	0.0
10	0.0	.001	.0008	0.0
11	0.0	.001	.0006	0.0
12	0.0	.7	1.7	0.0

APPENDIX F

INPUT DATA FOR EDI CASE FOUR

Gajan (1987) The system of units used is pound, inch, second

Shaft Material Properties

Density	.7764E-3	$(lb * s^2/in^4)$
Elastic Modulus	30.E6	(lb/in^2)
Shear Modulus	.82E11	(lb/in^2)

Concentrated Masses

Station Number	Concentrated Mass $(lb * s^2/in)$	Diametral Mom. of I. $(lb * s^2 * in)$	Polar Mom. of I. $(lb * s^2 * in)$
1	.05564	.14383	.2963
5	.015528	0.0	0.0
9	.040217	.108	.21580
11	.02976	.1056	.211
13	.031056	.109	.218
15	.031056	.109	.218
17	.031056	.109	.218
19	.031056	.109	.218
21	.031056	.109	.218
23	.029500	.1056	.211
25	.031056	.109	.218
27	.030800	.1079	.2158
29	.029762	.1056	.211
30	.037525	0.0	0.0
31	.010691	0.0	0.0
32	.015528	0.0	0.0
35	.035481	0.0	0.0
37	.004558	0.0	0.0

Shaft Description

Element Number	Length (in)	Outer Radius (in)
1	1.44	1.19
2	1.185	1.213
3	5.1875	1.25
4	13.125	1.2525
5	3.25	1.2550
6	1.3750	1.4975
7	1.5625	1.50
8	1.4380	1.50
9	2.3150	1.50
10	1.4380	1.50
11	2.3130	1.50
12	1.4380	1.50
13	2.3130	1.50
14	1.4380	1.50
15	2.3130	1.50
16	1.4380	1.50
17	2.3130	1.50
18	1.4380	1.50
19	2.3130	1.50
20	1.4380	1.50
21	2.3130	1.50
22	1.4380	1.50
23	2.3130	1.50
24	1.4380	1.50
25	2.3130	1.50
26	1.4380	1.50
27	2.3130	1.50
28	1.4380	1.50
29	2.1245	1.50
30	3.6225	1.50
31	2.3750	1.255
32	13.0	1.25
33	3.25	1.25
34	1.5	1.0
35	4.25	1.0
36	1.1250	.394

Bearing Description (both bearings)

Bearing 1 station number	4	
Bearing 2 station number	33	
Oil Viscosity	2.0E-6	$(lb * s/in^2)$
Bearing Length	1.0	(in)
Bearing Diameter	2.5	(in)
Bearing Radial Clearance	.003	(in)

Bearing Sommerfeld Number and Attitude Angle

Eccentricity Ratio	Sommerfeld Number	Attitude Angle (rad)
0.0	12.2	0.0
0.1	6.46	0.0
0.2	3.43	0.0
0.3	1.82	0.0
0.4	.965	0.0
0.5	.512	0.0
0.6	.272	0.0
0.7	.144	0.0
0.8	.0764	0.0
0.9	.0405	0.0
1.0	.0215	0.0

Bearing Dimensionless Stiffness Coefficients

Eccentricity Ratio	K_{xx}	K_{xy}	K_{yx}	K_{yy}
0.0	2.01	0.0	0.0	1.67
0.1	1.79	0.0	0.0	2.14
0.2	1.56	0.0	0.0	2.74
0.3	1.34	0.0	0.0	3.50
0.4	.863	0.0	0.0	4.49
0.5	.588	0.0	0.0	5.74
0.6	.400	0.0	0.0	7.35
0.7	.273	0.0	0.0	9.41
0.8	.186	0.0	0.0	12.0
0.9	.127	0.0	0.0	15.4
1.0	.0862	0.0	0.0	19.7

Bearing Dimensionless Damping Coefficients

Eccentricity Ratio	C_{xx}	$C_{x\dot{y}}$	C_{yx}	C_{yy}
0.0	35.0	0.0	0.0	30.0
0.1	18.6	0.0	0.0	22.4
0.2	9.85	0.0	0.0	16.4
0.3	5.22	0.0	0.0	11.9
0.4	4.59	0.0	0.0	8.94
0.5	3.13	0.0	0.0	7.50
0.6	1.95	0.0	0.0	7.58
0.7	1.06	0.0	0.0	9.20
0.8	.452	0.0	0.0	12.3
0.9	.105	0.0	0.0	17.0
1.0	0.0	0.0	0.0	23.2

Seal Descriptions

Seal Number	Station
1	9
2	11
3	13
4	15
5	17
6	19
7	21
8	23
9	25
10	27
11	29
12	30

Seal Stiffness Input
Part 1   Speed = 1100 rpm

Seal Number	K_{xx} (lb/in)	K_{xy} (lb/in)	$K_{x\phi}$ (lb/rad)	$K_{x\theta}$ (lb/rad)
1	686.	263.	-1600.	1600.
2	481.	194.	-1120.	1120.
3	483.	195.	-1123.	1123.
4	483.	196.	-1126.	1126.
5	487.	197.	-1129.	1129.
6	489.	198.	-1132.	1132.
7	493.	199.	-1135.	1135.
8	496.	200.	-1139.	1139.
9	499.	201.	-1146.	1146.
10	503.	202.	-1153.	1153.
11	348.	175.	-800.	800.
12	11834.	9622.	-.293E6	.293E6

Part 2   Speed = 1100 rpm

Seal Number	$K_{\phi z}$ (lb)	$K_{\phi y}$ (lb)	$K_{\phi\phi}$ (lb * in/rad)	$K_{\phi\theta}$ (lb * in/rad)
1	74.	186.	463.	48.
2	54.	129.	323.	36.
3	54.2	129.4	324.3	36.2
4	54.4	129.8	325.5	36.4
5	54.6	130.6	327.0	36.6
6	54.9	131.6	328.3	36.8
7	55.2	132.6	329.7	37.0
8	55.7	134.0	331.0	37.1
9	55.9	135.0	333.0	37.2
10	56.1	137.0	335.0	37.3
11	49.	95.	233.	30.5
12	20444.	14654.	.458E6	91398.

Seal Damping Input
Part 1   Speed = 1100 rpm

Seal Number	C_{xx} $(lb*s/in)$	C_{xy} $(lb*s/in)$	$C_{x\phi}$ $(lb*s/rad)$	$C_{x\theta}$ $(lb*s/rad)$
1	3.93	.311	.160	.160
2	3.13	.276	.137	.137
3	3.14	.279	.1375	.1375
4	3.15	.282	.138	.138
5	3.16	.285	.1385	.1385
6	3.17	.288	.1389	.1389
7	3.18	.291	.1393	.1393
8	3.19	.294	.1397	.1397
9	3.20	.297	.1399	.1399
10	3.21	.3	.141	.141
11	2.04	.19	.095	.095
12	246.2	33.25	72.	72.

Part 2   Speed = 1100 rpm

Seal Number	$C_{\phi x}$ $(lb*s)$	$C_{\phi y}$ $(lb*s)$	$C_{\phi\phi}$ $(\frac{lb*s*in}{rad})$	$C_{\phi\theta}$ $(\frac{lb*s*in}{rad})$
1	.116	1.1	.76	.057
2	.105	.876	.61	.0526
3	.1052	.879	.613	.05265
4	.1054	.882	.616	.0527
5	.1057	.885	.619	.05275
6	.1059	.888	.622	.0528
7	.1062	.891	.625	.05285
8	.1065	.893	.627	.0529
9	.1067	.895	.629	.05295
10	.107	.997	.63	.053
11	.07	.57	.4	.036
12	76.	494.	1897.	182.

Seal Inertia Input

Part 1   Speed = 1100 rpm

Seal Number	M_{xx} $(lb*s^2/in)$	M_{xy} $(lb*s^2/in)$	$M_{x\phi}$ $(lb*s^2/rad)$	$M_{x\theta}$ $(lb*s^2/rad)$
1	.003	0.0	-.002	.002
2	.002	0.0	-.001	.001
3	.002	0.0	-.001	.001
4	.002	0.0	-.001	.001
5	.002	0.0	-.001	.001
6	.002	0.0	-.001	.001
7	.002	0.0	-.001	.001
8	.002	0.0	-.001	.001
9	.002	0.0	-.001	.001
10	.002	0.0	-.001	.001
11	.0015	.00003	-.001	-.001
12	.3156	-.0032	-.7	-.7

Part 2   Speed = 1100 rpm

Seal Number	$M_{\phi x}$ $(lb*s^2)$	$M_{\phi y}$ $(lb*s^2)$	$M_{\phi\phi}$ $(\frac{lb*s^2*in}{rad})$	$M_{\phi\theta}$ $(\frac{lb*s^2*in}{rad})$
1	0.0	.0012	.001	0.0
2	0.0	.0012	.001	0.0
3	0.0	.0012	.001	0.0
4	0.0	.0012	.001	0.0
5	0.0	.0012	.001	0.0
6	0.0	.0012	.001	0.0
7	0.0	.0012	.001	0.0
8	0.0	.0012	.001	0.0
9	0.0	.0012	.001	0.0
10	0.0	.0012	.001	0.0
11	0.0	.005	.0005	0.0
12	-.007	.715	1.72	-.005

Seal Stiffness Input

Part 1   Speed = 3300 rpm

Seal Number	K_{xx} (lb/in)	K_{xy} (lb/in)	$K_{x\phi}$ (lb/rad)	$K_{x\theta}$ (lb/rad)
1	5948.	2544.	-15520.	15520.
2	4810.	2078.	-12707.	12707.
3	4830.	2085.	-12737.	12737.
4	4840.	2095.	-12747.	12747.
5	4870.	2105.	-12777.	12777.
6	4890.	2106.	-12807.	12807.
7	4930.	2108.	-12837.	12837.
8	4960.	2112.	-12867.	12867.
9	4990.	2117.	-12900.	12900.
10	5008.	2120.	-12951.	12951.
11	3672.	1854.	-9610.	9610.
12	.125E6	71134.	-.215E7	.215E7

Part 2   Speed = 3300 rpm

Seal Number	$K_{\phi x}$ (lb)	$K_{\phi y}$ (lb)	$K_{\phi\phi}$ $(lb * in/rad)$	$K_{\phi\theta}$ $(lb * in/rad)$
1	698.	1570.	4370.	442.
2	567.	1258.	3558.	366.
3	568.	1262.	3568.	367.
4	569.	1268.	3578.	368.
5	570.	1273.	3588.	369.
6	572.	1280.	3598.	371.
7	574.	1288.	3608.	373.
8	576.	1293.	3618.	374.
9	578.	1308.	3630.	375.
10	580.	1316.	3644.	377.
11	510.	966.	2703.	315.
12	.146E6	.156E6	.416E7	.751E6

Seal Damping Input

Part 1   Speed = 3300 rpm

Seal Number	C_{xx} $(lb*s/in)$	C_{xy} $(lb*s/in)$	$C_{x\phi}$ $(lb*s/rad)$	$C_{x\theta}$ $(lb*s/rad)$
1	12.64	.79	.51	.51
2	10.81	.69	.44	.44
3	10.83	.70	.44	.44
4	10.85	.70	.44	.44
5	10.87	.71	.44	.44
6	10.90	.71	.44	.44
7	10.92	.72	.44	.44
8	10.94	.72	.44	.44
9	10.96	.73	.44	.44
10	11.0	.74	.44	.44
11	7.3	.47	.31	.31
12	686.	97.1	210.	210.

Part 2   Speed = 3300 rpm

Seal Number	$C_{\phi x}$ $(lb*s)$	$C_{\phi y}$ $(lb*s)$	$C_{\phi\phi}$ $(\frac{lb*s*in}{rad})$	$C_{\phi\theta}$ $(\frac{lb*s*in}{rad})$
1	.311	3.45	2.33	.19
2	.272	2.95	2.0	.163
3	.275	2.95	2.02	.163
4	.278	2.96	2.03	.164
5	.281	2.96	2.04	.164
6	.284	2.97	2.05	.165
7	.287	2.97	2.06	.166
8	.290	2.98	2.07	.167
9	.296	2.98	2.08	.168
10	.3	3.0	2.1	.17
11	.2	2.0	1.4	.12
12	.220	1334.	5555.	524.

Seal Inertia Input
Part 1   Speed = 3300 rpm

Seal Number	M_{xx} $(lb*s^2/in)$	M_{xy} $(lb*s^2/in)$	$M_{x\phi}$ $(lb*s^2/rad)$	$M_{x\theta}$ $(lb*s^2/rad)$
1	.003	0.0	-.001	.001
2	.003	0.0	-.001	.001
3	.003	0.0	-.001	.001
4	.003	0.0	-.001	.001
5	.003	0.0	-.001	.001
6	.003	0.0	-.001	.001
7	.003	0.0	-.001	.001
8	.003	0.0	-.001	.001
9	.003	0.0	-.001	.001
10	.003	0.0	-.001	.001
11	.002	0.0	-.0008	.0008
12	.316	.003	-.7	.7

Part 2   Speed = 3300 rpm

Seal Number	$M_{\phi x}$ $(lb*s^2)$	$M_{\phi y}$ $(lb*s^2)$	$M_{\phi\phi}$ $(\frac{lb*s^2*in}{rad})$	$M_{\phi\theta}$ $(\frac{lb*s^2*in}{rad})$
1	0.0	.001	.0005	0.0
2	0.0	.001	.0005	0.0
3	0.0	.001	.0005	0.0
4	0.0	.001	.0005	0.0
5	0.0	.001	.0005	0.0
6	0.0	.001	.0005	0.0
7	0.0	.001	.0005	0.0
8	0.0	.001	.0005	0.0
9	0.0	.001	.0005	0.0
10	0.0	.001	.0005	0.0
11	0.0	.001	.0005	0.0
12	-.006	.70	1.726	-.0053

Seal Stiffness Input
Part 1   Speed = 6600 rpm

Seal Number	K_{xx} (lb/in)	K_{xy} (lb/in)	$K_{x\phi}$ (lb/rad)	$K_{x\theta}$ (lb/rad)
1	23116.	10716.	-65911.	65911.
2	18810.	8776.	-54222.	54222.
3	18910.	8786.	-54250.	54250.
4	19010.	8796.	-54300.	54300.
5	19110.	8806.	-54350.	54350.
6	19210.	8816.	-54400.	54400.
7	19250.	8826.	-54450.	54450.
8	19310.	8846.	-54500.	54500.
9	19390.	8866.	-54550.	54550.
10	19440.	8893.	-54625.	54625.
11	14134.	7726.	-40240.	40240.
12	.55E6	.255E6	-.886E7	.886E7

Part 2   Speed = 6600 rpm

Seal Number	$K_{\phi x}$ (lb)	$K_{\phi y}$ (lb)	$K_{\phi\phi}$ (lb * in/rad)	$K_{\phi\theta}$ (lb * in/rad)
1	2906.	6000.	18254.	1811.
2	2368.	4840.	14946.	1811.
3	2372.	4850.	14960.	1508.
4	2378.	4860.	14970.	1512.
5	2381.	4875.	14980.	1516.
6	2388.	4890.	15000.	1520.
7	2391.	4900.	15020.	1524.
8	2398.	4925.	15076.	1528.
9	2401.	4960.	15099.	1532.
10	2407.	5023.	15118.	1536.
11	2100.	3656.	11138.	1283.
12	.51E6	.687E6	.168E8	.286E8

Seal Damping Input
Part 1   Speed = 6600 rpm

Seal Number	C_{xx} $(lb*s/in)$	C_{xy} $(lb*s/in)$	$C_{x\phi}$ $(lb*s/rad)$	$C_{x\theta}$ $(lb*s/rad)$
1	26.7	1.35	1.05	1.05
2	22.92	1.19	.9	.9
3	22.99	1.2	.903	.903
4	23.03	1.21	.905	.905
5	23.06	1.22	.907	.907
6	23.08	1.23	.909	.909
7	23.10	1.24	.911	.911
8	23.12	1.25	.913	.913
9	23.14	1.26	.915	.915
10	23.16	1.28	.917	.917
11	15.36	.813	.657	.657
12	1320.	190.	408.	408.

Part 2   Speed = 6600 rpm

Seal Number	$C_{\phi x}$ $(lb*s)$	$C_{\phi y}$ $(lb*s)$	$C_{\phi\phi}$ $\left(\frac{lb*s*in}{rad}\right)$	$C_{\phi\theta}$ $\left(\frac{lb*s*in}{rad}\right)$
1	.56	7.2	4.72	.39
2	.49	6.2	4.12	.33
3	.5	6.2	4.13	.331
4	.5	6.2	4.13	.331
5	.5	6.2	4.13	.331
6	.5	6.2	4.13	.331
7	.5	6.2	4.13	.331
8	.5	6.2	4.13	.331
9	.5	6.2	4.13	.331
10	.52	6.25	4.15	.336
11	.35	4.15	2.75	.24
12	427.	2512.	11028.	1016.

Seal Inertia Input
Part 1   Speed = 6600 rpm

Seal Number	M_{xx} $(lb*s^2/in)$	M_{xy} $(lb*s^2/in)$	$M_{x\phi}$ $(lb*s^2/rad)$	$M_{x\theta}$ $(lb*s^2/rad)$
1	.002	0.0	-.002	.002
2	.002	0.0	-.002	.002
3	.002	0.0	-.002	.002
4	.002	0.0	-.002	.002
5	.002	0.0	-.002	.002
6	.002	0.0	-.002	.002
7	.002	0.0	-.002	.002
8	.002	0.0	-.002	.002
9	.002	0.0	-.002	.002
10	.002	0.0	-.002	.002
11	.001	0.0	-.001	.001
12	.316	0.0	-.7	.7

Part 2   Speed = 6600 rpm

Seal Number	$M_{\phi x}$ $(lb*s^2)$	$M_{\phi y}$ $(lb*s^2)$	$M_{\phi\phi}$ $(\frac{lb*s^2*in}{rad})$	$M_{\phi\theta}$ $(\frac{lb*s^2*in}{rad})$
1	0.0	.001	.0008	0.0
2	0.0	.001	.0008	0.0
3	0.0	.001	.0008	0.0
4	0.0	.001	.0008	0.0
5	0.0	.001	.0008	0.0
6	0.0	.001	.0008	0.0
7	0.0	.001	.0008	0.0
8	0.0	.001	.0008	0.0
9	0.0	.001	.0008	0.0
10	0.0	.001	.0008	0.0
11	0.0	.001	.0006	0.0
12	0.0	.7	1.7	0.0

APPENDIX G

INPUT DATA FOR CENTRITECH ROTOR

Murphy and Vance (1984) The system of units used is pound, inch, second

Shaft Material Properties

Density	.7272E-3	$(lb * s^2/in^4)$
Elastic Modulus	30.E6	(lb/in^2)
Shear Modulus	11.7E6	(lb/in^2)

Shaft Description

Element Number	Length (in)	Outer Radius (in)
1	.753	2.0
2	1.752	1.2505
3	1.752	1.2505
4	.762	2.0
5	1.8	1.25
6	2.021	1.0
7	3.0	1.0
8	4.998	4.95
9	2.021	1.005
10	3.0	1.005
11	4.996	4.95
12	2.012	1.0025
13	3.0	1.0025
14	5.004	4.95
15	2.075	1.0025
16	3.0	1.0025
17	2.756	1.25
18	1.750	1.25
19	1.760	1.25
20	2.2	1.25
21	1.0	1.005
22	1.001	1.005

Support Stiffness

Station Number	K_{xx} (lb/in)	K_{xy} (lb/in)	K_{yx} (lb/in)	K_{yy} (lb/in)
3	40400.	0.0	0.0	294000.
19	40400.	0.0	0.0	294000.

Support Damping

Station Number	C_{xx} (lb*s/in)	C_{xy} (lb*s/in)	C_{yx} (lb*s/in)	C_{yy} (lb*s/in)
3	359.	0.0	0.0	783.
19	359.	0.0	0.0	783.

APPENDIX H

INPUT DATA FOR CENTRITECH

ROTOR WITH MASSLESS HOUSING

The system of units used is pound, inch, second

Shaft Material Properties

Density	.7272E-3	$(lb * s^2/in^4)$
Elastic Modulus	30.E6	(lb/in^2)
Shear Modulus	12.E6	(lb/in^2)

Shaft Description

Element Number	Length (in)	Outer Radius (in)
1	.753	2.0
2	1.752	1.2505
3	1.752	1.2505
4	.762	2.0
5	1.8	1.25
6	2.021	1.0
7	3.0	1.0
8	4.998	4.95
9	2.021	1.005
10	3.0	1.005
11	4.996	4.95
12	2.012	1.0025
13	3.0	1.0025
14	5.004	4.95
15	2.075	1.0025
16	3.0	1.0025
17	2.756	1.25
18	1.750	1.25
19	1.760	1.25
20	2.2	1.25
21	1.0	1.005
22	1.001	1.005

Housing Material Properties

Density	.7383E-13	$(lb * s^2/in^4)$
Elastic Modulus	30.E6	(lb/in^2)
Shear Modulus	11.7E6	(lb/in^2)

Housing Description

Element Number	Length (in)	Outer Radius (in)	Inner Radius (in)
1	2.6	2.5	2.25
2	4.667	2.5	2.25
3	4.667	2.5	2.25
4	4.998	5.5	5.25
5	2.511	1.5	1.25
6	2.511	1.5	1.25
7	4.996	5.5	5.25
8	2.506	2.5	1.25
9	2.506	1.5	1.25
10	5.004	5.5	5.25
11	3.194	1.625	1.375
12	3.194	1.625	1.375
13	3.194	1.625	1.375
14	1.980	1.625	1.375
15	1.980	1.625	1.375
16	1.001	.875	.625
17	1.001	.875	.625

Support Stiffness

Station (Rotor)	(Housing)	K_{xx} (lb/in)	K_{xy} (lb/in)	K_{yx} (lb/in)	K_{yy} (lb/in)
3	2	80800.	0.0	0.0	588000.
19	14	80800.	0.0	0.0	588000.

Support Damping

Station (Rotor)	(Housing)	C_{xx} (lb * s/in)	C_{xy} (lb * s/in)	C_{yx} (lb * s/in)	C_{yy} (lb * s/in)
3	2	718.	0.0	0.0	1566.
19	14	718.	0.0	0.0	1566.

Housing Support Coefficients

Station Number	K_x (lb/in)	K_y (lb/in)	C_x (lb * s/in)	C_y (lb * s/in)
2	80800.	588000.	718.	1566.
14	80800.	588000.	718.	1566.

APPENDIX I

INPUT DATA FOR CENTRITECH

ROTOR WITH FLEXIBLE HOUSING

The system of units used is pound, inch, second

Shaft Material Properties

Density	.7272E-3	$(lb * s^2/in^4)$
Elastic Modulus	30.E6	(lb/in^2)
Shear Modulus	12.E6	(lb/in^2)

Shaft Description

Element Number	Length (in)	Outer Radius (in)
1	.753	2.0
2	1.752	1.2505
3	1.752	1.2505
4	.762	2.0
5	1.8	1.25
6	2.021	1.0
7	3.0	1.0
8	4.998	4.95
9	2.021	1.005
10	3.0	1.005
11	4.996	4.95
12	2.012	1.0025
13	3.0	1.0025
14	5.004	4.95
15	2.075	1.0025
16	3.0	1.0025
17	2.756	1.25
18	1.750	1.25
19	1.760	1.25
20	2.2	1.25
21	1.0	1.005
22	1.001	1.005

Housing Material Properties

Density	.7383E-3	$(lb * s^2/in^4)$
Elastic Modulus	30.E6	(lb/in^2)
Shear Modulus	11.7E6	(lb/in^2)

Housing Description

Element Number	Length (in)	Outer Radius (in)	Inner Radius (in)
1	2.6	2.5	2.25
2	4.667	2.5	2.25
3	4.667	2.5	2.25
4	4.998	5.5	5.25
5	2.511	1.5	1.25
6	2.511	1.5	1.25
7	4.996	5.5	5.25
8	2.506	2.5	1.25
9	2.506	1.5	1.25
10	5.004	5.5	5.25
11	3.194	1.625	1.375
12	3.194	1.625	1.375
13	3.194	1.625	1.375
14	1.980	1.625	1.375
15	1.980	1.625	1.375
16	1.001	.875	.625
17	1.001	.875	.625

Support Stiffness

Station (Rotor)	(Housing)	K_{zz} (lb/in)	K_{zy} (lb/in)	K_{yz} (lb/in)	K_{yy} (lb/in)
3	2	80800.	0.0	0.0	588000.
19	14	80800.	0.0	0.0	588000.

Support Damping

Station (Rotor)	(Housing)	C_{zz} (lb * s/in)	C_{zy} (lb * s/in)	C_{yz} (lb * s/in)	C_{yy} (lb * s/in)
3	2	718.	0.0	0.0	1566.
19	14	718.	0.0	0.0	1566.

Housing Support Coefficients

Station Number	K_x (lb/in)	K_y (lb/in)	C_x (lb * s/in)	C_y (lb * s/in)
2	80800.	588000.	718.	1566.
14	80800.	588000.	718.	1566.

APPENDIX J

INPUT DATA FOR JOHNSTON VERTICAL PUMP

The system of units used is pound, inch, second

Shaft Material Properties

Density	.7383E-3	$(lb * s^2/in^4)$
Elastic Modulus	30.E6	(lb/in^2)
Shear Modulus	11.7E6	(lb/in^2)

Shaft Description

Element Number	Length (in)	Outer Radius (in)
1	5.625	.84375
2	4.	.84375
3	5.	.84375
4	4.	.84375
5	5.	.84375
6	4.	.84375
7	5.	.84375
8	8.125	.84375
9	1.313	.625
10	14.21	.625
11	10.96	.625
12	10.96	.625
13	10.96	.625
14	12.631	.625
15	9.537	.625
16	9.537	.625
17	9.537	.625
18	9.537	.625
19	13.9	.625
20	10.65	.625
21	10.65	.625
22	10.65	.625
23	12.881	.625
24	9.787	.625
25	9.787	.625
26	9.787	.625
27	9.787	.625
28	13.59	.625

Element Number	Length (in)	Outer Radius (in)
29	10.34	.625
30	10.34	.625
31	10.34	.625
32	9.438	.625
33	9.594	.625
34	9.413	.625
35	9.413	.625
36	9.413	.625
37	9.413	.625
38	9.413	.625
39	12.123	.625
40	12.123	.625
41	3.1275	.625
42	6.375	.625
43	4.875	.8125
44	18.	.8125
45	18.	.8125

Concentrated Masses

Station Number	Concentrated Mass $(lb * s^2/in)$	Diametral Mom. of I. $(lb * s^2 * in)$	Polar Mom. of I. $(lb * s^2 * in)$
2	.0854887	.6013	.85035
4	.0854887	.6013	.85035
6	.0854887	.6013	.85035
10	.002817	.0032938	.0016285
19	.002817	.0032938	.0016285
28	.002817	.0032938	.0016285
33	.002817	.0032938	.0016285
42	.04608	.221	.1105

Constant Bearing Stiffness Coefficients

Station Number	K_{xx} (lb/in)	K_{xy} (lb/in)	K_{yx} (lb/in)	K_{yy} (lb/in)
1	552.2	452.2	-452.2	552.2
46	2.5E5	0.0	0.0	2.5E5

Constant Bearing Damping Coefficients

Station Number	C_{xx} $(lb * s/in)$	C_{xy} $(lb * s/in)$	C_{yx} $(lb * s/in)$	C_{yy} $(lb * s/in)$
1	43.82	18.6	-18.6	43.82
46	0.0	0.0	0.0	0.0

Seal Descriptions

Seal Number	Station
1	3
2	5
3	7
4	14
5	23
6	32
7	41
8	43

Seal Coefficient Input

Speed = 1398 rpm

Seal Number	K_{zz} (lb/in)	K_{zy} (lb/in)	C_{zz} $(lb*s/in)$	C_{zy} $(lb*s/in)$
1	.8496	3171.	29.22	4.961
2	.85	3171.	29.22	4.961
3	.85	3171.	29.22	4.961
4	52420.	0.0	23.98	0.0
5	52420.	0.0	23.98	0.0
6	52420.	0.0	23.98	0.0
7	2.498E5	0.0	285.	0.0
8	2.5E5	0.0	0.0	0.0

Speed = 1602 rpm

Seal Number	K_{zz} (lb/in)	K_{zy} (lb/in)	C_{zz} $(lb*s/in)$	C_{zy} $(lb*s/in)$
1	.8496	3171.	29.22	4.961
2	.85	3171.	29.22	4.961
3	.85	3171.	29.22	4.961
4	65670.	0.0	17.1	0.0
5	65670.	0.0	17.1	0.0
6	65670.	0.0	17.1	0.0
7	2.498E5	0.0	285.	0.0
8	2.5E5	0.0	0.0	0.0

Speed = 1800 rpm

Seal Number	K_{zz} (lb/in)	K_{zy} (lb/in)	C_{zz} $(lb*s/in)$	C_{zy} $(lb*s/in)$
1	.8496	3171.	29.22	4.961
2	.85	3171.	29.22	4.961
3	.85	3171.	29.22	4.961
4	95360.	0.0	25.7	0.0
5	95360.	0.0	25.7	0.0
6	95360.	0.0	25.7	0.0
7	2.498E5	0.0	285.	0.0
8	2.5E5	0.0	0.0	0.0

APPENDIX K

INPUT DATA FOR JOHNSTON VERTICAL

PUMP WITH FLEXIBLE HOUSING

The system of units used is pound, inch, second

Shaft Material Properties

Density	.7383E-3	$(lb * s^2/in^4)$
Elastic Modulus	30.E6	(lb/in^2)
Shear Modulus	11.7E6	(lb/in^2)

Shaft Description

Element Number	Length (in)	Outer Radius (in)
1	5.625	.84375
2	4.	.84375
3	5.	.84375
4	4.	.84375
5	5.	.84375
6	4.	.84375
7	5.	.84375
8	8.125	.84375
9	1.313	.625
10	14.21	.625
11	10.96	.625
12	10.96	.625
13	10.96	.625
14	12.631	.625
15	9.537	.625
16	9.537	.625
17	9.537	.625
18	9.537	.625
19	13.9	.625
20	10.65	.625
21	10.65	.625
22	10.65	.625
23	12.881	.625
24	9.787	.625
25	9.787	.625
26	9.787	.625
27	9.787	.625
28	13.59	.625

Element Number	Length (in)	Outer Radius (in)
29	10.34	.625
30	10.34	.625
31	10.34	.625
32	9.438	.625
33	9.594	.625
34	9.413	.625
35	9.413	.625
36	9.413	.625
37	9.413	.625
38	9.413	.625
39	12.123	.625
40	12.123	.625
41	3.1275	.625
42	6.375	.625
43	4.875	.8125
44	18.	.8125
45	18.	.8125

Housing Material Properties

Density	.7383E-3	$(lb*s^2/in^4)$
Elastic Modulus	30.E6	(lb/in^2)
Shear Modulus	11.7E6	(lb/in^2)

Housing Description

Element Number	Length (in)	Outer Radius (in)	Inner Radius (in)
1	2.5	6.25	5.815
2	0.5	3.9	3.4625
3	4.5	3.9	3.4625
4	2.188	4.5	3.9375
5	3.125	6.125	5.35
6	5.0	5.9	3.0
7	.875	6.0	4.15
8	3.125	6.125	5.35
9	5.0	5.8	3.0
10	.875	6.0	4.15
11	3.125	6.125	5.35
12	5.0	5.8	3.0
13	.875	6.0	4.15
14	55.47	6.0	5.69
15	3.094	6.1	5.45
16	46.77	6.0	5.69
17	46.77	6.0	5.69
18	3.094	6.1	5.45
19	46.77	6.0	5.69
20	46.77	6.0	5.69
21	3.094	6.1	5.45
22	63.	6.0	5.69
23	1.5	12.0	5.69
24	22.75	8.25	7.94
25	2.5	8.25	3.0
26	11.88	8.25	7.94
27	36.0	8.25	6.575

Concentrated Masses

Station Number	Concentrated Mass $(lb * s^2/in)$	Diametral Mom. of I. $(lb * s^2 * in)$	Polar Mom. of I. $(lb * s^2 * in)$
2	.0854887	.6013	.85035
4	.0854887	.6013	.85035
6	.0854887	.6013	.85035
10	.002817	.0032938	.0016285
19	.002817	.0032938	.0016285
28	.002817	.0032938	.0016285
33	.002817	.0032938	.0016285
42	.04608	.221	.1105

Constant Bearing Stiffness Coefficients

Station Number		K_{xx} (lb/in)	K_{xy} (lb/in)	K_{yx} (lb/in)	K_{yy} (lb/in)
1	3	552.2	452.2	-452.2	552.2
46	28	2.5E5	0.0	0.0	2.5E5

Constant Bearing Damping Coefficients

Station Number		C_{xx} $(lb * s/in)$	C_{xy} $(lb * s/in)$	C_{yx} $(lb * s/in)$	C_{yy} $(lb * s/in)$
1	3	43.82	18.6	-18.6	43.82
46	28	0.0	0.0	0.0	0.0

Seal Descriptions

Seal Number	Rotor Station	Housing Station
1	3	6
2	5	9
3	7	12
4	14	15
5	23	18
6	32	21
7	41	25
8	43	27

Seal Coefficient Input
Speed = 1398 rpm

Seal Number	K_{xx} (lb/in)	K_{xy} (lb/in)	C_{xx} (lb * s/in)	C_{xy} (lb * s/in)
1	.8496	3171.	29.22	4.961
2	.85	3171.	29.22	4.961
3	.85	3171.	29.22	4.961
4	52420.	0.0	23.98	0.0
5	52420.	0.0	23.98	0.0
6	52420.	0.0	23.98	0.0
7	2.498E5	0.0	285.	0.0
8	2.5E5	0.0	0.0	0.0

Speed = 1602 rpm

Seal Number	K_{xx} (lb/in)	K_{xy} (lb/in)	C_{xx} (lb * s/in)	C_{xy} (lb * s/in)
1	.8496	3171.	29.22	4.961
2	.85	3171.	29.22	4.961
3	.85	3171.	29.22	4.961
4	65670.	0.0	17.1	0.0
5	65670.	0.0	17.1	0.0
6	65670.	0.0	17.1	0.0
7	2.498E5	0.0	285.	0.0
8	2.5E5	0.0	0.0	0.0

Speed = 1800 rpm

Seal Number	K_{xx} (lb/in)	K_{xy} (lb/in)	C_{xx} (lb * s/in)	C_{xy} (lb * s/in)
1	.8496	3171.	29.22	4.961
2	.85	3171.	29.22	4.961
3	.85	3171.	29.22	4.961
4	95360.	0.0	25.7	0.0
5	95360.	0.0	25.7	0.0
6	95360.	0.0	25.7	0.0
7	2.498E5	0.0	285.	0.0
8	2.5E5	0.0	0.0	0.0

Housing Support Coefficients

Station Number	K_x (lb/in)	K_y (lb/in)	K_θ (lb * in/rad)	K_ϕ (lb * in/rad)
1	0.0	0.0	0.0	0.0
23	2.5E6	2.5E6	3.0E6	3.0E6

` VITA

James Howard Kelly was born on the 5th of May, 1963 in Oklahoma City, Oklahoma to Mr. and Mrs. James B. Kelly. Following a few month stint in Oklahoma of which he remembers nothing, the family moved east to beautiful North Carolina where Mr. Kelly spent most of his childhood. Passing through South Carolina, back to North Carolina, and then through Louisianna, he arrived in the great state of Texas in the spring of 1978. He graduated from high school in 1981 in Woodlands, Texas before coming to Texas A&M University. There, he completed a Bachelor of Science degree in Aerospace Engineering in five years during which time he worked as a cooperative education student engineer with McDonnell Douglas Technical Services Company. Following a summer of overseas travel, Mr. Kelly began his graduate studies in the fall of 1986 again at Texas A&M University within the Mechanical Engineering Department. The primary focus of his graduate work has been in the area of rotordynamic modelling of turbomachinery.

Permanent mailing address:

1537D Pineridge

College Station, TX 77840

The typist for this thesis was J. Howard Kelly.